Role of vegetation in shaping ancient estuarine sedimentary architecture; a case study from the Carboniferous of Ireland

Bart van der Kwaak

In partial fulfilment of the degree of Master of Science
in the Earth Sciences

Department of Physical Geography, Utrecht University

Supervisors:
dr. William McMahon
dr. Harm Jan Pierik
Tim Winkels MSc
prof. dr. Maarten Kleinhans

Abstract

Vegetation plays a key role in fluvial and estuarine morphodynamics through promoted mud production, enhanced capture of muds and sediment stabilization by deep-rooting. Major stages in terrestrial flora evolution are co-eval with the radiation of morphodynamic features such as anastomosing river behaviour, point bar sedimentation and coal formation. In modern estuaries the effects of vegetation have been studied through modelling efforts, but their reflection in the rock record is poorly understood.

The present study aims to identify tangible evidence in a stratigraphic succession of the effects of vegetation on estuarine sedimentary processes through original fieldwork on an Early Viséan-aged (*ca.* 350 Ma, Early-Middle Carboniferous) case study which crops out in NW Ireland. The Carboniferous period is associated with its abundant, complex and tall-stature vegetation, familiar from museum dioramas and textbook illustrations of the 'coal age' equatorial wetlands. Within the stratigraphic succession of the Early Viséan case study, what sedimentary features are indicative of the sculpting role vegetation played at the time of deposition?

The study builds out from this individual effort to a comparison of estuarine strata through geological time, with a focus on the Early Palaeozoic rise and radiation of terrestrial flora. How have the sedimentary characteristics of estuarine successions changed over the course of the Early Palaeozoic under the influence of major developments in the evolution of terrestrial flora? What stratigraphic (dis)similarities between the Carboniferous case study and younger analogues may be attributed to post-Carboniferous evolutionary advances in terrestrial flora? To this extend, the fieldwork is bolstered by a literature survey of 19 studies on Cambrian to Cretaceous (541-66 Ma) estuarine strata.

Vegetation-dependent signatures in the Carboniferous case study are rhizoliths, fusain, coal seams and plant impressions. Vegetation-influenced signatures include packages of inclined heterolithic stratification (IHS) and mudrock deposits. While packages of IHS and mudrock may form abiotically, computer and analogue modelling efforts demonstrate vegetation promotes the development of these signatures.

The impact of vegetation is intricate in estuaries as these environments host a complex variation of morphodynamic conditions over a limited spatial scale. This is reflected in estuarine successions in the diversity of facies and architectural styles, even within architectural elements formed by similar mechanisms. For example, packages of IHS may be dominantly coarse-grained, fine-grained, comprise distinct heterolithic couplets or display a trend in couplet grain size.

A review of 19 Cambrian to Cretaceous-aged successions demonstrate a marked increase in IHS occurrence frequency and an increase in mudrock abundance of 1.3 orders of magnitude in post-Devonian (359-66 Ma) successions relative to older successions (541-359 Ma). These trends are co-eval with major steps in the Early Palaeozoic evolution of terrestrial flora.

Key in shaping estuaries are vascular and deep-rooting plants, which have evolved by the Early Viséan. The Cretaceous (145-66 Ma) advent of herbaceous, grass-like and salt marsh vegetation introduces new powerful ecosystem engineers to estuaries. As a result, crevasse splays may occur less frequently in (post-)Cretaceous estuaries as closely spaced reeds, a grass-like herbaceous plant, introduced a greater degree of vegetation density in the geomorphic landscape. Additionally, since the advent of salt marsh vegetation, potent in retaining muds, lateral channel mobility in estuaries may have been restricted more effectively than previously.

This work demonstrates the vegetation-dependent and vegetation-influenced sedimentary signatures in an Early Viséan estuarine case study. The occurrence of vegetation-influenced sedimentary features, such as packages of IHS and mudrock deposits, is promoted by the above-ground baffling and below-ground binding properties of vegetation. A 1.3 orders of magnitude increase in the abundance of these sedimentary features is found to be co-eval with land plant evolution through a literature survey that may serve as a pilot for future research.

Table of contents

List of figures, tables and appendixes

1. Introduction

1.1. Rationale

Recent studies of how vegetation affects the lithology and architectural build-up of fluvial systems (see Davies and Gibling, 2010a for review) have gained insight on the apparent co-pacing of land plant evolution and fluvial morphology. Vegetation plays a key role in stabilizing the floodplain (Kleinhans et al., 2018), and in the production and retention of mud (McMahon and Davies, 2018a). Roots mechanically strengthen banks and prevent floodplain erosion, secretion of organic acids facilitate an increased mud production, and the increased above-ground surface roughness provided by vegetation reduces water flow velocity sufficiently to promote the deposition of fines (Gurnell, 2014; Kleinhans et al., 2018). As a result, flow channelizes and tends to meander (Kleinhans et al., 2018). In ancient examples, McMahon and Davies (2018a) show that promoted mud production and retention coincides with major stages in land plant evolution. The proportion of mudrocks in preserved alluvium increased by 1.4 orders of magnitude after the evolution of land plants during the Palaeozoic (McMahon and Davies, 2018a).

The evolution of land plants must have additionally influenced estuarine environments downstream of these river deposits, *e.g.* impacting the spatial extent of mudflats and channelizing flow. However, studies in these realms are far scarcer, restricted to individual modelling efforts (Braat et al., 2017; van de Lageweg et al., 2018; Lokhorst et al., 2018) and rare studies of pre-vegetation paralic strata (Bradley et al., 2018).

Through original fieldwork, this research explores the tangible sedimentary features and sedimentary architecture reflective of the impact of vegetation on estuary morphodynamics, as recorded in the stratigraphy of the Carboniferous-aged *Largysillagh Sandstone* and *Shalwy Formation*. The fieldwork of this study is bolstered by an analysis of 19 reports of Cambrian to Cretaceous-aged estuarine successions in published literature to distil trends in the occurrence of sedimentary characteristics through geological time, co-eval with major steps in land plant evolution.

The Carboniferous case study forms the cornerstone of this research. In this period of geological time, vegetation was sufficiently abundant for the first time in Earth history to be a forcing actor on large-scale systems such as the geomorphic landscape, atmospheric composition and (global) climate (Davies et al., 2013). A number of land plant characteristics key in shaping estuarine morphodynamics have evolved by the Carboniferous. As such, the impact of vegetation on these systems must have been profound. Post-Carboniferous evolutionary advances may have introduced new traits to terrestrial flora that impact estuaries in a novel way. The Carboniferous case study is compared to a modern analogue through the lens of continued, post-Carbonifeous evolutionary advances of terrestrial flora.

1.2. Vegetation control modern rivers and estuaries

1.2.1. Modern rivers

Analogue and computer modelling efforts (van Dijk et al., 2013; Kleinhans et al., 2018) on modern river systems demonstrate that in rivers the presence of vegetation and the increase in vegetation-aided capture of muds have a combined effect on river planform and sedimentary architecture. Vegetation enhances the catchment-wide production of mud by accelerating chemical weathering aided by humic acids (Drever, 1994). A high mud supply stabilizes the floodplain as mud fills up the floodplain lows, reducing overbank flow velocities which decreases the frequency of chute cut-offs and lateral channel migration, promoting the tendency for a channel to meander (Kleinhans et al., 2018). Locally, *e.g.* on the floodplain and on point bars, vegetation baffles overbank flow and causes muds to be deposited closer to the channel, forming levees and further promoting a meandering planform (Davies et al., 2011; Kleinhans et al., 2018). Sediment binding through rooting increases bank stability and thus promotes flow channelization (Smith, 1976).

However, such laterally confined meander belts result in higher floodwater levels, increasing overbank flow velocities which increase the frequency of chute cut-offs and lateral channel migration, promoting a (weakly) braided planform. This results in a quasi-periodic 'resetting' of river planform: meandering is promoted by floodplain aggradation first, but leads to channel confinement elevating floodwater levels which promote chute cut-off, 'resetting' the river planform to a more straight-channel one, only for it to shift to a tendency to meander (Kleinhans et al., 2018, pp. 1).

Overall, modern river behaviour is affected by vegetation through (1) the increased availability of muds resulting from enhanced chemical weathering by humic acids, (2) increased sediment stability through the binding effects of plant roots and (3) the local baffling of flow that the enhances capture of muds. In turn, these effects promote flow channelization and a tendency for channels to meander (Kleinhans et al., 2018).

1.2.2. Modern estuaries

The impact of vegetation on modern estuaries is primarily felt by channelization and meandering in the fluvial zone (Braat et al., 2017), reduced tidal dynamics and expansion of mudflats in the mixed-energy zone (Lokhorst et al., 2018; Braat et al., 2019), and by increased tidal dynamics and retreat of mudflats in the outer zone (Braat et al., 2017; van de Lageweg et al., 2018) (Table 1).

The fluvial zone of estuaries is affected by vegetation similar to fluvial environments. Increased vegetation-aided mud capture results in stream channelization and meandering in the fluvial zone of estuaries (Lokhorst et al., 2018).

In the mixed-energy zone of the estuary a positive feedback loop exists between mud deposition and vegetation occurrence (Lokhorst et al., 2018). Waning tide (ebb) deposits muds on intertidal areas, elevating them to allow for the settling of seedlings and the development of vegetation. In turn, these vegetated areas in the intertidal zone enhance the capture and retention of mud by baffling flow. Over the course of decades, vegetated mudflats in the mixed-energy zone expand in areal extent, encroaching on and channelizing the main estuary channel (Lokhorst et al., 2018). This narrowing and channelization of the main channel reduces the tidal prism of the estuary, siphoning landward flood flow and increasing flood flow velocity in the outer reaches of the estuary (van de Lageweg et al., 2018).

Perhaps counterintuitively, this pushed the tidal limit of the estuary seaward and increases tidal dynamics in the outer reaches of the estuary, preventing widespread accumulation of muds (Braat et al., 2017) and restricting development of vegetation to the margins (Lokhorst et al., 2018).

Table 1: *summary of the effects of vegetation in each of the three estuary reaches (Lokhorst 2018; classification after Dalrymple, 1992).*

	mud supply, no vegetation	*mud supply with vegetation*	*expected signatures*
fluvially dominated *Kleinhans et al., 2018*	abiotically deposited mud create cohesive floodplain, yields meandering planform.	Vegetation-enhanced mud capture leading to levee development and channelization of main channel.	IHS, floodplain deposits, rootlets, fossils, coal seams
mixed-energy *Braat et al., 2017* *Lokhorst et al., 2018*	abiotically deposited muds develop into intertidal mudflats. Central channel migrates laterally and, mid-channel bars are present.	Vegetation-capture muds develop into vegetated mudflats that encroach on main channel, limiting lateral mobility and reducing tidal prism.	IHS, mudflat deposits, rootlets, fossils, coal seams
tidally dominated *Braat et al., 2017* *Lokhorst et al., 2018*	intertidal mudflats that flank a wide, laterally migrating central channel with sand flats and mid-channel bars.	Reduced tidal prism by mixed energy channelization enhances tidal dynamics, limiting vegetated mudflat developments to margins.	IHS

1.3. Early Palaeozoic evolution of terrestrial flora

Terrestrial flora evolved and radiated over the course of the Early Palaeozoic, developing key physiological characteristics to allow the gradual colonization of diverse continental niches (Boyce and Lee, 2017). Two of such characteristics, deep-rooting and vascular plants, are crucial to shaping river and estuary morphodynamics (Braat et al., 2017; Kleinhans et al., 2018; Lokhorst et al., 2018). The development of these characteristics is expounded in the coming section, followed by an overview of the Carboniferous world and a discussion of post-Carboniferous evolutionary steps relevant to the impact of vegetation on estuaries.

1.3.1. Chemical weathering accelerated by vascular plants

Vegetation-accelerated chemical weathering is associated with the advent of vascular plants in the Late Silurian and their substantial radiation in the Devonian (Boyce and Lee, 2017). Vascular plants produce humic acids that alter soil properties and increase the residence time of water in a given substrate (Drever, 1994). Prior to this evolutionary step, mechanical weathering was the primary mechanism for substrate reduction (Eriksson and Simpson, 1998). As a result, fine-grained sediment load in pre-vegetation systems would be relatively rich in silt rather than clay (Kennedy et al., 2006).

1.3.2. Sediment binding by deep rooting

The Late Devonian onset of deep-rooting plants (Boyce and Lee, 2017) enhanced sediment stability through sediment binding by roots. In unvegetated environments sediments lack the protection offered by rooting, resulting in intensified raindrop erosion, surface runoff of meteoric water (Thornes, 2009) and aeolian winnowing of fine-grained sediments (Eriksson

and Simpson, 1998). Hortonian overland flows coalesce to streams which tend to widen rather than incise when discharge is increased (Sønderholm and Tirsgaard, 1998). Surface infiltration of water is limited in unvegetated environments (Knighton, 2014).

Sediments bound by roots are much more resistant to erosion; sediments with 18-20% roots by volume are up to 20.000 times more stable than those without (Smith, 1976). Sediment stability promotes channelization of streams (Pollen-Bankhead and Simon, 2009) and surface infiltration of water (Knighton, 2014). Flows transitioned to a more perennial state with the introduction of vegetation to the landscape due to the improved upstream storage capacity of water which increasingly regulated discharge (Love and Williams, 2000).

1.3.3. Late Devonian and Carboniferous radiation

The earliest known vascular plants, *Cooksonia* from the Silurian-Early Devonian (*ca.* 440-400 Ma), were likely highly susceptible to erosion as they possessed little to no roots (Gensel et al., 2006), being washed away in flash floods easily. As such, their impact through accelerated chemical weathering on fluvial and estuarine systems is likely to have been small (Davies et al., 2010a). Lacking roots, *Cooksonia* were not an actor to stabilize its substrate through sediment binding but may have promoted above ground flow baffling aiding in the retention of muds on floodplains and point bars.

Deep-rooting vascular plants radiated over the course of the Devonian (Boyce and Lee, 2017), occupying low-land coastal plains by the Carboniferous (Fielding et al., 2009). Possessing roots, plants could better survive flood waters and baffle flow sufficiently to capture muds, promoting fine-grained floodplain aggradation (Davies and Gibling, 2010). A cohesive, fine-grained floodplain coupled with the bank stability provided by deep-rooting promotes a meandering channel planform (Kleinhans, 2018). In stratigraphy, the Silurian-Devonian is marked by an increase in sedimentary features representing a meandering planform (Davies et al., 2010b).

1.4. The Carboniferous world

By the Carboniferous, events took place in the context of the Pangea supercontinent, hosting large continental areas that lay within 25° of the palaeoequator (Torsvik and Cocks, 2004). Oceans covered and withdrew from large, low-lying areas (Heckel, 2008) as glacio-eustatic sea level fluctuated by as much as 120 metres (Rygel et al., 2008). The Mississippian climate was relatively arid, with more humid periods becoming prevalent by the early Pennsylvanian (Davies et al., 2013). These humid periods were marked by coals and extensive accumulation of plant material (Allen et al., 2011). By the late Middle Pennsylvanian aridity increased (Calder, 1998), in part representing northward continental drift (Schutter and Heckel, 1985), the presence of continental ice sheets and the establishment of a monsoonal regime (Tabor and Poulsen, 2008).

While land plant traits key in shaping estuaries have already evolved by the Carboniferous (vascular plants and deep rooting), a number of important evolutionary steps and reorganisation of floral communities took place during this period. The Devonian-Mississippian boundary (*ca.* 359 Ma) is marked by the extinction of archeopteridalean progymnosperms, with diverse arborescent lignophytes appearing in the early Tournaisian (Decombeix et al., 2011). By the late Mississippian cordaitaleans and conifers evolve, diversifying and radiating greatly over the course of the Pennsylvanian (DiMichele et al., 2010). In the Pennsylvanian extensive wetlands developed (Allen et al., 2011), familiar from museum diorama's and textbook illustrations of

the ‘coal age’. Increasing aridity at the base of the Kasimovian resulted in the collapse of rainforest biomes (Cleal and Thomas, 2005), extinction of diverse lycopsids and a shift in peat-mire settings from predominantly lycopsid vegetation to tree ferns (DiMichele et al., 2009).

The geomorphic landscape was affected significantly by these vegetational events (Gibling and Davies, 2012). The invent of seed habit in the late Devonian allowed vegetation to colonize drier alluvial plains, covering the arid Mississippian expanses (Davies et al., 2013). Coniferophytes substantially covered uplands (Falcon-Lang and Bashforth, 2005; Gibling et al., 2010), dryland alluvial plains, alluvial fans and similar dry environments by the Pennsylvanian, while wetland environments persisted along riparian corridors and coastal wetlands (Calder, 1994; DiMichele et al., 2010; Davies et al., 2013 and references therein).

Considerable changes in atmospheric composition, such as the Late Devonian-Carboniferous decrease in atmospheric CO_2, is related to the substantial increase in plant cover in this period of Earth history (Berner, 2006). Carboniferous glacial-interglacial oscillations are linked to these changes in atmospheric conditions (Davies et al., 2013).

By the Carboniferous, vegetation was sufficiently abundant to significantly alter the geomorphic landscape, force global climate and play a key role in shaping river and estuarine morphodynamics for the first time in Earth history. These changes drew a sharp contrast between the Carboniferous and its preceding geological periods when vegetation was sparse, glacial periods rare and continental landforms relatively uniform (Davies et al., 2013).

1.4.1. Post-Carboniferous evolutionary advances

After the Carboniferous, the Cretaceous (145 – 66 Ma) advent of herbaceous and salt marsh vegetation (Martinius and van den Berg, 2011; Boyce and Lee, 2017) introduced novel and powerful ecosystem engineers to estuarine environments (Lokhorst et al., 2018; Braat et al., 2017). Widespread grassland development followed in the Early Cenozoic (Boyce and Lee, 2017). Salt marsh vegetation comprises, *i.e.*, halophytic (salt-tolerant) grasses, herbs and shrubs (Woodroffe, 2002). These types of vegetation are very effective in baffling surface flow and capturing muds (Kleinhans, 2018), profoundly shaping brackish reaches of estuaries through the expansion of mudflats (Lokhorst et al., 2018).

2. Method

The present research comprises fieldwork on a Carboniferous estuarine case study and a literature survey of 19 Cambrian to Cretaceous (541-66 Ma) estuarine successions. Sedimentary features observed and quantified in the field are compared to other ancient estuarine successions in a literature review. Additionally, the Carboniferous case study is compared to a modern estuary through the lens of continued, post-Carboniferous evolution of terrestrial flora.

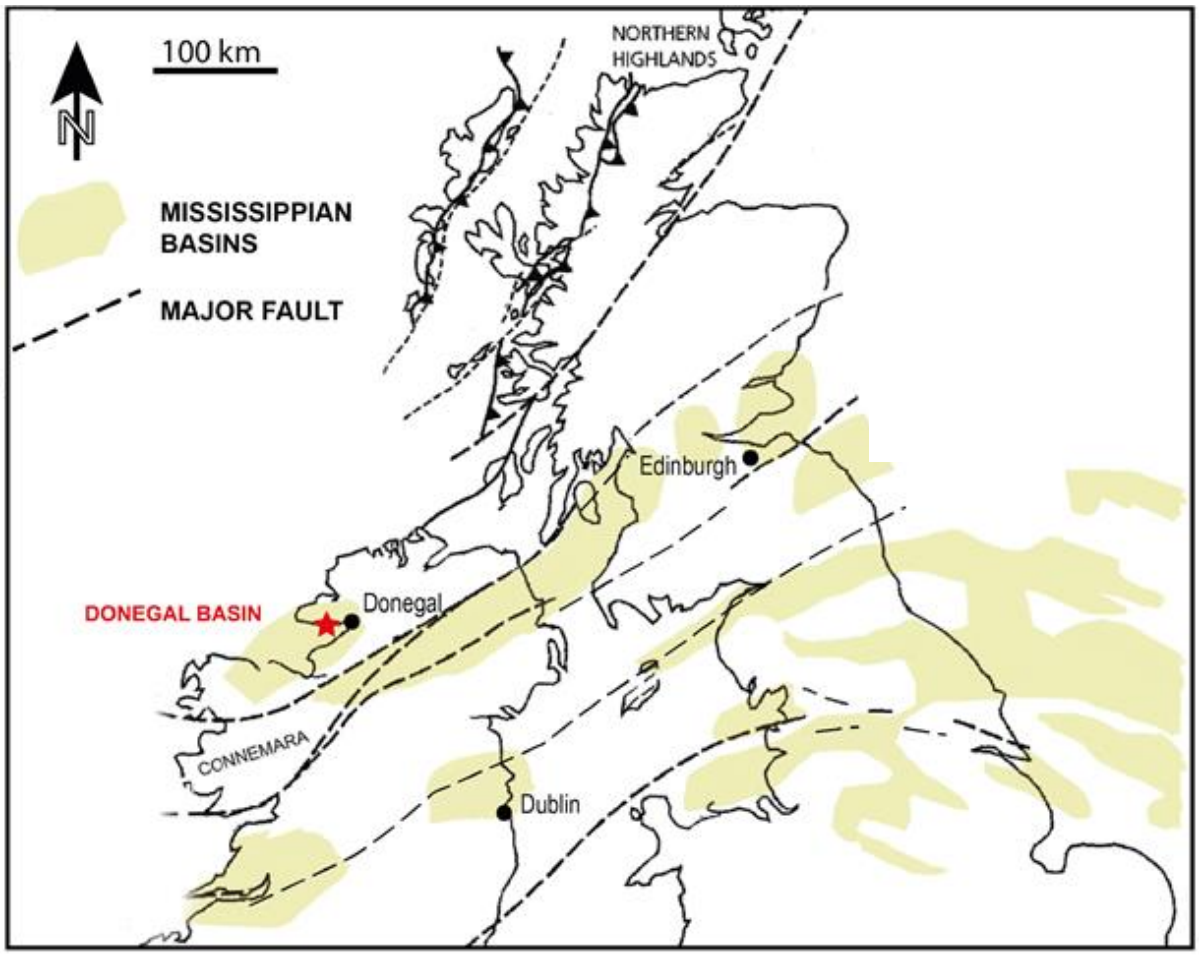

Figure 1: *Regional map showing major fault trends and distribution of Mississippian basins in Ireland and the UK, redrawn after Worthington and Walsh (2011). Shalwy Point study site marked by red star.*

2.1.1. Field site methods

High-resolution sedimentary logs on a decimetre-scale were taken through the estuarine sedimentary succession (Figure 3) as exposed at Shalwy Point in the north of the Republic of Ireland (Figure 1), comprising the *Largysillagh Sandstone* and *Shalwy Formation*. The strata are accessible and well-exposed, providing a continuous stratigraphic succession that can be walked out and outcrop windows that are typically several tens to some hundred metres wide. Thickness measurement for the high-resolution logs were done with a 2-metre folding ruler. Large-scale spatial characteristics, such as the lateral extent of a sediment body, were estimated in the field or from photographs using a person as an indicative scale.

The field site is suitable to observe a hierarchy of sedimentary features, such as sedimentary architectural elements (*e.g.* channels), package thickness and bed relations (*e.g.* an erosive bed base), and sediment composition and grain size (*e.g.* presence of shell fragments). In observing such features, emphasis was put on sedimentary features that may reflect a vegetation control on the estuary, based on what is known from studies on modern estuaries. For example, are there indicators for channel meandering or effective mud retention? What were the channel dimensions? Were these static or laterally mobile?

Methodically recording and quantifying the presence and abundance of sedimentary features allows for a relatively straightforward comparison of the case study with a modern analogue and with other estuarine successions in literature.

2.1.2. Case study comparison to modern analogue

The Carboniferous case study is compared to the Venice Lagoon estuary, a modern analogue system. The Venice Lagoon is considered a suitable analogue to the case study as channel dimensions are a similar order of magnitude (Brivio et al., 2016). The main advantages of a well-studied modern analogue are the constrained geomorphic landscape and the well-documented planform changes over temporal windows spanning seasons to decades. Such controls on sedimentary context are typically missing in stratigraphic successions.

Sedimentary characteristics of the Carboniferous case study are compared to the Venice Lagoon in light of the evolutionary advances of terrestrial flora since the Carboniferous, notably the advent of salt marsh vegetation during the Cretaceous (Boyce and Lee, 2017).

2.1.3. Ancient estuary database

A literature survey of Cambrian to Cretaceous-aged (541–66 Ma) estuarine successions was set up in an effort to distil a trend through geological time in the presence and abundance of key sedimentary features. This trend may be co-eval with the evolution of terrestrial flora. Terrestrial flora evolved and radiated over the course of the Palaeozoic era, with salt marsh vegetation evolving during the Cretaceous (Boyce and Lee, 2017)

The survey follows the methodology of Cotter (1978) and Davies et al. (2010a). The dataset used was compiled using the Web of Science search engine (www.webofknowledge.com), which is queried for 'estuary + Cambrian' or 'estuarine + Mississippian'. Period names are *sensu* the geological timescale of the International Commission on Stratigraphy (Cohen et al., 2013), with the Carboniferous also queried as 'Mississippian' and 'Pennsylvanian'. Such searches return papers that contain these terms in the title, abstract or listed keywords. These papers are individually reviewed to ascertain their suitability and to identify certain sedimentological characteristics. Papers are deemed suitable for inclusion when their results include lithostratigraphic logs based on outcrop data or core data, possibly supported by seismic data. The (reported) presence of packages of inclined heterolithic stratification (IHS) and the relative abundance of mudrock were compiled in a database to allow comparative analysis. These sedimentary characteristics are typically recorded by workers interrogating a sedimentary succession for a wide range of research questions.

Strata of clay-sized sediments, silt-sized sediments and shales are grouped as 'mudrock' (Ilgen et al., 2017). The abundance of mudrock is determined by measuring the cumulative thickness of mudrock sediments in a case study sedimentary log and is reported as a percentage of the total thickness of the (estuarine part of the) study's succession. Where researchers

identify multiple environments in their case studies only the interpreted estuarine facies are considered.

3. Geological setting and study area

3.1. Geological setting

Ireland was situated close to the palaeoequator in the Lower Carboniferous, and likely hosted a warm, alternatingly semi-arid and semi-humid climatic regime (Wright, 1990) during glacial cycles (Ketzer et al., 2002; Pfefferkorn et al., 2014). Graham (1996) indicates that the succession dates to the middle Viséan (~340 Ma), the second stage of the Mississippian. Bounded by land to the N-NW, the region saw a coastal to shallow-marine depositional environment that stretched from (modern) eastern Canada to eastern Europe (Graham, 1996). Inferred regional palaeocurrents from fluvial and deltaic deposits indicate a sediment transport direction to the south and southeast (Sevastopulo, 1981).

A phase of major northward marine transgression with intermittent regressive episodes characterizes the sedimentary signature in the region (Philcox et al., 1992; Guion et al., 2000; Sevastopulo and Jackson, 2009). Deposits from this long-term marine transgression unconformably overlie a Dalradian basement (Graham, 1996, 2010). Accompanying this transgression was a broad N-S to NNW-SSE trending crustal extension (Gawthorpe et al., 1989; Fraser and Gawthorpe, 1990, 2003; Johnston et al., 1996; Worthington and Walsh, 2011) leading to the development of a series of basins stretching 300 km across, covering parts of Ireland and northern Britain. In the north of the Republic of Ireland, these basins were bound by major NE-SW trending faults (Worthington and Walsh, 2011). Along these faults uplifted, emerged footwalls (*e.g.* the modern Ox Mountains and Curlew Mountains) separated basins from one another, allowing for little sediment transport between them (Worthington and Walsh, 2011).

3.2. Regional stratigraphy

The studied Carboniferous strata form part of the stratigraphy of the Donegal basin (Figure 2) (Graham, 1996). The overall net transgression across the region during the Lower Carboniferous is reflected in the Donegal Basin by a transition from basal alluvial conglomerates and fluvial sandstones, upwards into siliciclastic estuarine sediments and coastal calcareous deposits (Figure 2).

The onset of the transgression is marked by the unconformable contact of the Dalradian schist basement with the *Roulough Conglomerate Formation*, late Tournaisian or early Viséan (~345-350 Ma) in age (Ketzer et al., 2002), and is overlain by the sandstone dominated *Largysillagh Sandstone Formation*. The sandstone- and siltstone-rich *Shalwy Formation* follows, with overlying beds of bioclastic limestone and calcareous shales of the *Rinn Point Limestone* completing the fluvial to marine transition recorded in the regional stratigraphy (Graham, 1996).

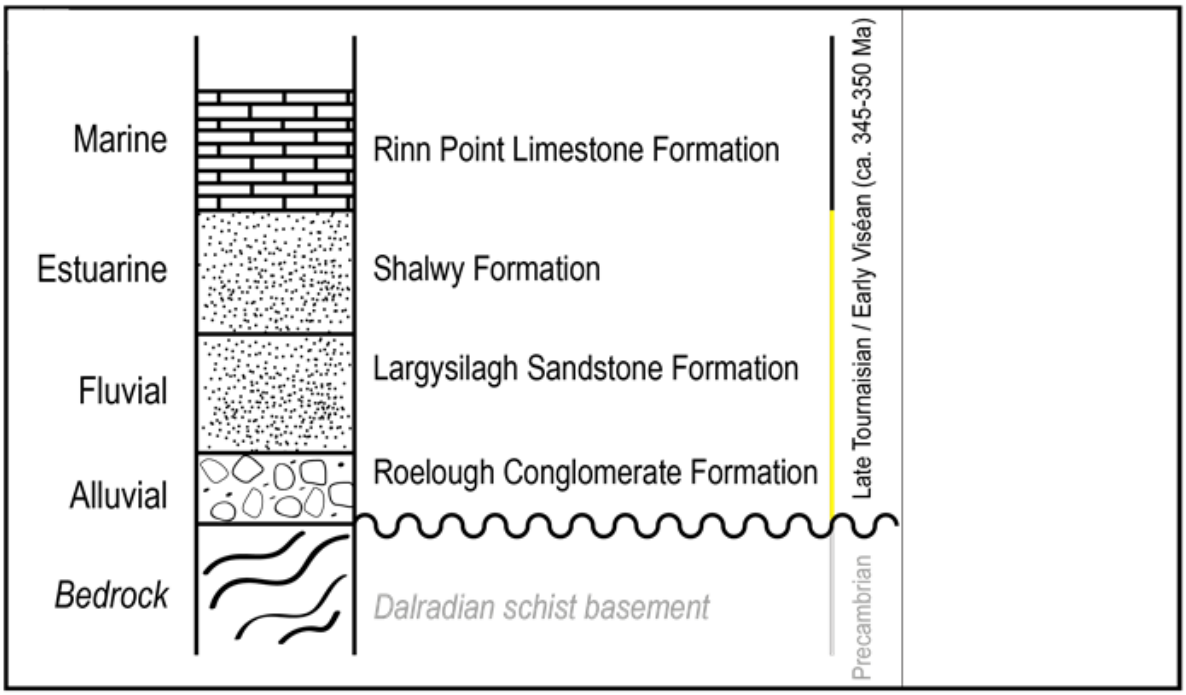

Figure 2*: Regional stratigraphic succession in the Donegal Basin. Studied section marked yellow, redrawn after Graham (1996).*

3.3. Field site succession

The logged succession is exposed in sea cliffs in the north of the Republic of Ireland, approximately 25 kilometres due west from Donegal at Shalwy Point (Figure 1). Previous work here mainly involved regional stratigraphic correlation (Graham, 1996; 2010) and work on the prominent fusain-rich point bar deposits (Nichols and Jones, 1992; Falcon-Lang, 1998).

At the field site, the clast-supported conglomerates of the *Roulough Conglomerate Formation* unconformably overlie the Dalradian basement. Despite the nature of the contact, the *Roulough Conglomerates* are virtually devoid of clasts of the basement's schists (Graham, 1996).

The *Largysillagh Sandstone Formation*, which erosively overlies the *Roulough Conglomerates*, comprises sandstones with frequent channel- and bar forms, occasional deposits of silt- and mudstone and some packages of inclined heterolithic strata (IHS) that are representative of point bar deposits (Thomas et al., 1987). Trace fossils gradually become more dense upwards in stratigraphy, particularly into the *Shalwy Formation*. In the *Shalwy Formation*, channel-form sandstones are less frequent and yield for sandstone beds with a tabular geometry.

Bioclastic sandstones and tempestite deposits are present close to the top of the studied succession. The uppermost strata recorded in the high-resolution logs comprise dark-coloured IHS rich in fusain and plant debris (Figure 3).

Above the studied succession, *Rinn Point Limestone* beds of bioclastic limestone, calcareous shales and hummocky cross-stratified sandstones gradually become more abundant (Graham, 2010).

4. Facies associations

The sedimentary facies identified in the studied succession are grouped based on lithology, ichnofauna and fossil presence, architecture and stratigraphic context. These results are presented concisely in table format (Table 2) and elaborated on in the successive text, with the stratigraphic succession graphically represented in the sedimentary logs (Figure 3).

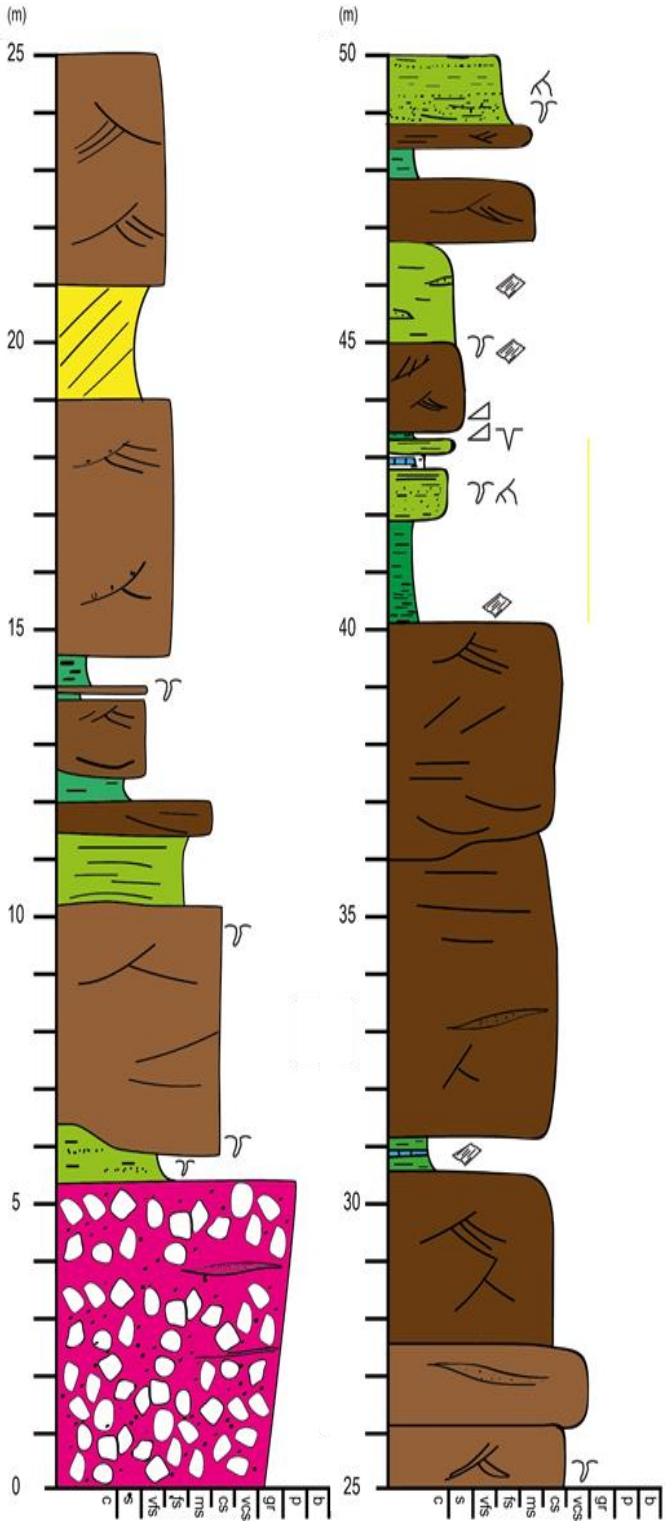

Figure 3: *Lower 50 metres of the stratigraphic log taken at Shalwy Point.*

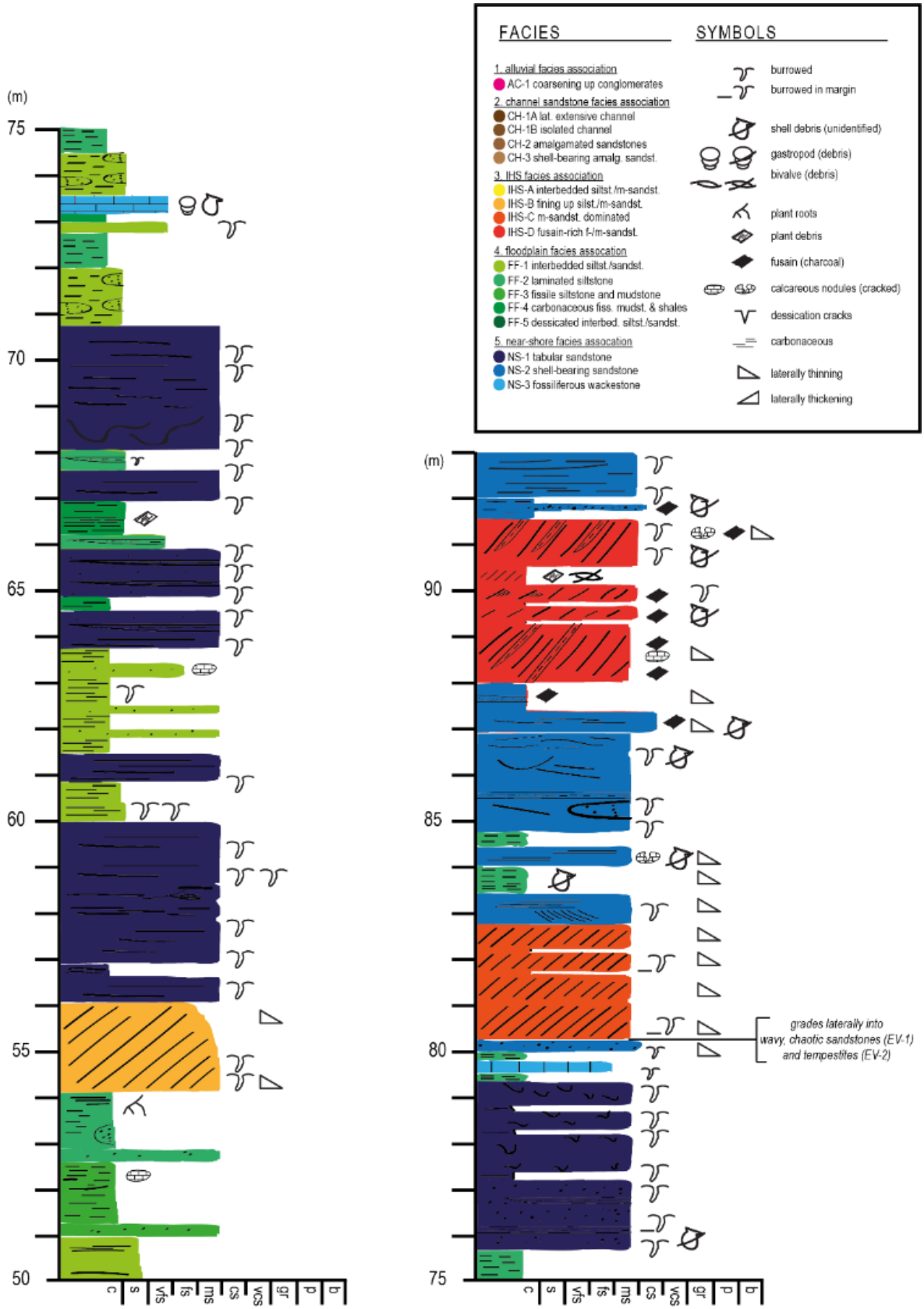

Figure 3 *(continued): Upper half of sedimentary log taken at Shalwy Point. Abbreviations in key: lat.: laterally; amalg.: amalgamated; sandst.: sandstone; siltst.: siltstone; mudst.: mudstone; fiss.: fissile; f-: fine-; m-: medium*

4.1. Facies association table

Table 2: *overview of the identified sedimentary facies and their associated figure number, texture, structure and interpretation.*

1. Alluvial facies association				
Facies code	*Figure №*	*Texture*	*Structure*	*Interpretation*
AC-1	Figure 4	Clast-supported, moderately rounded conglomerates, coarsening up from 4-8 (to 25) cm clasts to (8 to) 10-25 cm pebbles. Locally interbedded with disc. 10-40 cm siltstone lenses.	Siltstone lenses are laminated.	Alluvial fan deposit.
2. Channel sandstones facies association				
CH-1A	Figure 5	Laterally extensive channel-forms filled by medium-grained sandstone organised in 0.5-1 metre thick beds. Occasional coarse-grained sandstone to granules as initial fill. Channel-forms juxtaposed to irregularly bounded beds of CH-2. Channel-forms cut into fine-grained strata. Channel-forms 5-30 metres wide, 1-3 metres deep.	Parallel lamination and trough cross-bedding present in sandstone fill. Multi-storey channel-forms *ca*. 5-30 metres wide, 1-3 metres deep. Local sigmoidal sand lenses several metres in width. Dune topography preserved on exposed top surfaces.	Laterally migrating primary channel eroding older floodplain deposits on an active channel belt. Recorded flow conditions range from dune-forming to upper-flow regime conditions producing horizontal stratification and sigmoidal sand lenses.
CH-1B	Figure 5	Isolated channel-form filled asymmetrically with 10-40 cm beds of medium-grained sandstone. Channel-form *ca*. 25 metres wide, 2.5 metres deep.	Parallel lamination grading to trough cross-bedding in the top 20 cm. Current ripples on exposed top surface. Channel-form *ca*. 20 metres wide, 2.5 metres deep.	Short-lived primary channel downcutting into CH-2. Obliquely filled after abandonment.

CH-2	Figure 6	Medium to coarse-grained fining-up sandstone organised in an amalgamation of irregularly bounded 10-40 cm laterally thinning beds. Most bounding surfaces are erosive, few are draped by 2-10 cm thick dark-coloured siltstones. Rare *Chrondrites* trace fossils on some bounding surfaces. Rare plant debris 6-10 cm in size present.	Parallel lamination and trough cross-bedding in medium to coarse-grained sandstone.	Downstream migrating barforms in active channel belt. Siltstones and rare trace fossils occurrence indicate intervals of stasis.
CH-3	Figure 6	Medium-grained sandstone organised in an amalgamation of irregularly bounded 10-30 cm beds. Occasionally, an initial fill of coarse-grained sandstone occurs. Near the base 1-3 cm shell fragments are present frequently, as is a veneer of siltstone at the top.	Trough cross-bedding in medium-grained sandstone *Chrondrites* trace fossils frequently present close to base.	Brackish water channel, as indicated by presence of brackish-water fauna, with downstream migrating barforms.
3. Inclined Heterolithic Stratification (IHS) facies association.				
IHS-A	Figure 7	Cosets of inclined beds (10-12°) of alternating fine-grained and medium-grained sandstone organised in 1-5 cm beds. Medium-grained beds thicken towards top to 20-40 cm, but thin laterally to *ca*. 10 cm.	*Chrondrites* trace fossils burrowing down from medium-grained beds into the fine-grained beds.	Point bar in a fluvial channel with meandering planform. Seasonal discharge variability or tidal modulation results in grain size variation.
IHS-B	Figure 7	Cosets of inclined beds of alternating medium-grained sandstone (10-40 cm thick) and siltstone beds (2-9 cm thick); fining up to inverse alternations in upper half. The 2.5 metre thick package thins laterally to 0.5 metres. A singular 20 cm laterally continuous bed of bioclastic sandstone occurs within the package. Occasional 10-50 cm sized cracked carbonate nodules deform surrounding strata. Locally, 1-8 cm sized lenses of siltstone are present.	Frequent trough cross-bedding the medium-grained sandstone Frequent *Chrondrites* trace fossils throughout package and pervasive *Chrondrites* trace fossils in siltstone near top.	Point bar in tidally-influenced channel with meandering planform. Tidal modulation of flow results in grain size variation.

IHS-C	Figure 9	Cosets of inclined strata consisting of medium-grained sandstone organised in 10-40 cm beds, alternating with siltstone beds 1-4 cm in size. Plant debris 1-5 cm in size. Packages are frequently topped by 1-3 cm thick inclined siltstone beds. Rare 10-20 cm calcareous nodules deform strata.	Two modes are recognized based on structure: IHS-C1 sees a laterally varying number of bounding surfaces in the trough cross-bedded sandstone, with occasionally *ca*. 1 metre wide scours/channel forms near the top and frequent *Chrondrites* trace fossils towards the lateral margins. IHS-C2 sees 8-30 cm sandstone beds thinning laterally to *ca*. 10 cm. The top consists of a 1-3 cm veneer of siltstone with frequent *Chrondrites* trace fossils in the margins.	Point bar in tidally-dominated channel with meandering planform. Sandstones dominate as fine-grained sediments are reworked during subsequent depositional phases.
IHS-D	Figure 10	Cosets rich in fusain consisting of inclined beds, ranging from siltstone to coarse-grained sandstone 8 modes recognized, see text for detailed description. In general: rare *ca*. 10 cm sized cracked limestone nodules deforming surrounding strata; occasional 0.2-4 cm sized bivalve and shell debris; frequent 0.2-4 cm fusain debris, some modes are devoid of fusain.	Some *Chrondrites* trace fossils in siltstones and medium-grained sandstones are present. Infrequent 2-8 cm lenses of siltstone.	Point bar in channel with meandering planform proximal to estuary mouth (considering its stratigraphic context and shell-bearing lithology).
4. Floodplain facies association				
FF-1	Figure 11	Siltstone beds 0.5-3 cm in size alternate with 2-5 cm sandstone beds. in a *ca*. 70/30 siltstone./sandstone ratio, although becoming more sand-rich upwards. Siltstone beds are infrequently interjected by 1-3 cm discontinuous beds of medium-grained sandstone. Plant debris 1-4 cm in size in both siltstone and sandstone Locally, siltstone beds grade upward into carbonaceous mud.	*Chrondrites* trace fossils are present in top of siltstone units at contact with overlying tabular cross-bedded sandstone beds. Siltstone are infrequently interjected by parallel laminated sandstone beds with occasional *Chrondrites* trace fossils.	Proximal, poorly-drained floodplain on the active channel belt frequently interjected by overbank sands.

FF-2	Figure 11	Shales occasionally intercalated with 10-40 cm medium-grained sandstone of facies CH-2 and IHS-B. Infrequent interspersing 1-5 millimetre beds of fine-grained sandstone. Shell fragments 0.5-3 centimetres in size present locally.	Laminated shales., locally structureless siltstone, draped over underlying palaeotopography. The thick interjecting medium-grained sandstone beds comprise trough cross-bedding. The thin interspersing fine-grained sandstone beds host *Chrondrites* trace fossils.	Intermediately distal, poorly-drained floodplain on the active channel belt infrequently interjected by overbank sands. In the mixed-energy or tide-dominated section of estuary where shells are present in lithology.
FF-3	Figure 12	Siltstone locally grading to fissile muds bearing 1-5 cm sized plant debris. Infrequently interspersed by 5-10 cm thick beds of medium-grained sandstone and medium-grained sandstone lenses 1-4 cm thick. Occasionally, 2-8 cm calcareous nodules are present.	Siltstones comprise of 0.1-1 millimetre laminae. Medium-grained sandstone beds host frequent *Chrondrites* trace fossils.	Distal, poorly-drained floodplain on the active channel belt infrequently interjected by overbank sands.
FF-4	Figure 12	Very dark-coloured fissile muds and siltstones. Locally sees 0.5-3 cm plant debris as well as rare 1-2 cm coal seams.	Siltstone host 0.1-0.5 millimetre laminae.	Mire or very distal vegetated floodplain on the active channel belt.
FF-5	Figure 12	Medium-grained sandstone organised in beds 10-30 cm thick interbedded with 8-15 cm siltstone beds. Locally 2-4 cm discontinuous coal seams are present in the siltstones. Mudcracks occasionally present.	Pervasive *Chrondrites* trace fossils in both sandstone and siltstone.	Proximal floodplain on the active channel belt, frequently interjected by overbank sands or distal crevasse splays. Frequent exposure and depositional tranquillity as represented by mudcracks and pervasive ichnofauna.
5. Near-shore facies association				
NS-1	Figure 13	Tabular medium-grained sandstone organised in beds 10-40 cm thick. Bounding surfaces occasionally draped by 1-3 cm veneer of siltstone.	Tabular cross-bedding and parallel lamination displayed, though frequently disturbed by *Chrondrites* trace fossils, occasional along bounding surfaces and occasional pervasive throughout the bed. Dune topography on exposed top surface. Occasionally topped by 1-3 cm wavy veneer of siltstone.	Sand flat undergoing frequent upper-flow-regime conditions, with varying degree of inundation represented by varying presence of trace fossils.

NS-2	Figure 14	Medium-grained sandstone organised in beds of *ca*. 10 cm laterally thinning over tens of metres. Occasionally lined with 1-3 millimetre sized shell fragments. Locally 2-5 cm fusain-debris is present, in addition to cracked carbonate nodules *ca*. 8-15 cm in size.	Medium-grained sandstone display tabular cross-bedding.	Compound dunes in tidal channel with terrestrial input (fusain)
NS-3	Figure 14	Laterally continuous 10-30 cm beds of fossil-bearing limestone. Cracked limestone nodules 10-40 cm in size deforming surrounding strata.	Mud-supported.	Secluded, shallow lagoonal wackestone.
6. Event facies association				
EV-1	Figure 15	Medium to coarse-grained sandstone organised in laterally thinning 5-30 cm chaotic, wavy beds. Frequently lined with 1-6 cm sized plant debris and siltstone lenses. Frequently draped by siltstone veneer.	Locally sees occasional 1-3 cm sized shell debris. Locally fines laterally.	Crevasse splay element with brackish parent channel.
EV-2	Figure 15	Poorly sorted medium to coarse-grained sandstone with pervasive 1-5 cm fragments of gastropods, bivalves and unidentified bioclasts, organised into 10-30 cm fining-up beds. Locally 2-10 cm lenses of very fine sand are present. Beds are topped by 5-8 millimetres of fine to medium-grained sandstone.	Gastropod, bivalve and bioclast fragments are pervasive in the lower half of the bed. Upwards of this, medium to coarse-grained sandstone dominates. Top fine to medium-grained sandstone sees wavy laminae.	High-energy storm deposits in near-shore end of estuary.

4.2. Alluvial facies association

4.2.1. AC-1: coarsening up conglomerates

Unconformably overlying the Dalradian schist basement is a *ca.* 5 metre thick package of clast-supported conglomerates that coarsen upwards (Figure 4A). Moderately rounded clasts, typically around 4 to 8 cm in diameter with infrequent outliers to 25 cm near the base, coarsen to pebbles of 8 to 10 cm with infrequent outliers to 25 cm to the top (Figure 4B). 10-40 centimetre sized lenses of planar laminated siltstone and sandstone (Figure 4C) locally intersperse the conglomerates every several tens of centimetres.

Interpretation

These moderately rounded conglomerates with occasional sandstone lenses record an alluvial fan deposit (Blair and McPherson, 2009) and mark the onset of Carboniferous deposition in the area, with the sandstone lenses reflecting interspersed activity of fluvial processes. As this facies does not represent a (marginally) estuarine environment, it is outside the focus of this study and therefore described briefly.

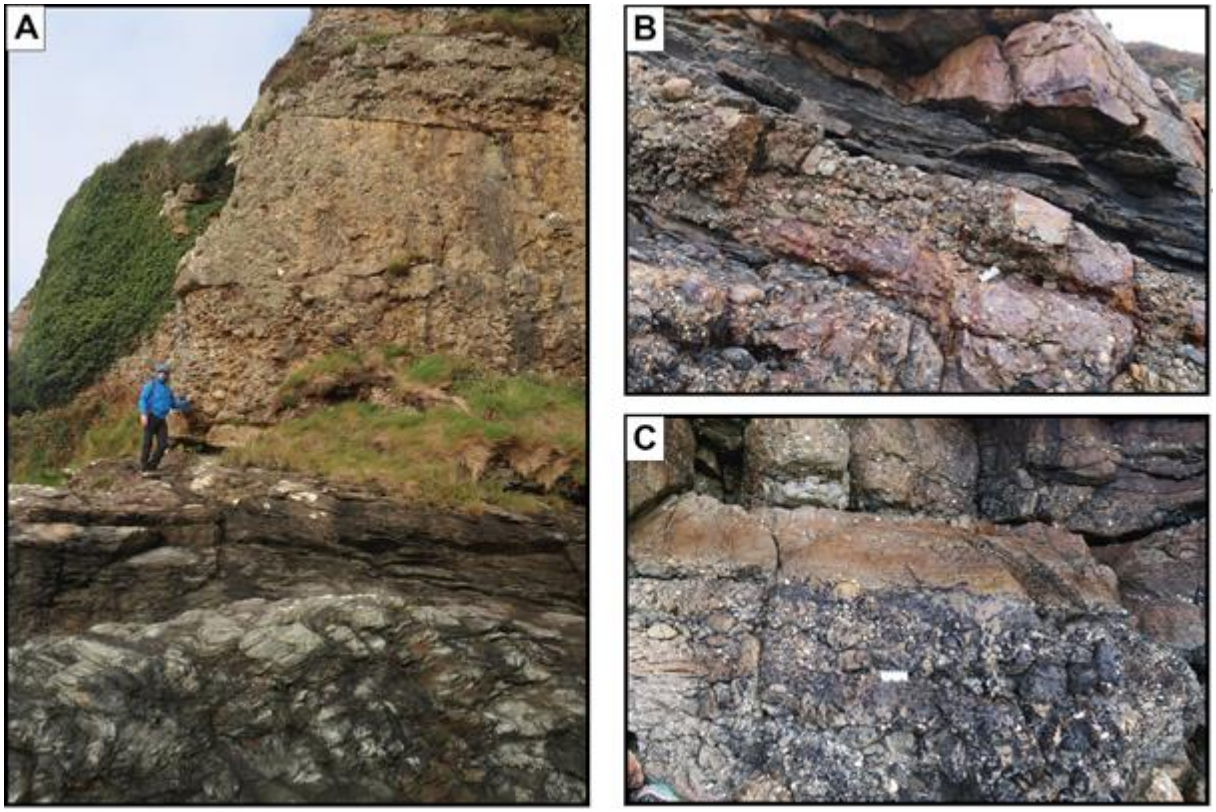

Figure 4: *(A) Top of Dalradian schist basement. Geologist (ca. 180 cm tall) hand on unconformably overlying conglomerates of facies AC-1. Note the overall fining up trend; (B) Detail of poorly sorted, moderately rounded conglomerates of facies AC-1. Note the sandstone lenses due left of scale bar. Overlain by sandstone deposits of the CPCB facies association. Scale bar dash length is 1 cm; (C) Detail of sandstone lens in conglomerates of facies AC-1. Note the overall fining up trend. Scale bar dash length is 1 cm.*

4.3. Channel sandstones facies association

In general, these intervals are organized in 1-4 metres thick packages containing 8-40 centimetres thick beds of cross-stratified or planar laminated medium- to coarse-grained sandstone. Granule- to pebble-size conglomerates are locally present. Channel-forms and irregular bounding surfaces are common throughout the facies association. On a succession scale, this facies association is frequently intercalated with the siltstone-dominated floodplain facies association (FF-1 to FF-5).

4.3.1. CH-1A: channel form, laterally extensive and multi-storey

These channel-forms (Figure 5A) are filled with medium-grained sandstone displaying well-preserved trough cross-bedding, planar laminations, occasionally fining up from an initial gravel to granule-sized fill. The fill is organised in beds 0.5-1 metres thick. The multi-storey channel-forms downcut into near-tabular strata of the siltstone-dominated floodplain facies association (FF-1 to FF-5). Channel-forms are 5-30 metres wide, 1-3 metres deep and laterally extensive over several tens of meters. The channel-forms are juxtaposed to beds irregularly bound by medium-grained sandstones of facies CH-2 (Figure 6A).

Locally, sigmoidal sand lenses up to several metres wide are present. To the top, the package forms a dune-like palaeotopography. Whereas the adjacent siltstone-dominated floodplain facies association (FF-1 to FF-5) contains trace fossils, these channel-forms are apparently ichnologically barren. Rare out-of-situ plant debris are observed in the sandstones.

4.3.2. CH-1B: channel form, isolated

These channel-forms are isolated architectural features and are not laterally extensive (Figure 5B). The channel form is filled by medium-grained, planar laminated sandstone, grading to cross-bedding in the top 20 centimetres. Beds 15-40 centimetres in thickness lie asymmetrically within the channel-form, thinning from the gentle to the steep side of the asymmetric channel form (right to left in Figure 5B). Flow ripples are present in the top of the exposed surface.

In the 22 metre wide outcrop, the channel-form thins from *ca.* 2.5 metres thick to *ca.* 1 metres thick before it is withdrawn from view. The channel-form margins are not exposed, but the preserved geometry implies they are not likely to be hidden from view by more than a few metres laterally. A reasonable approximate width for the channel-form would be 25 metres.

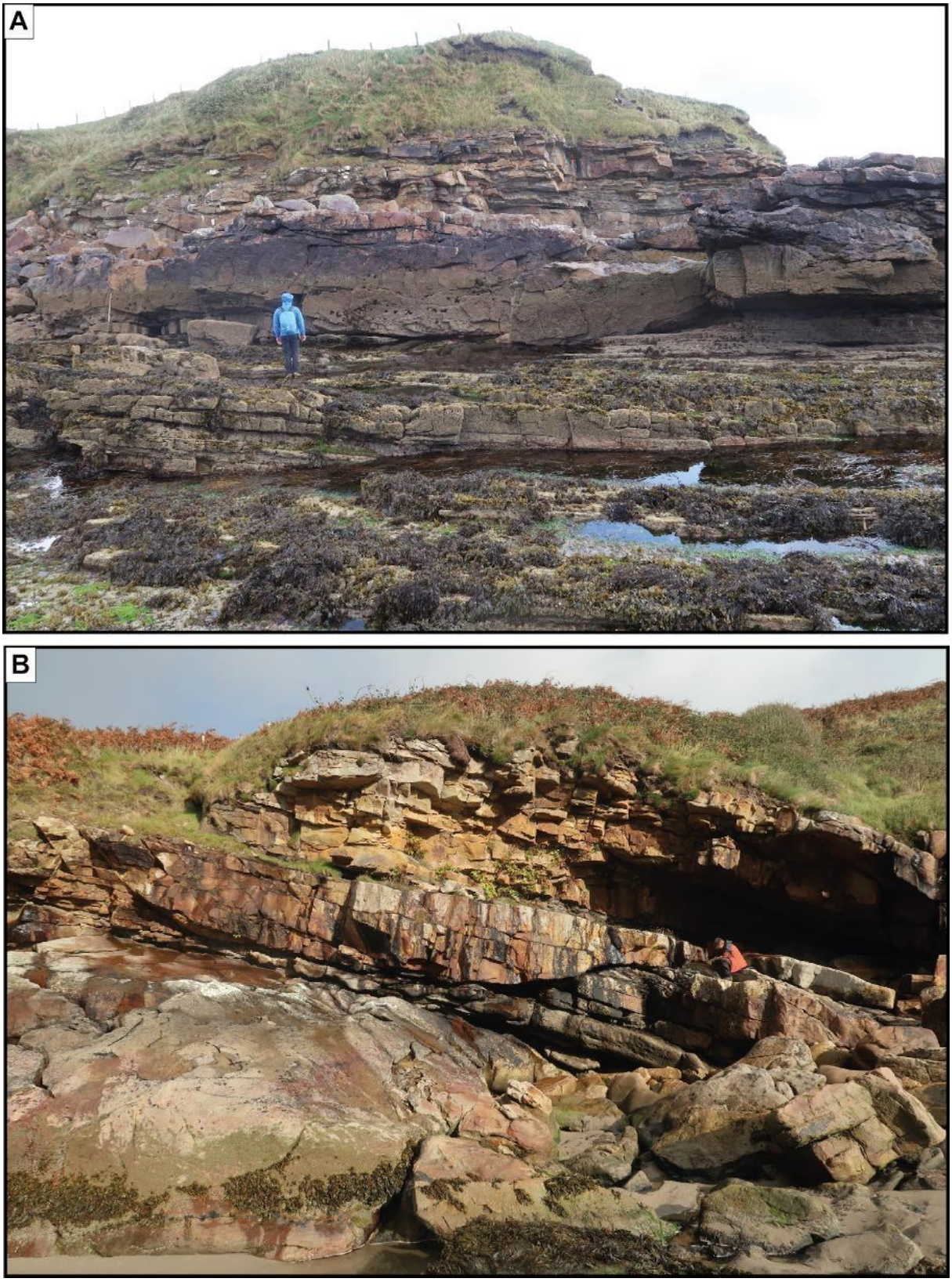

Figure 5: *(A) laterally extensive multi-storey channel complex of facies CH-1A cutting into proximal floodplain deposits of facies FF-1 and overlain by barforms of facies CH-2. Geologist is 180 cm tall; (B) Isolated channel form of facies CH-1B overlain by and cutting into barform of facies CH-2. Crouched geologist's height ca. 120 cm.*

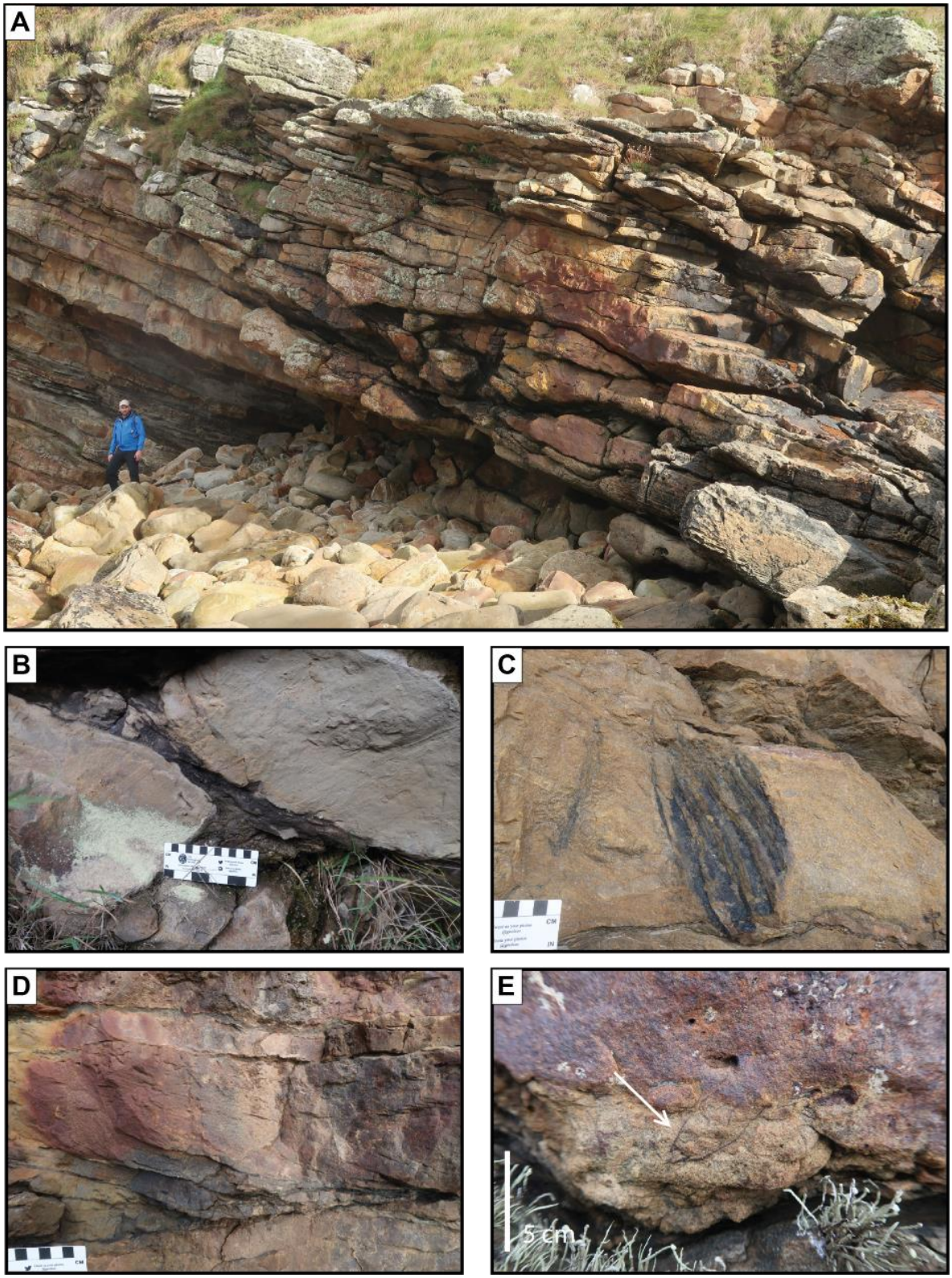

Figure 6*: (A) amalgamation of discontinuous wedging sandstones of facies CH-2 reflecting downstream migrating channel bars. Geologist is ca. 180 cm tall; (B) siltstone veneer of varying thickness separates wedging sandstones of CH-2. Scale bar dash length is 1 cm; (C) plant debris in sandstones of CH-2. Scale bar dash length is 1 cm; (D) Irregularly shaped bounding surfaces in sandstones of outcrop face of CH-3. Scale bar dash length is 1 cm; (E) Cross-cut shell fragments (white arrow) at bed base in sandstones of CH-3. View width ca. 20 cm.*

4.3.3. CH-2: amalgamated sandstones

These typically fining-upwards medium to coarse-grained sandstones (Figure 6A) display planar and trough cross-stratification. Amalgamated sandstone beds range between 10-40 centimetres in thickness and thin laterally over the course of several metres. They are separated by bounding surfaces that are irregularly shaped (Figure 6B) and are frequently draped by a 2-10 cm thick veneers of dark-coloured silts. Rare *Chrondrites* trace fossils and 5-10 centimetre sized plant debris occur (Figure 6C).

4.3.4. CH-3: shell-bearing amalgamated sandstones

This facies comprises medium-grained, trough cross-bedded sandstones in an amalgamated beds 10-30 centimetre thick (Figure 6D). Bounding surfaces occasionally host coarse-grained sandstone as the initial fill. *Chrondrites* trace fossils as well as 1-3 centimetre-sized shell (Figure 6E) fragments are present close to the bounding surfaces, with a siltstone veneer frequently capping individual beds.

Interpretation

Channelized sandstones (CH-1A) are interpreted to represent primary channels in an active channel belt of a laterally mobile stream. Individual channel (complex) dimensions vary but are all in the order of several to tens of metres wide and none are more than 1-3 metres deep. Occasional occurrence of plant debris (Figure 6C) reflects a vegetated hinterland.

Siltstone veneers which frequently cap beds record waning flow, likely resulting from temporal discharge variation, (upstream) channel migration, bar or levee elevation, or a combination of all three. Silt cohesion prevented the veneers from withering during deposition of subsequent sand beds (van Dijk et al., 2013).

Occurrence of *Chrondrites* trace fossils indicate periods of depositional stasis (Tipper, 2015). Bed bounding surfaces marked by *Chrondrites* suggest punctuated intervals of deposition and sedimentary stasis.

The channel-form sandstones are laterally and stratigraphically proximal to floodplain deposits (facies FF-1 to FF-5, discussed below) and point bar deposits (facies IHS-A to IHS-D, discussed below), implying a meandering planform for these channels (Thomas et al., 1987).

Facies CH-2, displaying outcrop faces marked by numerous co-sets of trough cross-bedding and co-sets with irregular bounding surfaces, are thought to represent an amalgamation of (partially preserved) channel barforms.

Presence of shell fragments in CH-3 implies (proximity to) brackish-water conditions. Shell fragments may have been flushed upstream from the coast during exceptionally high tides or storm events. Alternatively, shell species thrived locally. The present author argues for the latter, as evidence for high-energy conditions are lacking - no washed-out ripples, plane beds, indicators for flow reversal or poorly sorted storm beds are noted.

Channel architecture of CH-1A, CH-1B

The laterally extensive channel complex of CH-1A is cut into underlying and adjacent floodplain deposits (FF-1 to FF-5, discussed below). No packages of inclined heterolithic stratification (IHS-A to IHS-D, discussed below) reflective of point bar deposits (Thomas et al., 1987) are noted laterally or stratigraphically close, suggesting the channel complex migrated laterally with minimal vertical accretion.

The isolated channel of CH-1B cuts down into barform strata of CH-2 and lacks laterally adjacent channel forms or packages of IHS. Its 'clean' channel cut implies the channel did not migrate laterally. A chute channel would fit these observations but cannot be firmly stated as architectural context is missing, *e.g.* the presence of an adjacent main channel or upper flow regime elements (McMahon, 2018).

It is not a lack of stream power that would have limited lateral migration rate; the sandstone fill suggests stream power was not different from other (laterally migrating) channel complexes or downstream migrating bars seen elsewhere in the section. Rather, the sandstone filling reflects channel depression filling with a sustained stream power. Increased local sediment supply may yield such a result. Headward erosion in the formative stage of the chute channel provides a localized high sediment concentration as the bar erodes.

Oblique flow filling the channel depression accounts for the asymmetric fill of the channel depression (Okolo, 1983; Gibling, 2006).

4.4. Inclined heterolithic stratification (IHS) facies association

The term '*inclined heterolithic stratification (IHS)'* describes parallel to sub-parallel siliciclastic strata with an original (depositional) dip. These inclined strata are organised in alternating fine-grained and coarse-grained *sets*, jointly forming *couplets*. Packages of IHS form in a range of environments, but the overwhelming majority is the product of laterally accreting point bar deposits within meandering channels of *e.g.* fluvial or estuarine conduits (Thomas et al., 1987). Within estuaries and tidal rivers, differences in the sedimentological and ichnological character of individual IHS sets are reflective of the fluvial and tidal processes at play (Johnston and Dashtgard, 2014).

In the studied succession four types of IHS are distinguished based on their grain composition, grain size, bed thickness and presence of ichnofauna.

4.4.1. IHS-A: fine- and medium-grained sandstones alternations

Sigmoidal cosets of inclined heterolithic strata (IHS) consisting of fine-grained and medium-grained sandstones alternating in 1-5 centimetre thick beds (Figure 7A). In the upper half of the package, the medium-grained sandstones thicken to 20-40 centimetre beds that thin laterally to *ca.* 10 centimetres (Figure 8). Packages are inclined 10-12° with respect to the tectonic dip.

Chrondrites trace fossils appear to originate in the medium-grained beds and cut down into the underlying finer-grained horizons (Figure 7B).

4.4.2. IHS-B: fining up siltstone and medium-grained sandstone alternations

Sigmoidal cosets of IHS consisting of beds of medium-grained sandstones alternating with siltstone beds, trending up to fine-grained dominance (Figure 7C, D). The lower half of the package sees alternations of medium-grained, trough cross-bedded sandstone beds organised in 10-40 centimetre beds and 2-9 centimetre beds of siltstone (Figure 8). Frequent *Chrondrites* ichnofauna disturb and mix the sediment (Figure 7E). Thin lenses of siltstone, 1-3 centimetres thick, 2-8 centimetres wide are occasionally present in the sandstone beds.

The top half of the package sees inverse alternations: 10-40 centimetre beds of siltstone alternate with 2-9 centimetre beds of medium-grained, cross-bedded sandstone. The siltstone near the top of the package is heavily disturbed by bioturbation. Locally 10-50 centimetre sized cracked carbonate nodules deform surrounding strata (Figure 9C). The entire package thins laterally over tens of metres from 2.5 metres to 0.5 metres thick.

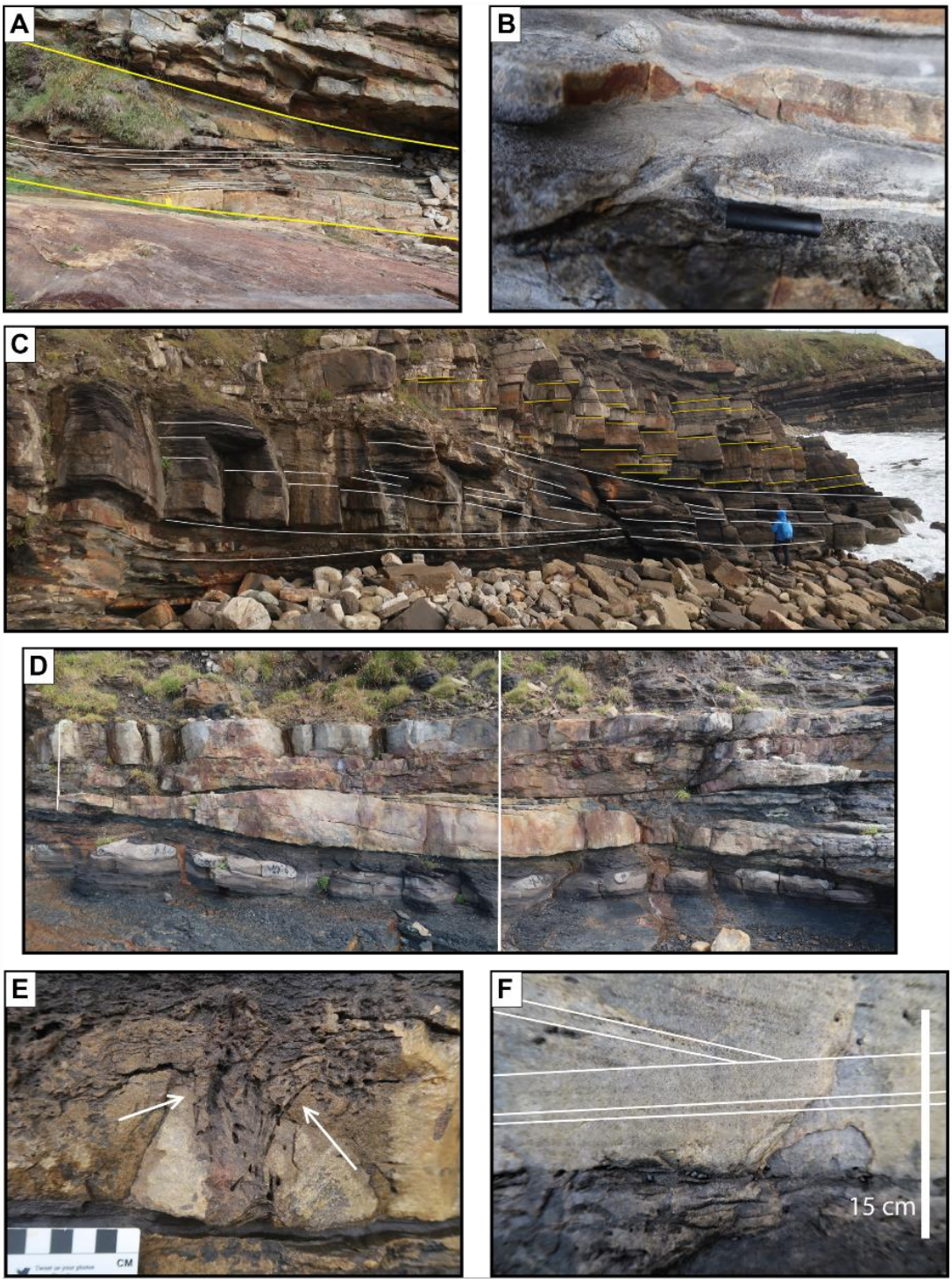

Figure 7*: (A) view on laterally accreting (LA) inclined heterolithic strata (IHS) of IHS-A (within yellow outline). White markings highlight depositional dip of IHS relative to tectonic dip. Yellow notebook is ca. 20 cm long; (B) Detail of alternations of medium-grained (thicker) sandstone beds and fine-grained sandstone beds in IHS-A. Pen cap is ca. 3 cm long; (C) view on package of IHS-B. Geologist is ca. 180 cm tall. White markings highlight depositional dip of IHS relative to tectonic dip (marked yellow) (D) Minor all-sandstone LA element of IHS-B in a context of shale-rich FF-2 deposits. Measuring stick left is 1 metre long; (E) Laminae deflection and sediment disturbance by Chondrites ichnofauna in sandstones of IHS-B. Scale bar dash length is 1 cm; (F) Bioturbated fine-grained sandstone (base) truncated by planar laminated cross-bedded sandstone, barren sandstone (middle) overlain by inclined bedded sandstone (top). White markings highlight cross-bedding.*

4.4.3. IHS-C: medium-grained sandstone dominated alternations

Coset of IHS dominated by trough cross-bedded sandstone organised into 10-40 centimetre beds, alternating with 1-4 centimetre sized beds of siltstone (Figure 9A) which display 1-5 centimetre sized plant debris (Figure 9B; Figure 8). Two modes of this IHS facies are recognized. IHS-C1 displays a laterally varying number of bounding surfaces in the sandstone. Occasional *ca.* 1 metre wide scour/channel-forms and frequent *Chrondrites* trace fossils are noted towards the margins.

The sandstone beds in the other mode, IHS-C2, range in thickness from 8-30 centimetres, topped by a 1-3 centimetres thick siltstone bed. Towards the margins, these sandstone beds thin to *ca.* 10 centimetres. The siltstones host *Chrondrites* trace fossils in these margins. Rare 10-20 centimetre sized calcareous nodules deform the sediment (Figure 9C).

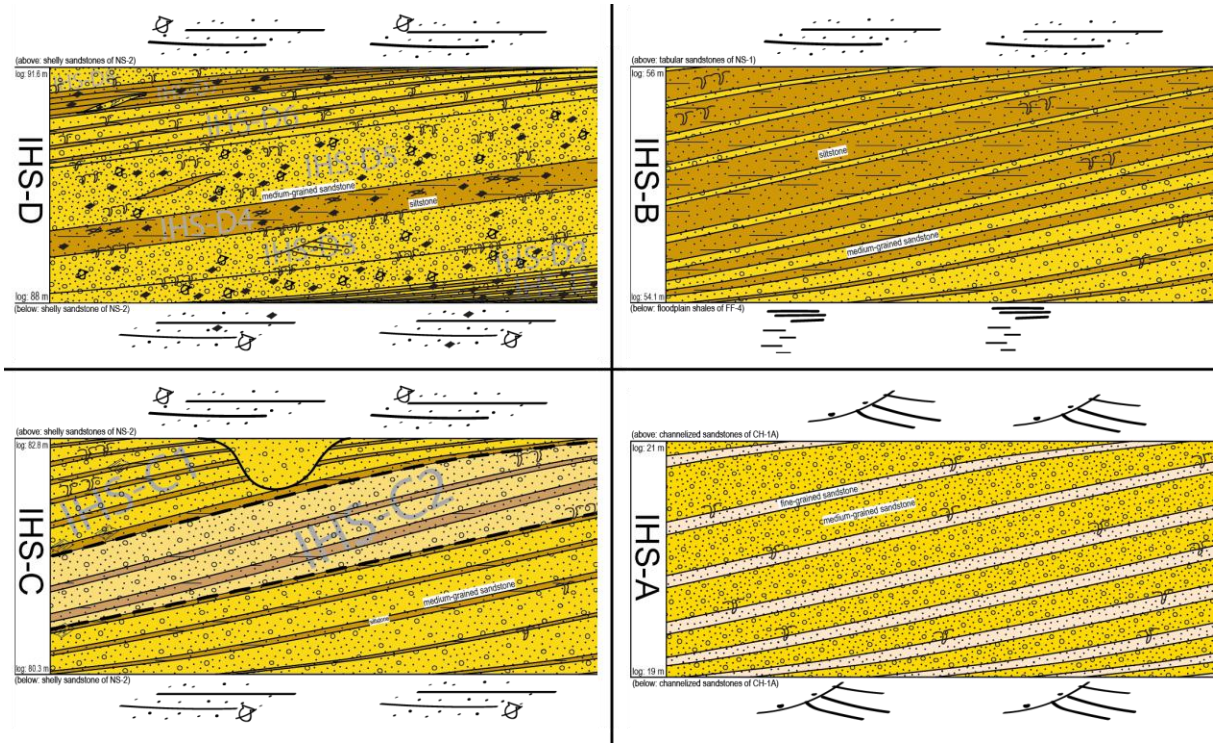

Figure 8: *schematic representation of identified types of IHS, see text for details. See log (Figure 3) for symbol key.*

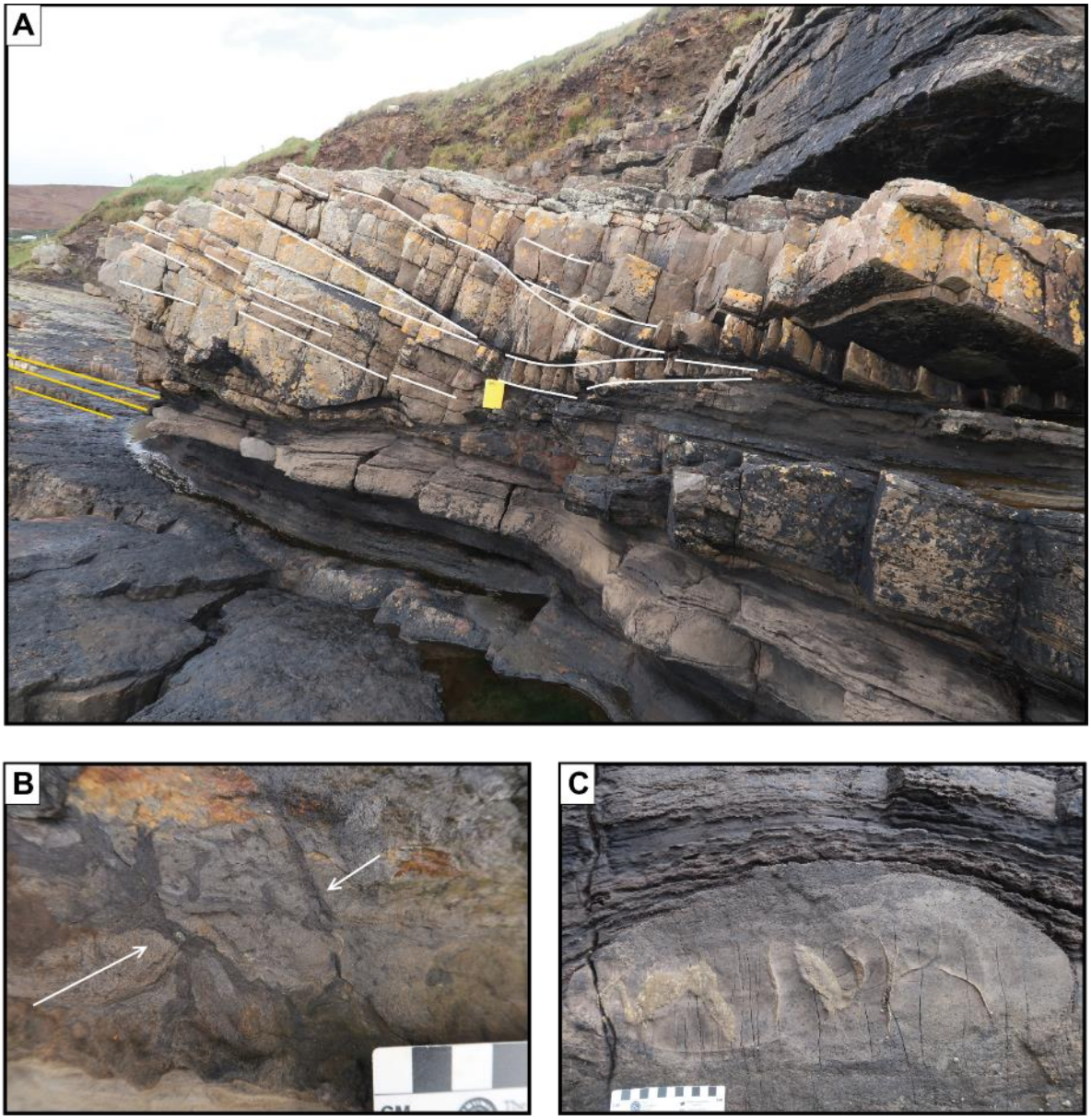

Figure 9: *(A) View on LA-IHS deposits of IHS-C from the side. White markings highlight pinching of beds, yellow markings highlight tectonic dip. Yellow notebook is ca. 20 cm long; (B) Plant debris (white arrows) in sandstones of IHS-C. Scale bar dash length is 1 cm; (C) Representative calcareous nodule seen at multiple horizons in the section. This particular nodule deforms surrounding strata of IHS-B. Scale bar dash length is 1 cm;*

4.4.4. IHS-D: fusain-dominated medium to coarse-grained sandstone alternations

Cosets of IHS notable for their dark-coloured sets rich in fusain (fossiliferous charcoal (Skolnick, 1958) debris (Figure 10A, E; Figure 8). This facies is partitioned into 8 sub-facies that are present within the inclined package.

- IHS-D1 contains laterally thinning equal alternations of 0.3-2 centimetre beds of fine-grained sandstone and siltstone rich in 0.2-2 centimetre scale fusain debris (Figure 10B). *Ca.* 10 centimetre, uncracked limestone nodules are locally present.
- IHS-D2 is characterized by a homolithic medium-grained sandstone with fusain (Figure 10C) and 0.2-2 centimetre scale shell debris.
- IHS-D3 comprises of a generally homolithic medium-grained sandstone displaying cross-bedding only in the middle of the 0.5 metre thick unit. The top and base of the unit is intensely bioturbated with *Chrondrites.* Siltstone veneers regularly overly bed tops. Infrequent 1-4 millimetre pyritized shell and fusain debris occur throughout the section (Figure 10D).
- IHS-D4 consists of siltstone with frequent 0.2-4 centimetre sized bivalve and fusain debris.
- IHS-D5 is a medium-grained, intensely bioturbated sandstone rich in 1-4 millimetre sized shell debris and with occasional 0.2-4 centimetre sized fusain. 2-8 centimetre sized lenses of siltstone occasionally interject.
- IHS-D6 has fine-grained sandstone beds 8-12 centimetre in size alternating with 2-5 centimetre beds of siltstone. The fine-grained sandstone beds comprise *Chrondrites* trace fossils and occasionally *ca.* 10 centimetre sized cracked limestone nodules (Figure 10E). The alternations thin laterally to *ca.* 5 centimetres in thickness.
- IHS-D7 is marked by 2-12 centimetre sizes beds of siltstone with 3-8 centimetre lenses consisting of coarse-grained sandstone with plentiful 0.2-4 centimetre sized shell and fusain debris. The siltstones occasionally host 1-3 centimetre sized fusain debris.
- IHS-D8 hosts a medium-grained sandstone organised in *ca.* 10 centimetre thick beds with frequent *Chrondrites* trace fossils at bed interfaces. Fusain debris is notably absent in these sandstones towards the top of the inclined package.

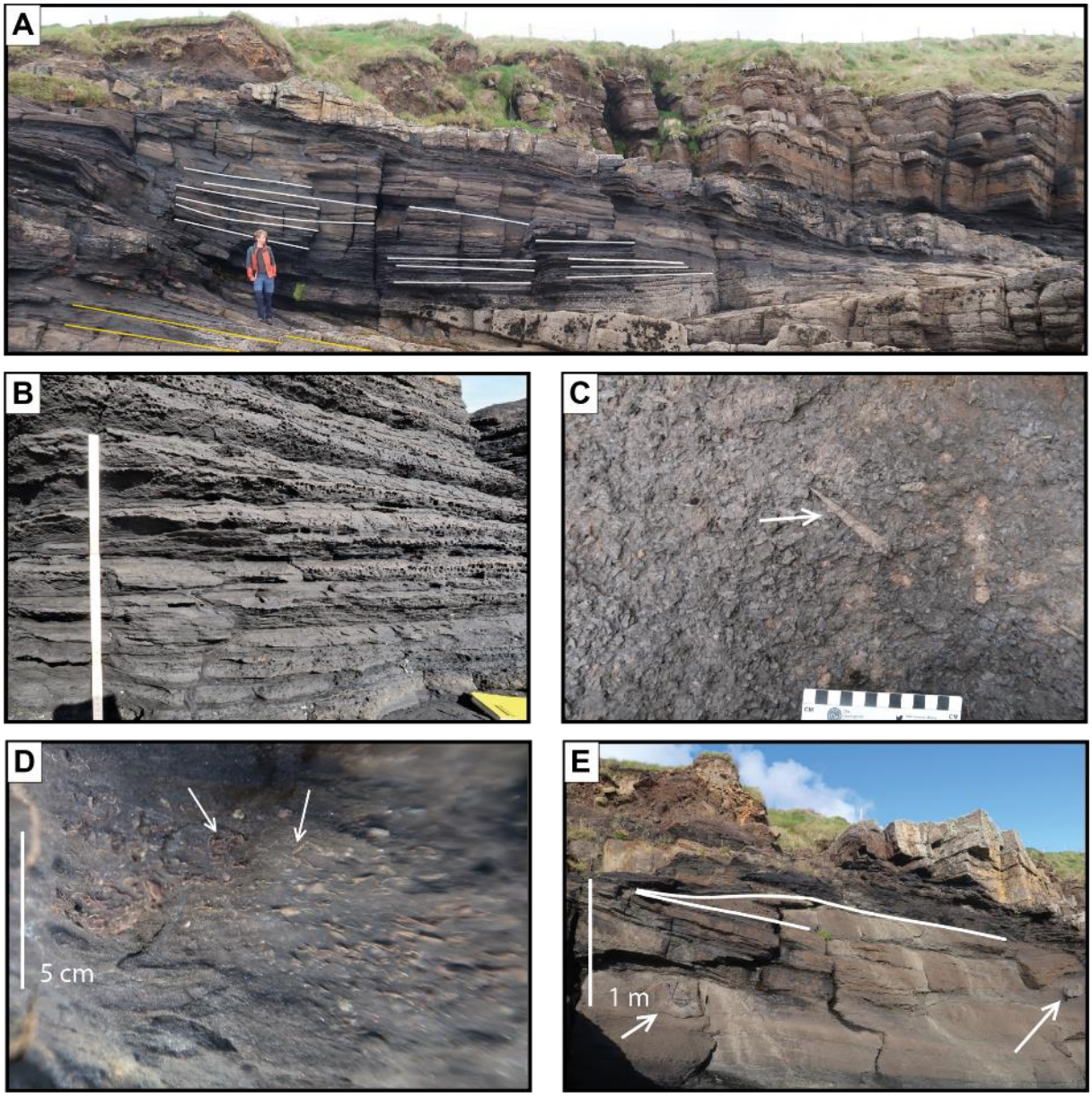

Figure 10: *(A) View on LA-IHS deposits of fusain-rich IHS-D. Note pinching of strata to right. White markings highlight depositional dip of beds, yellow markings highlight tectonic dip. Geologist ca. 185 cm tall; (B) Closer view of alternations of fusain-laden medium-grained sandstone and siltstone of IHS-D. Measuring stick 50 cm long; (C) Detail of fusain from IHS-D, note large fragment (white arrow). (D) Pyritized shell fragments (white arrows) in siltstone of IHS-D; (E) View on locally wedging beds of IHS-D, highlighted in white. Note the cracked calcareous nodules (white arrows).*

Interpretation

The packages of inclined heterolithic strata (IHS) in the studied succession are interpreted to represent point bar deposits in channels with a meandering planform (Thomas et al., 1987) because of their stratigraphic context that is reflective of a fluvial and tidally-influenced depositional environment.

Alternating sets within the four identified types of IHS generally display contrasting grain sizes, alternating between fine-grained sediments and medium- to coarse-grained

sediments (Figure 8). Going up in the succession, cosets of IHS alternate between fine-grained and medium-grained sandstone (IHS-A), siltstone and medium-grained sandstone (IHS-B), cosets dominated by medium-grained sandstones (IHS-C), and medium- and coarse-grained sandstones lined with fusain and shell debris (IHS-D).

Such grain size alternations within a package of IHS may result from changes in the grain size of the sediment supply, changes in flow conditions, or both (Johnson and Dashtgard, 2014). Sediment supply may be affected by *e.g.* seasonal variability in discharge and hinterland erosion (Sisulak and Dashtgard, 2012). Flow conditions in nearcoast alluvial environments are influenced on a system-scale by tides (Ainsworth and Walker, 1994). Tides influence flow conditions by accelerating flow during receding tide and deceleration flow with incoming tide (Ainsworth and Walker, 1994). Within the fluvial-dominated reach of estuaries this tidal modulation of flow is dampened going upstream. Closer to the estuary mouth, flow is distorted by increasing influence of wave and tidal action.

Tidal modulation of flow at the scale of the entire alluvial system provides an explanation for the contrasting grain sizes between the identified types of IHS. In terms of changing flow conditions the packages of IHS in the succession would grade from relatively stable flow conditions with minor fluctuations (IHS-A), to fluctuating or modulated flow conditions (IHS-B), to stable flow conditions (IHS-C), to fluctuating or modulated flow conditions (IHS-D) (Figure 16).

IHS-A, which comprises alternations of fine- and medium-grained sandstone, has a stratigraphic context comprising fine-grained floodplain deposits (FF-1 to FF-5) and channelized sandstones (CH-1A, -1B, -2). The sigmoidal geometry of the inclined packages and fluvial stratigraphic context likely renders this IHS-A a point bar deposit of a channel with a meandering planform in a fluvially dominated environment. Minor differences in set grain size, compared to the set grain size contrasts as observed in IHS-B and IHS-D, may be the result of small flow deviations, attributed to minimal tidal modulation or minimal (seasonal) discharge variability.

IHS-B, comprising sigmoidal sets with alternating siltstone and medium-grained sandstone, overlies fluvial floodplain (FF-1 to FF-5) and channelized sandstones (CH-1A, -1B, -2) and is in turn overlain by (near-shore) tabular sandstones (NS-1). The grain size contrast in IHS-B is greater than the other three identified IHS packages and could reflect a relatively high degree of tidal modulation of flow. IHS-B is interpreted as a point bar of a tidally-influenced meandering channel.

IHS-C is dominated by medium-grained sandstone and at the same stratigraphic level as the near-shore tabular sandstones of NS-1, implying the inclined strata would experience tidal influence. Returning high flow conditions (during incoming tide) would deposit and preserve coarser sediments (medium-grained sandstones) and erode finer-grained sediments (siltstones or mudstones) that were deposited during low tide. IHS-C is interpreted as a point bar in a tidally-dominated meandering channel.

IHS-D hosts alternating sets of medium- and coarse-grained sandstones and is stratigraphically above storm (tempestite) deposits of EV-2, and below the belemnite and coral-rich strata of the *Rinn Point Limestone Formation* (Graham, 1996). Shell debris and fusain litter the inclined strata, indicative of both a (near-)coast and a terrestrial sediment provenance. Low-density fusain settled from suspension from a basinward directed flow (receding tide). Shell debris may have been transported as bedload in a landward directed flow (rising tide). Additionally, brackish water conditions may have allowed some shell species to thrive *in-situ*.

Considering its stratigraphic proximity to tempestite deposits and calcareous marine deposits, IHS-D is interpreted as a point bar deposit in proximity to the estuary mouth. An alternative interpretation as a channel fill is rejected as the strata possess a depositional dip, accrete laterally and wedge out laterally (Figure 10A, laterally accreting to the left, wedging out to the right).

4.5. Floodplain facies association

4.5.1. FF-1: interbedded burrowed siltstones and sandstones

Beds of laminated siltstones alternate with beds of medium-grained, tabular cross-bedded sandstones (Figure 11A, B). Bed thickness and occurrence ratio of both lithologies varies throughout the section. Thin alternations with siltstone beds of 0.5 to 3 centimetres and sandstone beds of 2 to 5 centimetres thick have a siltstone/sandstone ratio of *ca.* 70/30. Conversely, thick alternations with siltstone beds of 5 to 12 centimetres and sandstone beds of 10 to 30 centimetres have an inverse siltstone/sandstone ratio of *ca.* 30/70.

Grey to dark grey siltstone is locally interspersed by 1-3 centimetre beds of medium-grained, parallel laminated sandstones that are laterally discontinuous over several metres. The base of these packages is usually draped over the underlying strata's palaeotopography.

Occasionally, plant debris of 1-4 centimetres in size is present in both siltstone and sandstone beds. *Chrondrites* trace fossils are frequently present in siltstones directly under the base of the sandstone beds (Figure 11B).

Locally the siltstone beds fine-up to carbonaceous mud of facies FF-4.

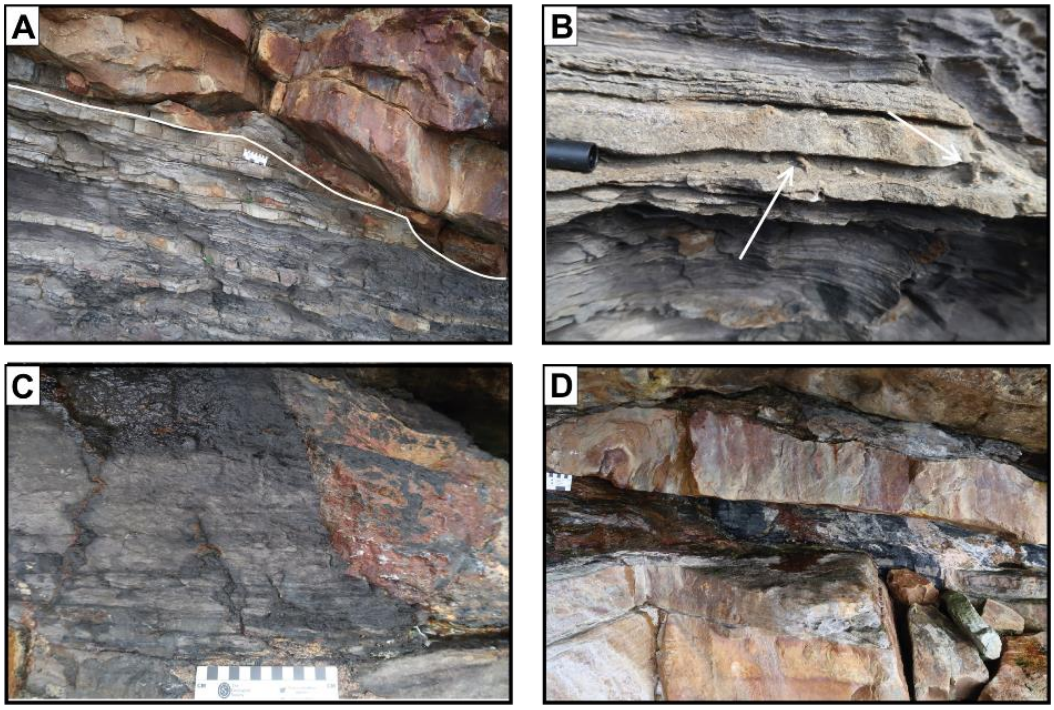

Figure 11: *(A) interbedded siltstone and sandstone of facies FF-1. Note erosive contact (marked white) with overlying amalgamated wedging sandstones of CH-2. Scale bar dash length is 1 cm; (B) detail of sandstone bed with Chrondrites trace fossils (white arrows) in FF-1. Pen cap is ca. 3 cm long; (C) Dark-grey shales of FF-2. Note the contrasting red weathering colour. Scale bar dash length is 1 cm; (D) Dark-grey shales of FF-2 interjected by wedging sandstone of CH-2. Scale bar dash length is 1 cm.*

4.5.2. FF-2: laminated siltstones

These dark-coloured laminated or locally structureless shales are draped over any underlying palaeotopography (Figure 11C). Occasionally interjected by 10-40 centimetre medium-grained, trough cross-bedded sandstones of facies CH-2 (Figure 12D). Infrequently, fine-grained sandstone beds of 1-5 millimetres intersperses the siltstone. These sands locally host *Chrondrites* trace fossils. Shell fragments 0.5-5 centimetres in size occasionally line the shales when in stratigraphic proximity to sandstones of the near-shore facies association (NS-1 or NS-2).

4.5.3. FF-3: fissile siltstones to mudstones

Siltstones locally grading to mudstones, both are fissile in structure and ichnologically barren (Figure 12A, C). These fine-grained deposits comprise 0.1-1 millimetre-scale laminae and are infrequently interspersed with laterally thinning 5-10 centimetre-thick beds of medium-grained sandstone with *Chrondrites*. Occasionally, 1-4 cm thick medium-grained sandstone lenses, 2-8 cm plant debris (Figure 12B) and 2-8 cm calcareous nodules are present.

4.5.4. FF-4: carbonaceous fissile mudstones and shales

This facies comprises fissile mudstones and 0.1-0.5 millimetres laminated siltstones, characterized mainly by their very dark colour (Figure 12C, E). Plant debris 0.5-3 centimetre is size is present (Figure 12D), as well as 1-2 centimetre coal seams.

4.5.5. FF-5: desiccated interbedded mudstones and sandstones

Beds of medium-grained sandstone, 10-30 centimetres thick, are interbedded with mudstone beds 8-15 centimetres in size. Mudcracks occasionally line the exposed sediment surface (Figure 12F).

Chrondrites trace fossils occur frequently throughout the beds, in both the siltstone as the sandstone. Discontinuous 2-4 centimetres thick coal beds of facies FF-4 are locally present in the siltstone beds.

Interpretation

This dominantly fine-grained facies association is thought to represent floodplain deposits of varying proximity. FF-5 and FF-1 to FF-4 describe a gradient from proximal to distal floodplain sediments (Figure 16).

The most proximal deposits comprise FF-1 with laterally continuous sandstone beds deposited during bankfull conditions and silts falling out of suspension when flow subsides. *Chrondrites* trace fossils suggest periods of stasis under (frequently) sufficiently wet and moist, waterlogged conditions (Buatois and Mángano, 2002; Baucon et al., 2014). Sustained submerged conditions were likely as escape burrows underneath the sand beds indicate live burrowing organisms up until the next bankfull flood or crevasse splay.

A similar ratio of siltstone and sandstone is recorded in FF-5, implying a comparable position on the floodplain as FF-1. However, emergence is recorded in FF-5, as is a greater organic content reflected in the presence of coal seams. FF-5 is on a similar position in the proximal to distal gradient as FF-1, although slightly more secluded or elevated resulting in emergence and colonization by vegetation.

Increasing in siltstone content, FF-2 represents a more distal position on the floodplain. Discontinuous sandstone beds could represent distal crevasse splays, where flow turbidity has waned enough for organised beds to develop (Fielding, 2006), but proximal enough to keep fines in suspension. Local occurrence of shell fragments indicates a position in the marine-influenced part of an estuary.

The fissile siltstone and mudstone of FF-3 records a more distal position still. Infrequent interjection of sandstone (lenses) is ascribed to a similar mechanism of exceptional bankfull discharge, or distal reached of a crevasse splay. The presence of calcareous nodules is not well understood. Davies and Gibling (2003) ascribe calcareous nodules in their Carboniferous alluvial siltstones to well-drained conditions, though without elaborating any mechanism for calcareous nodule formation.

FF-4 is interpreted as a very distal floodplain considering the (very) fine-grained nature of the deposits. The abundant presence of clays is reflected in the fissile structure of these deposits, indicative of the very distal position on the floodplain. High organic content yields the very dark discolouration of the mudstone and is underpinned by the presence of plant debris and 1-2 centimetre thick coal seams. A proximal mire or swamp interpretation is rejected as this facies lacks thin beds of sandstone indicating (seasonal) floods.

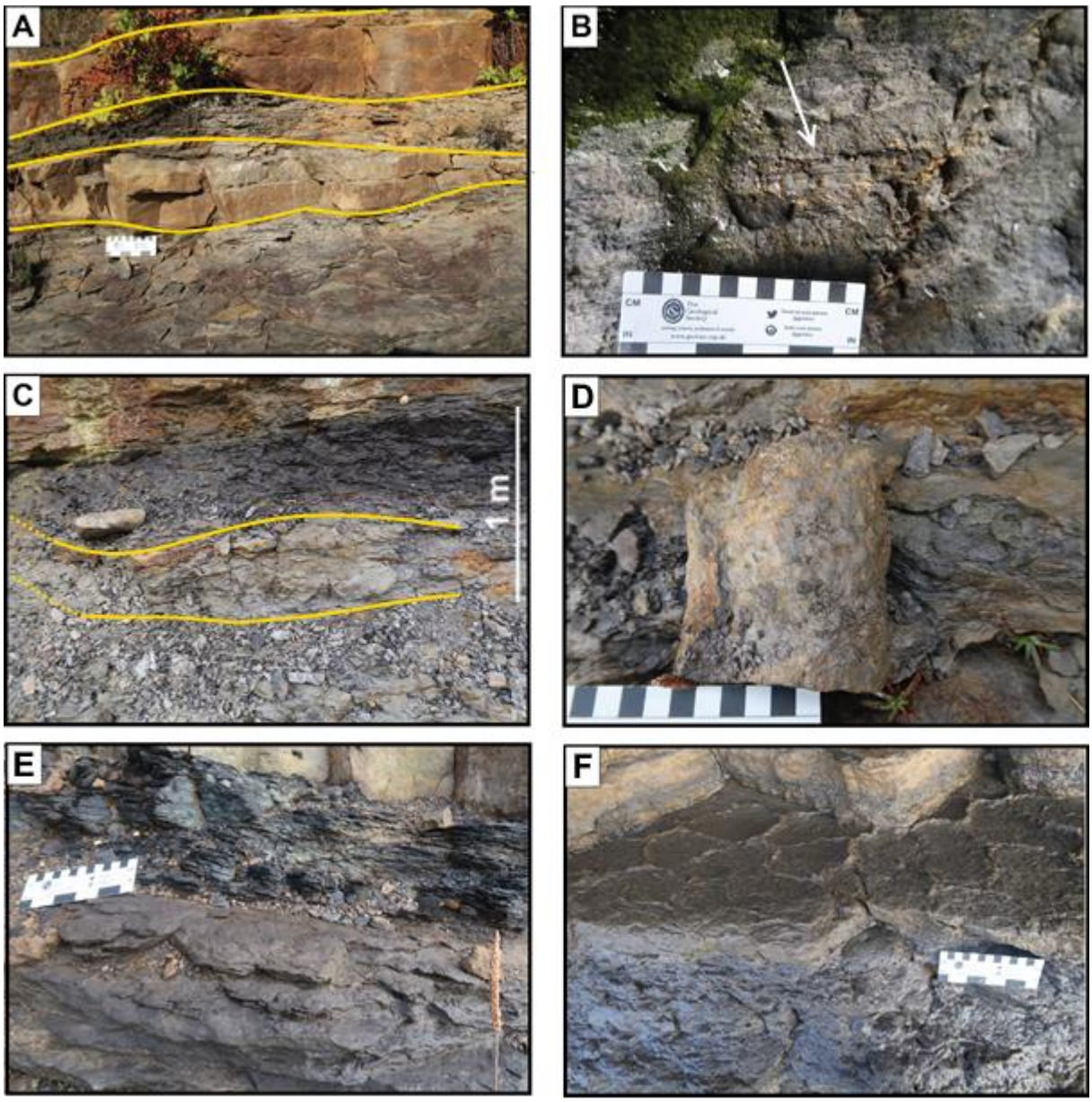

Figure 12: *(A) Grey siltstone of FF-3 interjected by wedging sandstone of CH-2 (yellow outline). Note upward grading to fissile siltstone above the interjection. Scale bar dash length is 1 cm; (B) Plant debris (white arrow) in grey siltstones of FF-3. Scale bar dash length is 1 cm. (C) shales grading to fissile mudstone of facies FF-3, interjected by 5-10 cm discontinuous fine-grained sandstone (yellow outline); (D) Lepidodendron fossil in fissile mudstone of facies FF-4. Scale bar short dash length is 1 cm; (E) fissile mudstone grading up to carbonaceous of facies FF-4. Scale bar dash length is 1 cm; (F) desiccation cracks on outcrop surface in mudstone of FF-5. Scale bar dash length is 1 cm.*

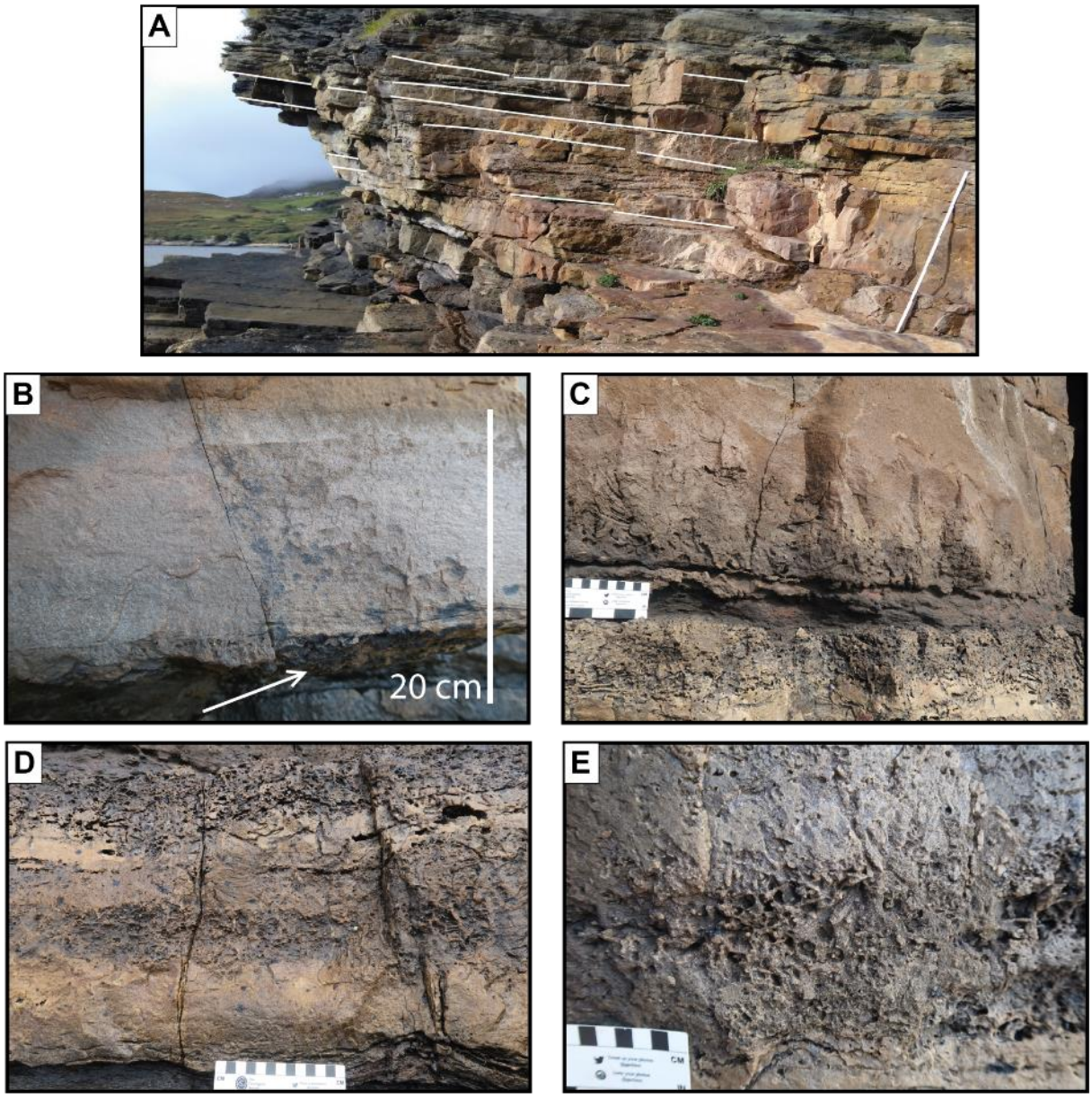

Figure 13*: (A) View on successive tabular sandstones of NS-1. Note lateral variation above measuring stick between tabular sandstone beds of NS-1 (left, highlighted white) and interbedded sand- and siltstones of FF-1. Measuring stick 1 metre long; (B) Detail of barren medium-grained sandstone of NS-1. Chondrites ichnofauna localized at base of bed (white arrow); (C) Detail of sandstones of NS-1 with Chondrites ichnofauna along bounding surfaces. Note siltstone veneer separating beds. Scale bar dash length is 1 cm; (D) Detail of sandstones of NS-1 with Chondrites ichnofauna localized along bounding surfaces not highlighted by siltstone veneer. Scale bar dash length is 1 cm; (E) Detail of sandstone of NS-1 with pervasive Chondrites ichnofauna. Scale bar dash length is 1 cm.*

4.6. Near-shore facies association

4.6.1. NS-1: tabular sandstones with varying degree of burrowing

Medium-grained, tabular sandstone organised in beds of 10-40 centimetres thick (Figure 13A). Cross-bedding and planar lamination are abundant in sections which lack *Chrondrites* (Figure 13B). Such trace fossils, when present, line connecting bounding surfaces (Figure 13C, D), and can be occasionally pervasive throughout a bed (Figure 13E). Locally, bounding surfaces are draped by a 1-3 centimetre veneer of siltstone. A dune-like palaeotopography is preserved on planform exposures, locally accentuated by a 1-3 centimetre veneer of wavy siltstone.

Interpretation

Planar cross-stratification and frequent planar lamination in these sandstones indicate upper flow regime conditions (Fielding, 2006). Considering the tabular nature of the sandstone beds, these sediments are interpreted as compound dunes and upper flow regime deposits in a nearshore setting (*e.g.* sand flats at the seaward end of an estuary (Dalrymple et al., 1992). *Chrondrites* trace fossils at bed bounding surfaces indicate periods of stasis between deposition of subsequent beds. Prolonged stasis is recorded in pervasively burrowed beds.

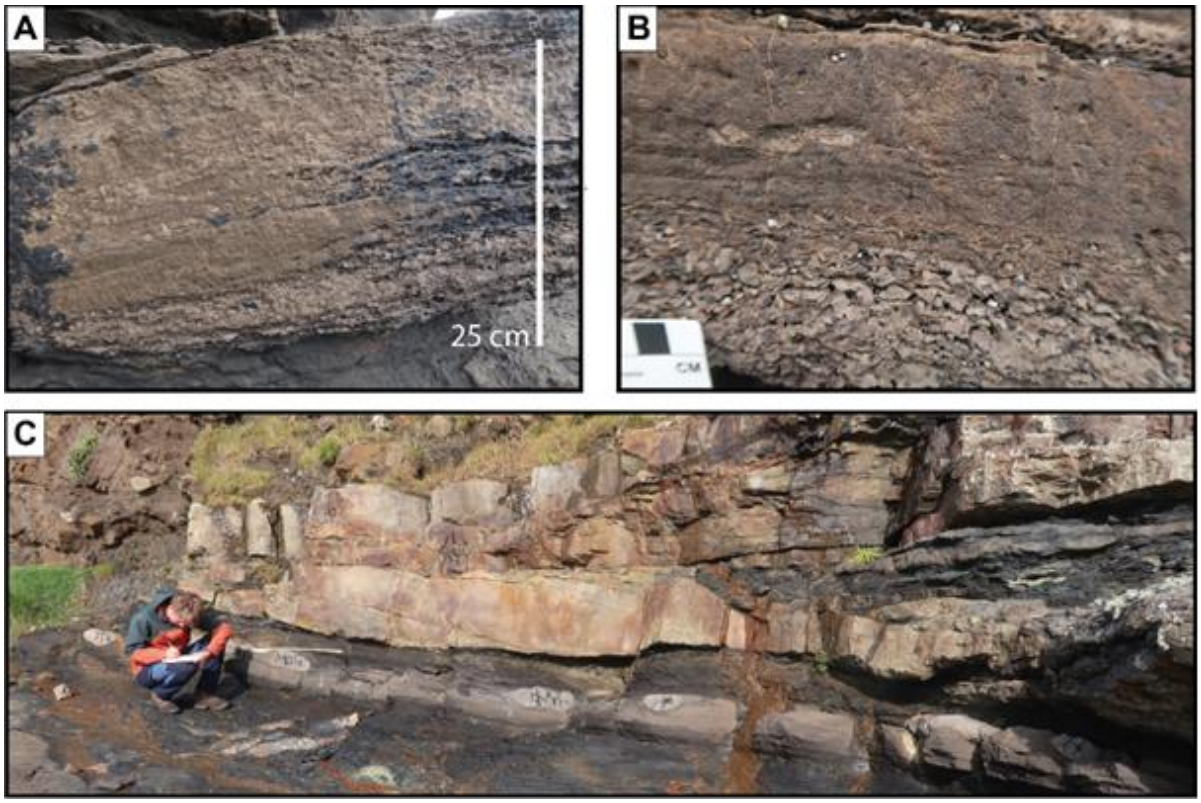

Figure 14: *(A) View on bioclastic sandstone of NS-2. Note elongated sandstone lens between coarse-grained beds; (B) Detail of sandstone lens interface with bioclastic beds. Note frequent presence of shell fragments within sandstone lens. Scale bar dash length is 1 cm; (C) View on laterally continuous limestone of NS-3, at knee height of crouched geologist. Fossiliferous limestone is interspersed by calcareous nodules. Crouched height of geologist ca. 120 cm.*

4.6.2. NS-2: laterally discontinuous shell-bearing sandstone

These medium-grained sandstones displaying tabular cross bedding are occasionally lined with 1-3 millimetre shell fragments (Figure 14A, B). Fusain debris 2-5 centimetres in size is also locally present. The sandstones are organised in *ca.* 10 centimetre thick beds. The package thins laterally over the course of tens of metres. Cracked limestone nodules approximately 8-15 centimetres in size locally deform sediments.

Interpretation

Inclined planar cross-stratification and frequent planar lamination in these sandstones indicate upper flow regime conditions (Fielding, 2006; Plink-Björklund, 2005; Dalrymple et al., 1992). Considering the tabular nature of the sandstone beds, these sediments are interpreted as compound dunes deposits. Similar to NS-1, the inclined planar cross-stratification and frequent planar lamination in these sandstones indicate upper flow regime conditions during time of formation (Plink-Björklund, 2005; Dalrymple et al., 1992).

Occurrence of shell fragments and fusain debris point to bidirectionality in currents, as fusain debris is sourced from the hinterland while shell fragments are likely washed in from the sea, although shell species may have thrived locally in brackish-water conditions. A small tidal channel interpretation is favoured, with channel margins no more than a few tens of metres apart.

4.6.3. NS-3: fossiliferous wackestone

This facies sees laterally continuous beds of mud-supported gastropod fossil-bearing wackestone (Figure 14C). Cracked limestone nodules 10-40 centimetres in size are present locally, deforming the surrounding strata.

Interpretation

These wackestones are interpreted to have formed in a near-shore, shallow setting (Singh and Andotra, 2000), likely in a (small) secluded, shallow lagoon or lake with negligible clastic sediment supply.

4.7. Event facies association

4.7.1. EV-1: wavy and chaotic medium- to coarse-grained sandstone

This medium to coarse-grained structureless sandstone facies is organised in chaotic, wavy beds 5 to 30 centimetres in size (Figure 15A), thinning and locally fining laterally over the course of several metres. Underlying strata display sandstone-filled *Chrondrites* burrows (Figure 15C). Siltstone lenses and plant debris (Figure 15B, C) 1 to 6 centimetres in size frequently line the sediments. Beds are typically topped with a siltstone veneer. 1 to 3 centimetre sized shell fragments occur locally.

Interpretation

The chaotic, structureless sandstones littered with plant and shell debris likely record crevasse splay elements (Burns et al., 2017, 2019). The presence of both plant debris and shell fragments likely reflect terrestrial but brackish conditions in the parent channel. Alternatively, shell fragments were previously washed landward from the sea and subsequently reworked to be deposited in this crevasse splay element.

4.7.2. EV-2: bioclastic sandstone

This diverse facies comprises a poorly sorted medium to coarse-grained sandstone mired in 1-5 centimetre sized fragments of gastropods, bivalves and other undetermined bioclasts. The *ca.* 80 centimetre package is organised in *ca.* 10-30 centimetre thick beds that fine upwards. Pervasive shell fragments and bioclasts line the base of the bed, gradually reducing in number upwards until their disappearance approximately halfway up the bed, where the medium to coarse-grained sand dominates. The top of the bed is draped by wavy fine to medium-grained sandstone laminae several millimetres in thickness. Locally lenses 2-10 centimetres in size of millimetre-scale laminated very fine sand are present.

Interpretation

These bioclastic sandstones reflect high-energy deposits, with gastropod, bivalve and other bioclasts washed in from the sea landwards during storm conditions. Considering their stratigraphic proximity to pervasively burrowed sandstones (NS-1) and other shell-bearing strata (NS-2), these tempestites are interpreted to have formed in the mixed-energy or tide-dominated part of an estuary.

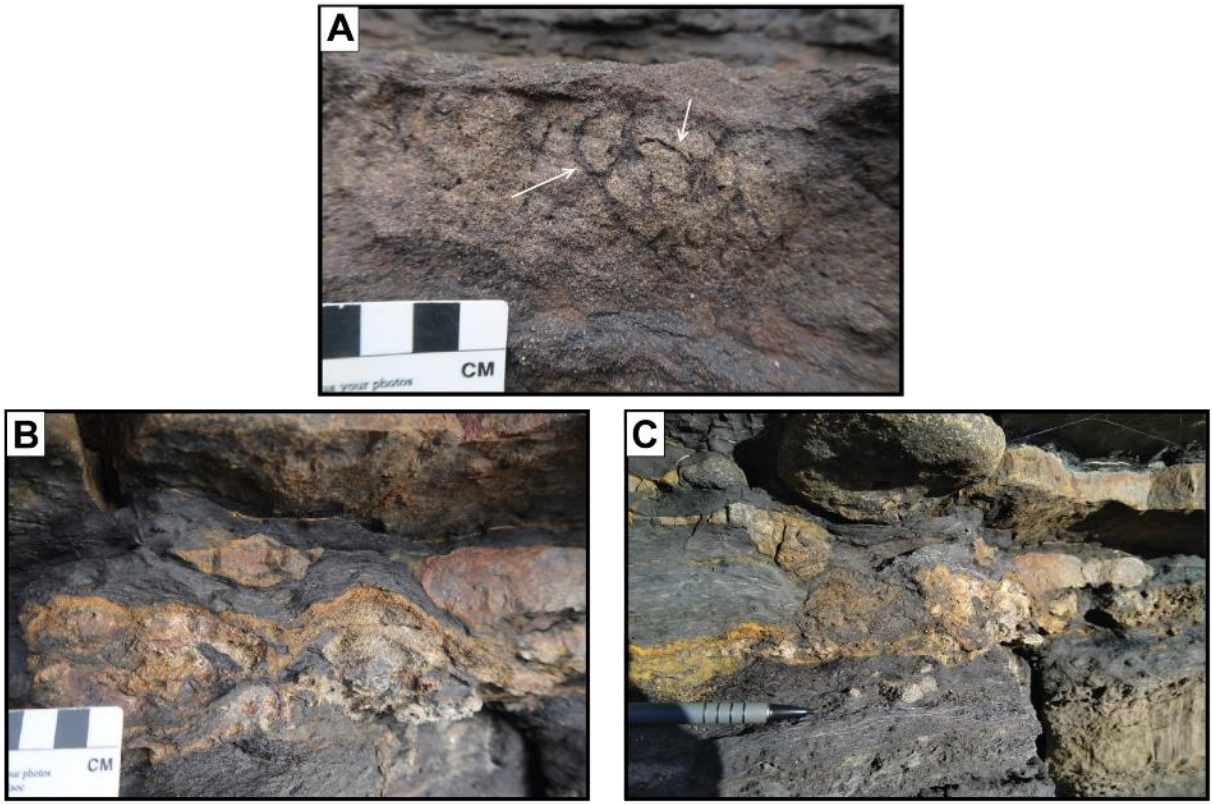

Figure 15: *(A) Detail of plant imprints in wedging coarse-grained sandstone in EV-1. Scale bar dash length is 1 cm. (B) chaotic, wavy siltstone lined with plant debris and frequently interspersed by sandstone lenses of facies EV-1. Scale bar dash length is 1 cm; (C) Detail of discontinuous sandstone lenses interspersing wavy siltstones of facies EV-1. Note sandstone-filled Chondrites ichnofauna right of pencil tip. Visible part of pencil is ca. 8 cm long.*

5. Environmental summary

The 93 studied metres of the strata exposed at Shalwy Point record a transition from an alluvial, fluvially dominated realm to an overall marginal marine environment.

Following the estuary classification of (Dalrymple et al., 1992), the succession is crudely partitioned into: 1) a fluvial zone; 2) a fluvially dominated but tidally influenced zone; 3) a mixed-energy zone; and 4) a tidally dominated but fluvially influenced zone. The following section summarizes the approximate position of the identified facies within this partitioning (Figure 16), and draws a comparison between estuary stratigraphy and estuary planform.

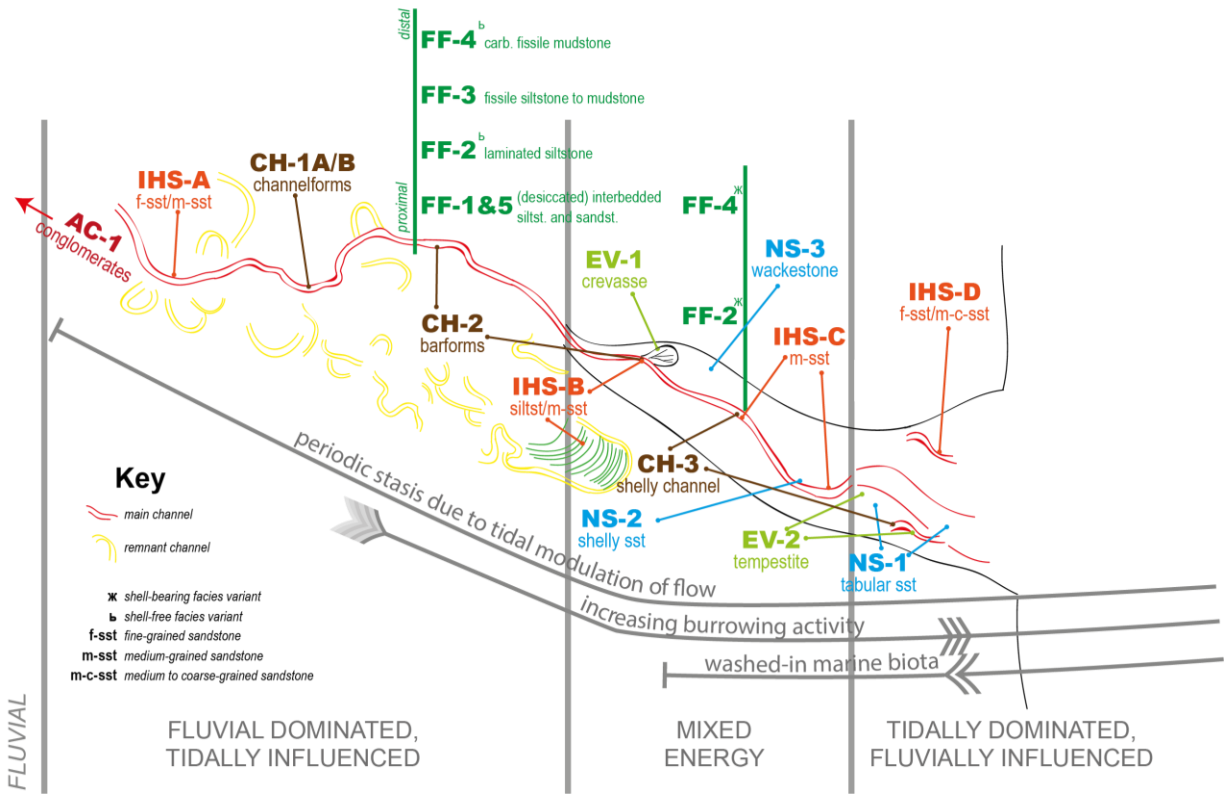

Figure 16: *Schematic representation of the approximate location of the identified facies in an idealized estuary. The text colours of the facies codes correspond to the colour groups in the sedimentary logs of Figure 3.*

5.1. Facies in estuary zones

Coarse-grained conglomerates of facies AC-1 mark the start of sedimentation in the basin with alluvial fans covering the Dalradian schist basement.

Fluvial processes gained dominance with channel sandstones (CH-1A/B), siltstones (FF-1 to FF-3, FF-5) and shales (FF-4) recording fluvial channels, bars (CH-2) and floodplains. Laterally extensive outcrops of channel sandstones (CH-1A) and packages of IHS (IHS-A) reflect sinuous, meandering channels that are laterally mobile (Thomas et al., 1987). Isolated channel sandstones (CH-1B) may be reflective of chutes. Minor burrowing activity reflects periods of stasis. Periods of stasis may have been sanctioned by tidal modulation of flow, waning flow sufficiently to provide a temporal window for sedimentary non-deposition. Siltstone drapes record a similar tidal modulation, waning flow to allow for the settling of silts. Channel deposits, floodplain deposits and packages of IHS contain plant debris and are free of shells or calcareous debris indicating the net sediment transport direction was basinward.

Increasing abundance of burrowing activity and incoming marine fauna mark the mixed-energy part of the estuary. Sinuous channels were still widespread in this part of the estuary as recorded by shell-bearing channel sandstones and barforms (CH-2, CH-3) and by packages of IHS (IHS-B, IHS-C). Flanking these channels were (very) fine-grained floodplains and mudflats (FF-2, FF-4). In small, secluded lagoons fossiliferous wackestone formed (NS-3).

Tidal dominance is reflected in high-energy deposits such as upper flow regime tabular sandstones (NS-1) and tempestites (EV-2). Relatively little mudrock is present in this part of the estuary. Packages of IHS (IHS-D) reflect sinuous channels, likely in a relatively secluded position close to the margins of the estuary mouth. Extensive deposits of fusain in IHS-D reflect wildfire events in the hinterland.

5.2. Meander bend migration recorded in IHS coset trends

Small-scale autogenic variability may be recorded in accretional features in a sedimentary system, such as in point bar deposits reflected in packages of IHS. In the following section a conceptual model is presented of how lateral meander bend migration may be recorded as a subtle grain size trend in the cosets of a single package of IHS, such as the coset grain size trend observed in IHS-B. Superimposed on the siltstone and medium-grained sandstones alternations of IHS-B is an overall 'set' fining upward trend. That is, the relative thickness of siltstone sets in these alternations increases going up in the IHS package (Figure 8). This trend may be expounded by variation in flow conditions on the scale of the meander bend resulting from autogenic meander bend migration, but may also be an artefact of the angle of outcrop cut relative to the original planform (Figure 17).

The migration of a meander bend produces a series of point bar deposits that accrete in the migration direction of the bend and are displayed in outcrop as IHS cosets. During the deposition of a single set a downstream fining trend governed spatial grain size distribution on the point bar: coarser-grained sediments were deposited on the upstream part of the point bar and finer-grained sediments on the downstream part (Jackson, 1976; Smith et al., 2009).

Laterally accreting point bars form in meander bends and may migrate (1) laterally parallel to the bend axis; (2) laterally parallel to the bend axis and in the downstream direction; or (3) laterally parallel to the bend axis and in the upstream direction (Figure 17) (Thomas et al., 1987). An outcrop cut through a series of point bar cosets may display a 'set' fining upward or coarsening upward trend if the outcrop cut is oblique to the direction of meander migration.

For example, a stationary spectator observes a meander bend from the position of the bend axis (convergence point of red lines in Figure 17). The meander bend migrates both laterally and in the upstream direction and produces a series of point bars with the locus of coarse-grained sediment deposition shifting upstream relative to the stationary spectator. If the spectator would make an outcrop cut parallel to the original bend axis, that is, straight to the opposite channel bank, a 'set' fining upward trend would be laid bare.

The 'set' fining trend observed in IHS-B could represent a similar case, with a meander bend migrating laterally and upstream. However, underdetermination hampers drawing such conclusions as it is not possible in the studied succession to ascertain what angle the outcrop cut makes with respect to the original planform of the meandering channel. Additionally, the outcrop likely cuts over the point bar in a random direction, rather than originating from the stationary spectator's position. Multiple exposures of the same series of accreted point bars would be required to determine the relative angle between exposures and through this infer the most likely scenario for meander bend migration.

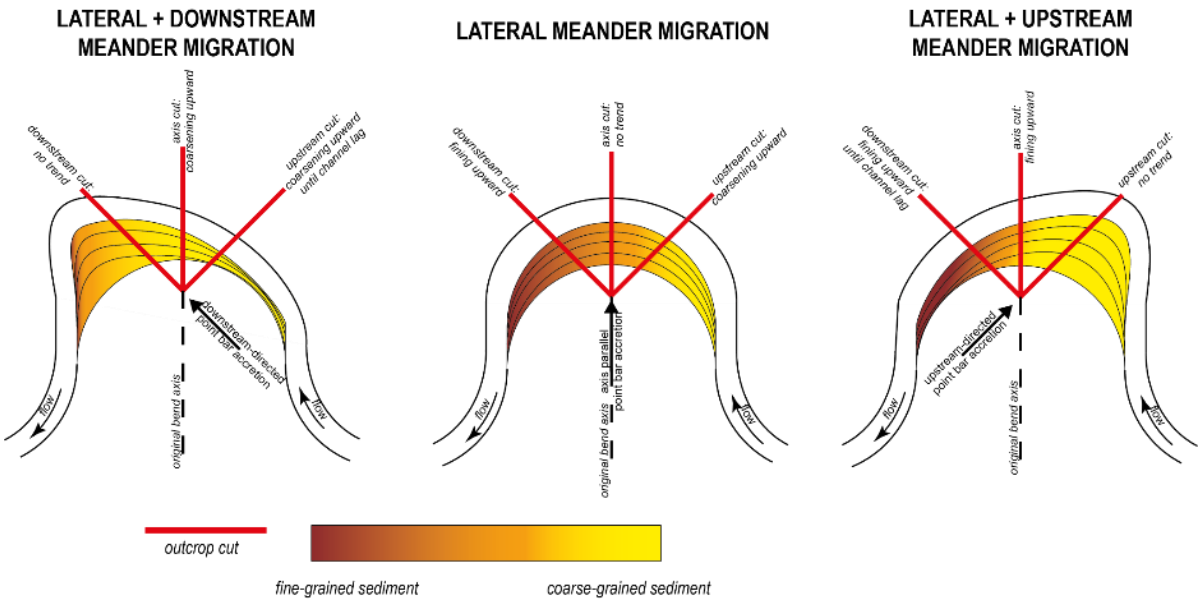

Figure 17: *Schematic representation of set grain size trends observed in IHS outcrops in three meander migration scenarios and under three modes of outcrop cuts.*

6. Signatures of vegetation

Vegetation has a greatly influences processes at play on the Earth's surface (Istanbulluoglu and Bras, 2005). The primary aim of the present study is to identify the sedimentary signature of vegetation in the studied estuarine succession. What tangible geological evidence in the studied succession points to vegetation affecting sedimentary processes? And, as evolutionary stages in the development of plant life are found to coincide with the proliferation of distinct types of fluvial morphology and sedimentary architecture (McMahon and Davies 2018b), how does the signature of vegetation in the studied succession compare to that of estuaries in other geological periods?

The Middle Mississippian age of the studied succession in Ireland puts it in a context of significant and steadily increasing impact of vegetation on the geomorphic landscape, (global) climate and the morphodynamics of rivers and estuaries. However, the studied succession is from before the 'vegetation apex' of the Pennsylvanian, when equatorial wetlands were extensive and coniferophytes occupied upland and dryland environments (DiMichele et al., 2010). Nonetheless, the geomorphic landscape in which estuaries occur, coastal plains, was profoundly vegetated by the Middle Mississippian (Decombeix et al., 2011; Boyce and Lee, 2017).

The coming section considers the sedimentary signature of vegetation in the studied succession and is followed by a comparison with estuarine successions from other geological periods through a literature survey. This literature survey may distil a trend in presence and abundance of key sedimentary features co-eval with major steps in the evolution of terrestrial flora.

6.1.1. Equifinality and underdetermination

Drawing conclusions on the effects of biology on sedimentary processes and its products in geological outcrops is hampered by underdetermination and equifinality (Davies et al., 2020).

Underdetermination is a phenomenon referring to situations often found in Earth science, where lines of evidence are not sufficient to ascertain which explanation from a plural of possibilities is the true cause of the observed feature (Kleinhans et al., 2005).

Equifinality is the concept that end-states can potentially be explained by various causes (Beven, 1996). The signature recorded in stratigraphy. in beds and outcrops. is essentially an end-state relative to the depositional conditions (Davies et al., 2019) and many sedimentary signatures can have a multitude of possible forming mechanisms, both biotic and abiotic. Research on the perceived likelihood of a biotic origin of certain sedimentary signatures helps observers interpret ambiguous sedimentary signatures in outcrops (Davies et al., 2020).

Additionally, estuaries are complex systems. This complexity is reflected in the diversity of facies in the studied succession, recording starkly contrasting morphodynamic conditions. Laterally shifting environments within an estuary over geological time render estuaries autogenically highly variable systems. This introduces a degree of uncertainty to studying estuarine outcrops that is not present in modelling studies that provide a planform view over long timescales (Braat et al., 2017).

However, despite the challenges underdetermination, equifinality and complex estuaries pose, there are numerous signatures of vegetation observed in the studied succession.

6.1.2. Signatures of vegetation in studied succession

Davies et al. (2020) provide a comprehensive overview of the numerous signatures of biology in the Earth's sedimentary record of fluvial environments, listing features in outcrops ascribed to the result of microbiota, fauna and flora altering sedimentary processes.

Davies et al. (2020) draw a subdivision of the signatures of biology in the sedimentary record between (1) biologically dependent signatures (BDS) and (2) biologically influenced signatures (BIS). Biologically dependent signatures are those that can unequivocally be ascribed to biological activity, while biologically influenced signatures are those most likely ascribed to biological activity but can have alternative abiotic explanations. Davies et al. (2020) elaborated how life alters sedimentary processes and their products in the sedimentary record of alluvial environments.

This study explores what features listed by Davies et al. (2020) are observed in the estuarine setting of the studied succession and how vegetation made an impact. Focus is on the impact of vegetation as terrestrial flora, presently occupying *ca.* 87% of the Earth's total biomass (Bar-on et al., 2018), are powerful ecosystem engineers. Whilst the studied succession hosts ichnofauna, fossil-bearing limestone and shell-debris, the focus of this study is on the role of plants as ecosystem engineers.

6.1.2.1. Root structures (BDS)

Root structures are present in the studied succession as oxidized rhizoliths (Hillier et al., 2008). Plant roots stabilize sediments, promote bank stability and limit reworking in fluvial settings. (Kleinhans et al., 2018; Davies et al., 2020).

In studied succession

Root structures have been observed in two facies in the studied succession: in proximal floodplain sandstones (Figure 18A) and in distal floodplain siltstones, both within the fluvial parts of the succession.

The sediment stabilizing effect of plant roots noted in fluvial environments (Davies et al., 2020) is argued to be similar in estuaries. The notable lack of abundantly preserved root structures in mixed-energy zones of the estuarine succession likely reflects their poor preservation potential due to their susceptibility to autogenic reworking and post-depositional oxidization, rather than a scarcity of plant (roots) in the palaeolandscape.

6.1.2.2. Fusain (fossiliferous charcoal) (BDS)

Fusain (fossiliferous charcoal) is the product of the combustion of plant material, typically by wildfires (Glasspool et al., 2004). Their existence directly relies on the presence of vegetation, providing fuel, and relies indirectly on vegetation as an agent for an oxygenated atmosphere (Diessel, 2010). The Carboniferous in particular was marked by high atmospheric oxygen levels, 22% by the Viséan (*ca.* 350 Ma) and reaching 32-35% by the end of the Pennsylvanian (*ca.* 300 Ma) (Scott and Glasspool, 2006). Incidence of wildfires increased concomitantly (Falcon-Lang, 2000).

In studied succession

Extensive deposits of fusain have been observed in the package of inclined heterolithic strata (Figure 10B, Figure 18B) in the tidally dominated part of the succession, where fusain fragments several centimetres in size are present in a matrix of siltstones and sandstones. Being the product of wildfires (Glasspool et al., 2004), fusain has a terrestrial provenance. Its presence

in the tidally-dominated part of the succession (IHS-D, section 4.4.4, page 34) is thus indicative of a basinward component of sediment transport in the tidally-dominated reaches of the estuary.

Although the presence of fusain is evidence for wildfire events, which drastically change the geomorphic landscape and promote surface runoff (Falcon-Lang, 1998), the fragments themselves behave as clasts under the principles of particle-motion physics (Clark, 1988) and do not alter sedimentary processes or their products. Contemporaneous charcoal fragments are initially transported in suspension owing to their low bulk density, but are gradually transported as bedload as the fragments become more waterlogged (Skolnick, 1958).

Wildfires strip the ground surface of vegetation, promoting surface runoff and sediment load by rill and gully erosion (Benda et al., 2003). The enhanced sediment supply following wildfire events has been associated in modern environments with river terrace construction (Benda et al., 2003), mass failure through the loss of sediment-stabilizing root networks (Mills, 1989) and unusually high water levels as the water buffering effect of vegetation (peat bogs in particular) is diminished (Johnson, 1984).

For the fusain-rich packages of IHS at the top of the studied section (facies IHS-D, Figure 10), the present author concurs with Nichols et al. (1992). These authors associate the enhanced sediment supply following the palaeowildfire to the relatively poorly-sorted nature of the packages of IHS and their draping over underlying bedforms.

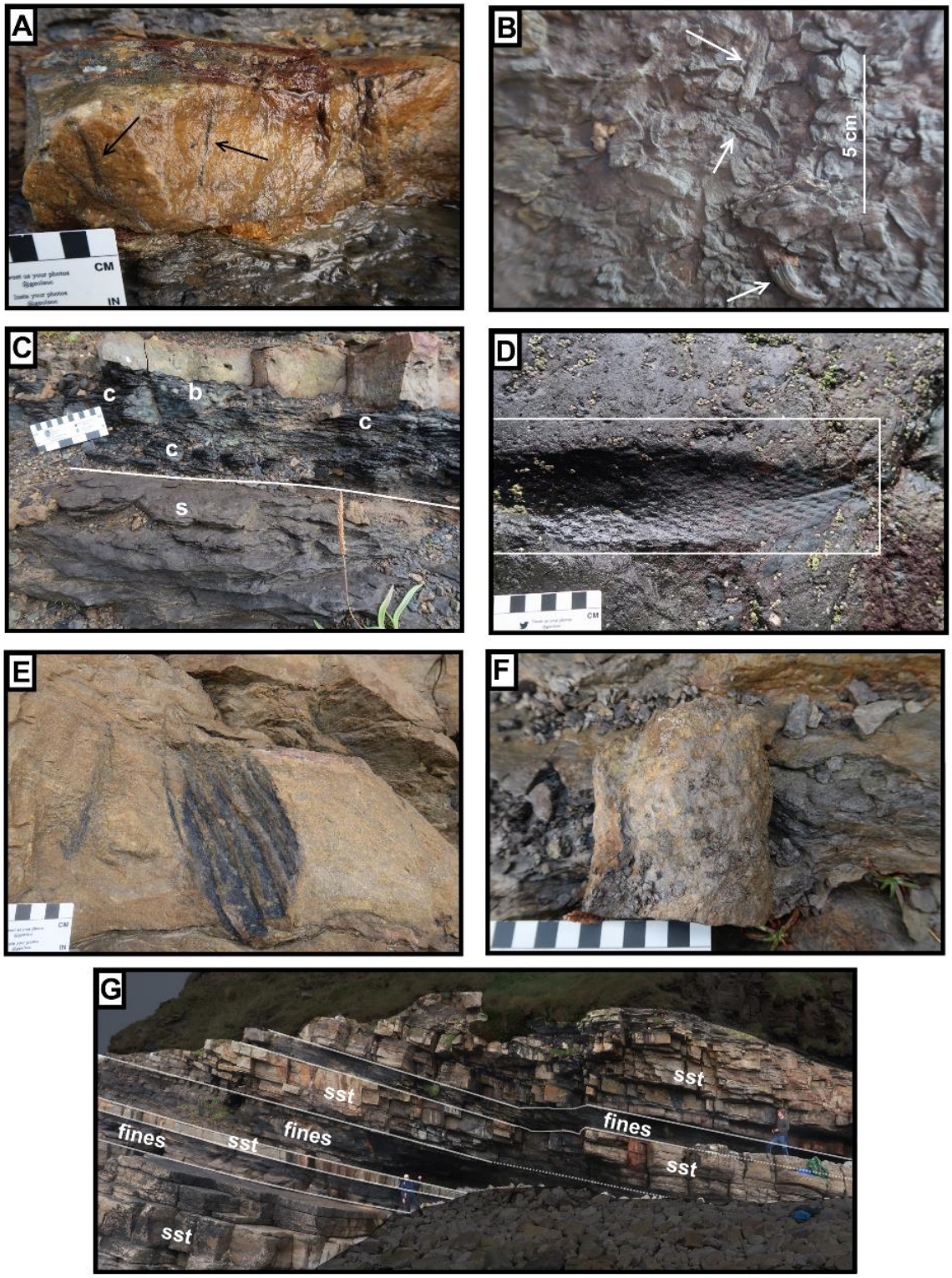

Figure 18*: (A) black arrows indicate root structures in a bed of sandstone in proximal floodplain facies FF-1; (B) fragments of fusain (charcoal) in a fine-grained sandstone matrix in facies IHS-D. White arrows indicate fragments with recognizable woody texture; (C) carbonaceous mudrock (c) overlying shales (s) in distal floodplain facies FF-3 and FF-4. Note Chrondrites burrows (b) at top of mudrock package; (D) imprint of Lepidodendron fragment; (E) imprint of plant debris in proximal floodplain facies FF-1; (F) woody debris in siltstones of proximal floodplain facies FF-3; (G) exposure of alluvial mudrock and siltstone (fines) contrasting sandstones (sst). Both geologists ca. 185 cm tall. A, C, D, E, F: scale bar dash length is 1 cm.*

6.1.2.3. Carbonaceous muds and coal seams (BDS)

Coal seams and pre-cursor lithology carbonaceous mudrock are formed by an accumulation of organic debris that compacts and (partially) coalifies (Nelsen et al., 2016), with woody vegetation primarily associated with coal. Sufficient areal extent of vegetation, particularly woody trees, is required to accumulate ample organic matter to form carbonaceous mudrock and coal seams (Davies et al., 2019).

Conditions in the near-shore parts of estuaries would be too dynamic to allow for sufficient areal extent (Braat et el., 2018; Lokhorst et al., 2018). Calm, waterlogged environments such as oxbow lakes, wetlands and poorly-drained floodplains produce conditions for the formation of coal and are generally found in fluvial or fluvio-deltaic settings (Braat et al., 2017; Lokhorst et al., 2018).

Carbonaceous mudrocks first start to develop in the Early Devonian (Kennedy et al., 2013), with coal appearing in the Middle Devonian (Kennedy et al., 2013), before rapid proliferation during the Carboniferous (Boyce and Lee, 2017).

In studied succession

Coal seams and carbonaceous mudrocks (Figure 12E, Figure 18C) occur primarily in the fluvially-dominated zone and to a limited extend in the mixed-energy zone of the succession. The two lithologies are directly dependent on the presence of vegetation, as coal would not develop without (woody) vegetation.

In fluvial environments, the areal extent offered by wide floodplains allows for sufficient dispersal of vegetation. Tidal dynamics in the near-shore reaches of the estuary limit development of extensive vegetated floodplains and mudflats (Lokhorst et al., 2015), prohibiting the formation of carbonaceous mudrocks and coal seams.

Before the proliferation of woody vegetation, the landscape was covered by non-woody vegetation. Woody vegetation alters morphodynamics through the introduction of sturdy, woody debris that form obstacles for flow. The effects on fluvial and estuarine morphodynamics in the transition to a landscape covered by woody vegetation is argued to have been subtle compared to the profound impact on fluvial and estuarine morphodynamics of the introduction of vegetation to a barren landscape.

6.1.2.4. Plants impressions and woody debris (BDS)

Plant casts (Figure 18D, *Lepidodendron*), plant carbonaceous impressions (Figure 18E) and woody debris (Figure 18F) form the clearest recorders for the presence of vegetation in the (hinterland of) the studied succession. Large woody debris encourages channel switching through avulsion by reducing or blocking streamflow (Davies et al., 2020).

In studied succession

Plant impressions and woody debris are observed in the fluvial-dominated and mixed-energy parts of the studied succession. These features are observed out-of-situ in channelized sandstones and both out-of-situ and in-situ in proximal floodplain deposits.

Despite being clear recorders of the *presence* of vegetation, plant impressions and woody debris alone do not record the effects of vegetation on sedimentary. Recognition of, for example, streamflow blockage by large woody debris is ambiguous as such conclusions are hampered by underdetermination. That is, the observation of woody debris implies nothing else than mere presence of it, unless it is found within a channel accompanied by other debris blocked by the obstruction and is found adjacent to a channel the streamflow avulsed to.

Nevertheless, terrestrial plants are important ecosystem engineers and evidence for their presence in the form of plant impressions and woody debris is indicative that plants have played a role in the studied system.

6.1.2.5. Alluvial mudrock (BIS)

Alluvial mudrocks are deposits of fine-grained sediments in an alluvial setting. The deposition of clay to silt-sized sediments in alluvial settings is promoted twofold by land plants: (1) catchment-wide by the promotion of chemical weathering and mud production in conjunction with fungi (Davies, 2017, 2019; McMahon and Davies 2018a, Fischer, 2018), and (2) locally by the capture of suspended fines through baffling surface water flow and below-ground stabilization through rooting (Gurnell, 2014).

In studied succession

Alluvial mudrock (Figure 18G) comprise *ca.* 16 % of the studied succession (Figure 2) and occur in the fluvially-dominated, mixed-energy and the marine-dominated parts of the succession. As discussed previously (section 1.4, page 10), the hinterland of this Carboniferous estuary must have been densely vegetated and thus provided ample supply of very fine-grained sediment. Within the estuary, observed plant roots indicate the presence of vegetation that aided capture of muds.

6.1.2.6. Channel-form deposits and lateral accretion sets of inclined heterolithic strata (BIS)

Vegetation impedes the formation of wide, sheet-like flows. Rather, flow tends to coalesce into streams when vegetation stabilizes floodplain sediments, restricting sediment winnowing by aeolian and fluvial processes (Kleinhans et al., 2018). Such streams produce channel-form bodies of sediment, as opposed to wide, tabular bodies of sediments in a barren geomorphic landscape (Davies et al., 2020). Evidence for meandering behaviour of channels is recorded in packages of inclined heterolithic strata organised in lateral accretion sets (Long, 2011; McMahon and Davies, 2018a).

In studied succession

Two contrasting types of channels are recorded in the stratigraphy of the studied succession: (1) channels migrating laterally over several tens of metres, producing wide channel-form sandstone deposits (facies CH-1A, Figure 5A), and (2) relatively static channels, reflected in stratigraphy as isolated channel-form sandstone deposits (CH-1B, Figure 5B). The presence of vegetation in the Carboniferous geomorphic landscape has limited the lateral extent of surface flow, resulting in channelization of flow into laterally mobile channels (Davies et al., 2020). The lateral mobility of channels may be further restricted by types of vegetation that are very effective at retaining muds, such as herbs, grasses and shrubs which evolve by the Cretaceous. The effects of these types of vegetation on channel mobility is discussed in section 7.4, page 61.

Four packages of IHS are observed in the studied succession (Figure 8), in the fluvially-dominated, mixed-energy and marine-dominated parts. In conjunction with (laterally extensive) channelized sandstone bodies (facies CH-1A/B) these packages of IHS record the presence of meandering channels throughout the estuary.

Packages of IHS also are observed in the tidally-dominated parts (IHS-D), despite tidal dynamics in the tidally-dominated part of the estuary preventing the formation of extensive

vegetated areas and thus limiting the capture of cohesive sediments (Lokhorst et al., 2018). The presence of meandering channels could also be expounded by abiotic deposition of mud on the tidal flat during slackwater periods in tidal cycles; a mechanism very conceivable in the tidally-dominated parts of an estuary.

7. Ancient estuary database

In an effort to distil a trend through geological time in the presence and abundance of key sedimentary features in estuarine successions co-eval with the evolution of terrestrial flora, a literature survey was set up comprising 19 Cambrian to Cretaceous-aged (541 – 66 Ma) estuarine successions. Major steps in terrestrial flora evolution occur in this timeframe (see section 1.3, page 9), such as the Silurian-Devonian development of vascular plants and the Devonian onset of deep-rooting (Boyce and Lee, 2017).

The presence of packages of IHS and the relative abundance of mudrock in the estuarine successions is compiled in the database. These two sedimentary characteristics of a succession are most likely to be reported on in stratigraphic successions that are interrogated for a variety of research goals.

7.1. Limitations and mitigation

Cotter (1978) and Davies et al. (2010a, 2013) list a number of limitations with a literature survey of this kind: (1) Early Palaeozoic interpretations are under-represented in literature, in part due to exposure constraints; (2) different tectonic and climatic settings are represented by the various case studied; and (3) comparability issues exist between case studies conducted by different workers to answer different research questions using an array of different diagnostic criteria and conceptual models. Furthermore, a literature survey on estuarine settings is hampered by (4) the difficulty interpreting an estuary in the sedimentary record, requiring evidence of bidirectional flow and bidirectionally sourced sediment. Sedimentary successions recording sequence drowning are often identified as a fluvial to marine transition, fluvio-deltaic deposits or near-shore deposits. Queries for any of these terms, *e.g.* 'fluvial to marine + Carboniferous', return up to 8 times more results than queries for 'estuary + Carboniferous' but do not necessarily return studies on estuarine successions. To conclude, (5) the database spans 20 studies (including the present study), which is a sufficient number to suggest trends, but is not numerous enough to draw conclusions with any statistical foundation.

Effort has been put in to mitigating these limitations but the problem of under-representation of Early Palaeozoic successions in compiled literature is unfortunately unavoidable.

The second problem of differing climatic and tectonic settings represented in the successions is mitigated by aiming to include case studies with a diverse mix of tectonic and climatic backgrounds in the database. These efforts are hampered by the limited amount of suitable studies that are available and by studies that are lacking information on tectonic or climatic regime.

The problem of comparability is mitigated relatively simple. The database is compiled to compare well-identifiable, tangible sedimentary characteristics between studies. Most workers at least briefly describe the sedimentary characteristics observed, while many present their observation in a table or graphic format. The presence of IHS and the abundance of mudrock are typically recorded by workers in a plethora of research fields. This makes it relatively easy to ascertain the abundance, the absence or presence of certain sedimentary characteristics in the succession of reported case studies.

The fourth problem, the difficulty of interpreting an estuary, limits the amount of studies available. For many purposes – *e.g.* palaeotectonics, reconstruction of marine ingressions, sequence stratigraphy – it suffices to constrain a succession represents a fluvial to marine transition, or fluvio-deltaic deposits. An estuarine interpretation typically surfaces in detailed

sedimentological studies for *e.g.* hydrocarbon exploration or in palaeoecology work where brackish water species are studied.

An attempt was made to mitigate this issue by extending the range of search queries to include facies commonly associated with estuarine environments, such as tidal flats and tidal channels. However, this primarily returned search results of papers on tidal shorelines and beaches, as tidal flats and tidal channels are even more common in these environments. Available studies on estuarine successions thus remain limited.

Lastly, the limited scope of this literature survey inhibits drawing conclusions founded on statistical analysis. A more expansive study, if possible with the limited incidence of reported estuaries, would enable analysis on the relevance of perceived trends strengthening links made and conclusions drawn.

Table 3: *Reported age, unit, location and type of exposure for selected studies through geological time reporting estuarine successions. Number in first column corresponds to number in Table 4.*

#	Reported age	Unit	Location	Exposure	Main references
1	Early to Medial Cambrian	Altona Fm.	Quebec basin	outcrop	Brink et al. (2019)
2	L. Cambr. to Early Ordov.	Santa Rosita	NW. Argentina	outcrop	Buatois et al. (2003)
3	Early Ordovician	Alto del Condor Fm.	Bolivia	outcrop	Sánchez et al. (2007)
4	Late Ordovician	Melaz Shuqran Fm., Mamuniyat Fm.	SW. Libya	outcrop	El-Ghali et al. (2005)
5	Ordovic. to Early Silurian	Tumblagooda Sandstone	W. Australia	outcrop	Bradley et al. (2018)
6	Silurian	Kepingtage Member	Tarim Basin, W. China	slabbed core	Zhang et al. (2008)
7	Late Silurian	Gray Sandstone Group	Wales, UK	outcrop	Hiller et al. (2004)
8	Devonian	Sperm Bluff Fm.	S. Victoria Land, Antarctica	outcrop	Savage et al. (2013)
9	Medial to Late Devonian	Old Red Sandstone	Onega Lake, W. Russia	outcrop	Mikulaš et al. (2013)
10	Late Devonian	Ignacio Fm.	Colorado, USA	outcrop	Evans et al. (2019)
11	Medial Mississippian	Largysillagh and Shalwy Fm.	N. Rep. of Ireland	outcrop	this study
12	Late Mississippian	Buffalo Wallow Fm.	W. Kentucky, USA	outcrop	Greb et al. (2016)
13	Late Carb. to Med. Perm.	Nuayyim Fm.	SE. Saudi Arabia	slabbed core	Polo et al. (2018)
14	Late Permian	Faraghan Fm.	Central Iran	well core	Vennin et al. (2015)
15	Early Triassic	Dongchuan Fm.	S. China	outcrop	Zhang et al. (2017)
16	Early Jurassic	Sjøgrenfjellet Mb.	Svalbard	outcrop	Oluassen et al. (2018)
17	Medial Jurassic	Dhruma Fm.	Saudi Arabia	well core	Al-Hussaini et al. (2019)
18	Early to Medial Jurassic	Iroquois Fm.	USA East Coast	well core	O'Conner et al. (2018)
19	Early Cretaceous	Mulichinco Fm.	W. Argentina	outcrop	Olivo et al. (2019)
20	Late Cretaceous	Puesto El Moro Fm.	W. Argentina	outcrop	Varela et al. (2019)

Table 4: *Reported age, mudrock abundance in percentage and presence or absence of packages of IHS for selected studies reporting estuarine successions. Number in first column corresponds to number in Table 3.*

#	Reported age	% mudrock	& architecture	Comments	Main references
1	Early to Medial Cambrian	17%	-	sub-equatorial arid climate	Brink et al. (2019)
2	L. Cambr. to Early Ordov.	15%	IHS	-	Buatois et al. (2003)
3	Early Ordovician	30%	-	-	Sánchez et al. (2007)
4	Late Ordovician	8%		polar climate	El-Ghali et al. (2005)
5	Ordovician to Early Silurian	0%	-	-	Bradley et al. (2018)
6	Silurian	12%	-	-	Zhang et al. (2008)
7	Late Silurian	35%	IHS	-	Hiller et al. (2004)
8	Devonian	6%	-	-	Savage et al. (2013)
9	Medial to Upper Devonian	19%	-	-	Mikulaš et al. (2013)
10	Upper Devonian	18%	IHS	semi-arid climate; formation age debated	Evans et al. (2019)
11	Medial Mississippian	16%	IHS	alternating humid and arid climate	this study
12	Late Mississippian	35%	IHS	alternating humid and arid climate	Greb et al. (2016)
13	Late Carb. to Med.Perm.	12%	IHS	post-glacial ameliorating climate	Polo et al. (2018)
14	Late Permian	43%	-	-	Vennin et al. (2015)
15	Early Triassic	25%	-	-	Zhang et al. (2017)
16	Early Jurassic	45%	-	high latitude climate	Oluassen et al. (2018)
17	Medial Jurassic	21%	IHS	equatorial humid climate	Al-Hussaini et al. (2019)
18	Early to Medial Jurassic	53%	IHS	age debated	O'Conner et al. (2018)
19	Early Cretaceous	24%	IHS	temperate humid climate	Olivo et al. (2019)
20	Late Cretaceous	50%	IHS	-	Varela et al. (2019)

Table 5: *abundance of mudrock in stratigraphic successions in literature case studies, grouped into stages representing successive advances in land vegetation cover.*

Timeframe (study number)	vegetation stage	mudrock abundance (range | median)
Cambrian-Ordovician (1-5)	pre-vegetated landscapes	0-30% | 15%
Silurian-Devonian (6-10)	rise of terrestrial flora	6-35% | 18%
Carboniferous-Cretaceous (11-20)	abundant vegetation cover	12-53% | 30%

7.2. Abundance of mudrock and IHS frequency

Results

The 20 estuarine succession considered, 19 from literature and the present study (Table 3, Table 4), are grouped into three vegetation stages that represent successive advance in land vegetation cover (Table 5). Mudrock is present in nearly all database case studies (Figure 19).

Relative mudrock abundance in the successions of the Cambrian to Ordovician group (*ca.* 541 - 443 Ma) of studies ranges from 0% to 30% (median 15%). Estuarine systems from this period in geological time functioned in a barren geomorphic context (Boyce and Lee, 2017). During the Silurian-Devonian (*ca.* 443 – 359 Ma) rise and radiation of terrestrial flora (Boyce and Lee, 2017), relative abundance of mudrock ranges 6% to 35% (median 18%).

From the Carboniferous on (*ca.* 359 Ma) the relative abundance of mudrock increases markedly, ranging 12% to 53% (median 30%), an increase of 1.3 orders of magnitude (Table 5, Figure 19). By this period, the geomorphic landscape is extensively covered by vegetation (Boyce and Lee, 2017). Similarly, packages of IHS, indicative of channel meandering, occur more frequently from the Devonian onwards (Figure 19).

Discussion

The post-Devonian increase in mudrock abundance and IHS presence in estuarine successions are argued to be the effects of vegetation, newly introduced to the geomorphic landscape over the course of the Silurian and Devonian (Boyce and Lee, 2017). As vegetation radiated its effects on estuarine morphodynamics became increasingly profound, enhancing the catchment-wide production of mud and promoting mud retention and sediment stabilization.

These large-scale trends are similar in fluvial environments. However, estuaries are complex environments and the stage for a variety of morphodynamic conditions. Trends in a coarse proxy like the bulk properties of a stratigraphic succession do not capture this intricate heterogeneity accurately (van de Lageweg et al., 2018). For example, abiotic deposition of mud through the settling of fines during slackwater periods in a tidal cycle plays a significant role in estuaries alongside biologically influenced deposition of mud. These abiotic, marine muds shape estuary behaviour by promoting the development of mudflats along the flanks of the estuary mouth (van der Lageweg et al., 2018) but are indistinguishable in stratigraphy from biologically influenced mud deposits.

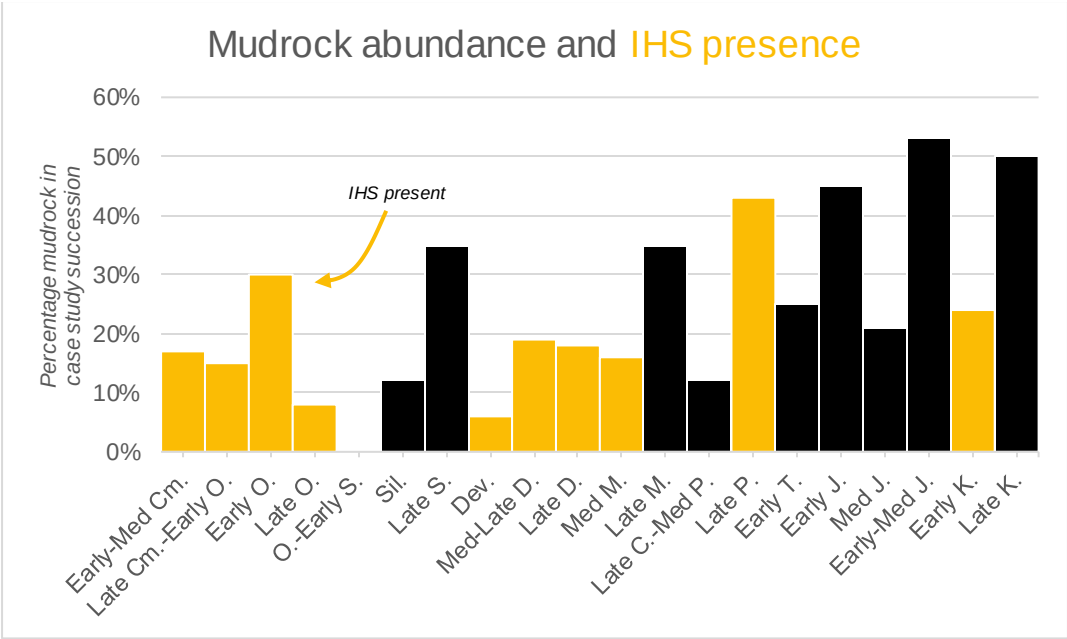

Figure 19: *Graph illustrating the relative abundance of mudrock in each of the case studies' successions. Coloured bars indicate the presence of packages of IHS in the case study's succession. Med.: Medial; Cm.: Cambrian; O.: Ordovician; S./Sil.: Silurian; D./Dev.: Devonian; M.: Mississippian; P.: Pennsylvanian; T.: Triassic; J.: Jurassic; K.: Cretaceous.*

7.3. Estuary autogenic morphodynamic variability

The mudrock abundance varies in post-Devonian case studies, ranging from 12% to 53% (Table 4). The high degree of morphodynamic variability in estuaries leading to great spatial variability in mud deposition (Braat et al., 2017; van de Lageweg et al., 2018) may result in a large range of mudrock abundance in stratigraphy. Put simply, autogenic variability is greater in estuaries than in rivers. For example, the mixed-energy part of an estuary is tranquil enough to allow deposition of muds (Braat et al., 2017; Lokhorst et al., 2018), while a few kilometres downstream tidal dynamics prevent widespread accumulation of fine-grained sediment. Conversely, in rivers the morphodynamic conditions do not change as much in the span of a few kilometres. Fine-grained sediment settles on river floodplains while channels host coarse-grained lag deposits; a distribution that is much the same a few kilometres downstream.

Furthermore, estuaries are systems governed by the relative magnitude of river influence, tidal influence and wave-action influence (Dalrymple et al., 1992). Estuaries ruled by river influence see a heterogenous spatial distribution of sediment, becoming muddier to the estuary mouth (van de Lageweg et al., 2018), while those impacted also by tides separate out sediment and primarily deposit muds close to the flanks (Braat et al., 2017; van de Lageweg et al., 2018). Addition of wave-action prevents deposition of mud near the estuary mouth (van de Lageweg et al., 2018). To add to the complexity, the relative magnitude of each of these constituents may change over time as a result of changing boundary conditions, *e.g.* an upstream avulsion limiting the impact of fluvial processes in the estuary.

In stratigraphy this translates to a wide variety of morphodynamic conditions recorded in estuarine successions and may be reflected by a wide range of mudrock abundance between case studies. An accurate reconstruction of morphodynamic conditions based on bulk properties of a succession, *e.g.* relative abundance of mudrock or the presence of IHS, is not feasible as different morphodynamic conditions may result in similar bulk properties (van de Lageweg et al., 2018).

7.4. Lagged impact of halophytes

The widespread colonization of the continents by land plant in the Early Palaeozoic (Davies and Gibling, 2010) served to retain mud on the continents by two distinct processes, baffling and binding, in addition to the greater production of mud resulting from enhanced chemical weathering (Davies et al., 2020). It is not well-constrained when halophytic vegetation became widespread as halophytic traits in land plants appear to have evolved independently numerous times over geological time (Flowers et al., 2015). That means the local effects of vegetation may have lacked behind in brackish parts of some ancient estuaries as halophytic vegetation was yet to radiate.

Modern halophytes are primarily angiosperms (Cheeseman, 2015), which evolved by the Cretaceous (Cheeseman, 2015; Boyce and Lee, 2017) and are an important constituent of the salt marsh vegetation palette (Woodroffe, 2002). Pre-Cretaceous halophytes include mangroves (Raymond and Philips, 1983) and some gymnosperms and lycophytes (DiMichelle et al., 1996; Falcon-Lang, 2003).

Salt marshes evolved by the Cretaceous and are effective in capturing muds and play a key role in estuary morphodynamics (Lokhorst et al., 2018). Pre-Cretaceous estuaries may have seen a skewed impact of vegetation as the local effects of mud capture through flow baffling was missing due to the lack of widespread salt marsh vegetation. However, mangrove vegetation in modern estuaries has an equifinal effect on the bulk properties (*e.g.* relative

abundance of mudrock) of estuarine successions as salt marsh vegetation (Kakeh et al., 2016). Mangrove vegetation may have taken up the bulk of the engineering role that salt marshes play in pre-Cretaceous estuaries.

Intricate details, not recorded by the bulk properties of a stratigraphic succession, may be different between pre-Cretaceous (mangrove) estuaries and post-Cretaceous (salt marsh) estuaries. The studied Carboniferous succession hosts ample evidence for laterally migrating, meandering channels, recorded as laterally expansive bodies of channelized sandstone (CH-1A) and packages of IHS (IHS-A to IHS-D). In comparison, meandering channels in the present-day Venice Lagoon are relatively immobile with a lateral migration rate of several centimetres per year (Brivio et al., 2016). Channel dimensions are similar between the Carboniferous case study and the Venice Lagoon case study: several tens of metres wide (Brivio et al., 2016). One of the key differences between the two estuarine settings is the widespread presence of salt marsh vegetation in the Venice Lagoon (Brivio et al., 2016; D'Alpaos et al., 2017). Salt marsh vegetation may be more effective at baffling flow and capturing mud than pre-Cretaceous vegetation, better promoting floodplain aggradation and flow channelization. In turn, this more effectively limits the lateral mobility of a meandering channel. In post-Cretaceous stratigraphy, this translates to narrower bodies of channelized sandstones, limited in capacity to migrate laterally, compared to pre-Cretaceous counterparts.

7.5. Crevasse splays

In the studied succession crevasse splays are recorded in facies EV-1 as wavy, chaotic sandstones, with shell fragments recording the nearshore nature the facies. Crevasse splays are sheet-like progradational deposits that are lobe-shaped in plan-view (Burns et al., 2017). Crevasse splays typically develop when floodwaters overtop the levee of an established channel and break through the levee, initiating a new, point-source conduit over the adjacent floodplain (Mjøs et al., 1993).

The occurrence and spatial extent of crevasse splays in a Holocene nearshore, backbarrier setting appears to be related to contemporaneous wetland vegetation type and density (Albernaz et al., in review). A dense vegetation cover restricts overbank flow and distal sediment deposition, resulting in narrow but elevated levees and a limited occurrence frequency of crevasse splays (Albernaz et al., in review).

Wetlands covered by reed vegetation are relatively dense as reed stalks grow close to one another, whereas the geomorphic landscape is relatively porous when wetlands are vegetated by woody shrubs and trees. Over the course of the Early Holocene Old Rhine estuary the wetland vegetation cover transitioned from reed-dominant to wood-dominant, recorded in stratigraphy as a shift from reed peat to wood peat (Stouthamer, 2001; van Asselen et al., 2009). Consequently, crevasse splay deposits are more frequent in the packages of wood peat (Albernaz et al., in review).

Reeds are grass-like herbaceous plants, a family that evolved by the Cretaceous (Boyce and Lee, 2017). As such, dense vegetation cover by reeds were not a feature in the geomorphic landscape of pre-Cretaceous estuaries, *e.g.* the Carboniferous case study, to limit the occurrence of crevasse splays. Rather, the geomorphic landscape is likely to have been relatively porous, covered by woody cordaitalean trees (Boyce and Lee, 2017). Crevasse splays may occur less frequently in post-Cretaceous estuaries than in pre-Cretaceous estuaries as reed-like vegetation restricts crevasse splay development.

8. Summary

This research considers the impact of terrestrial flora and its evolution on the sedimentary features recorded in the stratigraphy of estuarine successions from the Cambrian to the Cretaceous (*ca.* 541 – 66 Ma) based on original fieldwork on an Early Viséan (*ca.* 340 Ma; Carboniferous) case study and a literature survey. The case study dates from a period in geological time when vegetation was sufficiently abundant for the first time in Earth history to be a forcing actor on large-scale systems such as the geomorphic landscape, atmospheric composition and (global) climate (Davies et al., 2013).

The strata of the Carboniferous case study are well-exposed in sea cliffs in the north of the Republic of Ireland. The succession reflects a fluvial to marine transition as recorded in (channel-form) sandstones, mudrocks and rare paralic limestone, with bioturbation and abundance of shell fragments increasing to the top of the succession.

The impact of vegetation on the contemporaneous morphodynamics of the estuarine case study is reflected in numerous sedimentary characteristics of the studied succession. Flow channelization and channel meandering (Braat et al., 2017; Lokhorst et al., 2017; Kleinhans et al., 2018) is recorded in channel-form sandstones and packages of inclined heterolithic stratification (IHS). Extensive deposits of alluvial mudrock mirror accelerated production and improved retention of mud by vegetation (McMahond and Davies, 2018a). Further indicators of (the effects of) vegetation include the presence of rhizoliths, fusain (fossiliferous charcoal), plant imprints, woody debris, carbonaceous mudrock and coal seams.

Terrestrial flora evolved over the course of the Early Palaeozoic (Boyce and Lee, 2017; Davies et al., 2020). The abundance of key sedimentary characteristics reflective of a vegetation control on estuarine morphodynamics is co-eval with the evolution of terrestrial flora. The presence of packages of IHS and the relative abundance of mudrock is compiled in a database spanning 20 studies of Cambrian to Cretaceous aged (541-66 Ma) estuarine succession. These sedimentary characteristics are typically recorded by workers interrogating a succession for a variety of research questions.

From the Devonian onwards, a marked increase in the presence of IHS and an order 1.3 magnitude greater relative abundance of mudrock is observed in the database successions. This trend is linked to the substantial radiation of two key traits in land plants: (1) the Late Silurian advent of vascular plants, which accelerate chemical weathering through the excretion of humic acids; and (3) the Late Devonian advent of deep-rooting, providing stability and resistance to erosion to plants and sediments.

Subsequent evolutionary advances in terrestrial flora relevant to estuarine morphodynamics are the Cretaceous (145-66 Ma) advent of herbaceous, grass-like and salt marsh vegetation (Boyce and Lee, 2017). Salt marsh vegetation appears to be very effective at immobilizating channels, restricting lateral channel migration. This is exemplified by the presence of laterally extensive channel sandstone deposits in the Carboniferous case study, contrasting with the lack of notable lateral migration of channels in the present-day Venice Lagoon (Brivio et al., 2016). As such, lateral channel mobility in estuaries may have been hampered markedly since the Cretaceous advent of salt marsh vegetation.

Similarly, the development of crevasse splays may be limited since the Cretaceous advent of grass-like vegetation (Boyce and Lee, 2017). Reeds, which grow in populations of closely spaced stalks, may have introduced a greater degree of vegetation density to a geomorphic landscape previously covered by cordaitalean trees. A high vegetation density restricts overbank flow and distal sediment deposition, which limits the incidence of crevasse splays

(Albernaz et al., in review). This implies crevasse splays may occur less frequently in estuaries since the Cretaceous emergence of grass-like vegetation such as reeds.

To summarize, the impact of vegetation on estuarine morphodynamics is reflected in stratigraphy by the presence of key sedimentary features, such as the presence of packages of IHS, channelized sandstones and abundance of mudrock. Frequent presence and increased abundance of these sedimentary features is co-eval with the Early Palaeozoic radiation of terrestrial flora. The effects of subsequent evolutionary advances on estuary morphodynamics may include reduced incidence of crevasse splays and restricted lateral mobility of channels since the Cretaceous advent of grass-like and salt marsh vegetation.

9. Conclusions

The present study explores the effects of vegetation and its evolution on the sedimentary features recorded in the stratigraphy of estuarine successions through the Palaeozoic and Mesozoic based on an Early Viséan (*ca.* 340 Ma) case study and a literature survey.

The case study succession reflects an estuary in a gradual fluvial to marine transition. Direct and indirect signatures of vegetation are recorded in the studied succession as rhizoliths, fusain, coal seams, carbonaceous mudrocks, plant impressions, packages of inclined heterolithic stratification (IHS) and mudrock deposits. The mechanisms through which vegetation alters sedimentary processes and products is similar in fluvial and estuarine environments, with catchment-wide vegetation-promoted mud production, local vegetation-enhanced capture of muds and sediment stabilization through deep-rooting. However, estuaries host a complex variety of morphodynamic conditions over a limited spatial scale that render the impact of vegetation intricate. This may translate to stratigraphy as IHS coset grain size trends and a wide range of relative abundance of mudrock between individual estuaries.

The literature survey demonstrated a marked and sustained Early Palaeozoic increase in mudrock content and occurrence of packages of IHS in the sedimentary record co-eval with the evolution of land plants. Land plant traits key in shaping estuaries, such as vascular plants, deep-rooting and increased above-ground surface roughness, have fully evolved by the Early Viséan, with salt marsh vegetation, grasses and herbs evolving during the Cretaceous (145-66 Ma).

Salt marsh vegetation may have introduced a greater degree of channel immobilization, resulting from their effective retention of muds. As such, increased floodplain stability following the introduction of salt marsh vegetation to the geomorphic landscape may have restricted lateral channel migration more effectively in post-Cretaceous estuaries than their pre-Cretaceous counterparts.

The introduction of grass-like reeds in post-Cretaceous estuaries may have limited crevasse splay occurrence frequency as the geomorphic landscape became more densely vegetated with closely-spaced reed stalks compared to a geomorphic landscape previously covered by cordaitalean trees.

This work has demonstrated tangible geological evidence for the impact of vegetation in an Early Viséan estuarine case study, and has distilled a co-eval pacing of the occurrence of sedimentary features in estuaries with land plant evolution through a database which may serve as a pilot for future research.

10. Acknowledgements

I would like to express my gratitude to my supervisors prof. dr. Maarten Kleinhans, dr. William McMahon, dr. Harm Jan Pierik and Tim Winkels MSc for formulating the project and for their extensive input and support before and during this project. Many thanks in particular to Will for his great tuition in the outdoors of Ireland, good company there and plentiful assistance during the write-up process back in Utrecht. In Ireland that good company was most definitely boosted by dr. Francesco Salese.

Thank you, not in the least, to Ailleen for her love, care and uplifting rallying during these long 37.5 credits. And thank you to my family for their warmth, support and encouragement.

11. References

Ainsworth, R. B., & Walker, R. G. (1994). Control of estuarine valley-fill deposition by fluctuations of relative sea-level, Cretaceous Bearpaw-Horseshoe Canyon transition, Drumheller, Alberta, Canada.

Albernaz, M. B., Roelofs, L., Pierik, H. J., Kleinhans, M. G. (in review). Natural levee and floodbasin evolution in vegetated fluvial-tidal environment. ESPL.

Alekseev, A. S., Kononova, L. I., & Nikishin, A. M. (1996). The Devonian and Carboniferous of the Moscow Syneclise (Russian Platform): Stratigraphy and sea-level changes. Tectonophysics, 268(1-4), 149-168.

Allen, P. A. (2008). Landscape evolution: Denudation, climate and tectonics over different time and space scales.

Allen, J. P., Fielding, C. R., Gibling, M. R., & Rygel, M. C. (2011). Fluvial response to paleo-equatorial climate fluctuations during the late Paleozoic ice age. GSA Bulletin, 123(7-8), 1524-1538.

Aqrawi, A. A. (1995). Correction of Holocene sedimentation rates for mechanical compaction: The Tigris-Euphrates delta, Lower Mesopotamia. Marine and Petroleum Geology, 12(4), 409-416.

Athy, L. F. (1930). Density, porosity, and compaction of sedimentary rocks. AAPG Bulletin, 14(1), 1-24.

Bar-On, Y. M., Phillips, R., & Milo, R. (2018). The biomass distribution on earth. Proceedings of the National Academy of Sciences, 115(25), 6506-6511.

Baucon, A., Ronchi, A., Felletti, F., & de Carvalho, C. N. (2014). Evolution of crustaceans at the edge of the end-Permian crisis: Ichnonetwork analysis of the fluvial succession of Nurra (Permian–Triassic, Sardinia, Italy). Palaeogeography, Palaeoclimatology, Palaeoecology, 410, 74-103.

Benda, L., Miller, D., Bigelow, P., & Andras, K. (2003). Effects of post-wildfire erosion on channel environments, Boise River, Idaho. Forest Ecology and Management, 178(1-2), 105-119.

Berner, R. A. (2006). GEOCARBSULF: a combined model for Phanerozoic atmospheric O2 and CO2. Geochimica et Cosmochimica Acta, 70(23), 5653-5664.

Beven, K. (1996). 12 equifinality and uncertainty in geomorphological modelling. Paper presented at the The Scientific Nature of Geomorphology: Proceedings of the 27th Binghamton Symposium in Geomorphology, Held 27-29 September 1996

Blair, T. C., & McPherson, J. G. (2009). Processes and forms of alluvial fans. Geomorphology of desert environments (pp. 413-467) Springer.

Boyce, C. K., & Lee, J. (2017). Plant evolution and climate over geological timescales. Annual Review of Earth and Planetary Sciences, 45, 61-87.

Braat, L., Kessel, T. v., Leuven, J. R., & Kleinhans, M. G. (2017). Effects of mud supply on large-scale estuary morphology and development over centuries to millennia. Earth Surface Dynamics, 5(4), 617-652.

Braat, L., Leuven, J. R., Lokhorst, I. R., & Kleinhans, M. G. (2019). Effects of estuarine mudflat formation on tidal prism and large-scale morphology in experiments. Earth Surface Processes and Landforms, 44(2), 417-432.

Bradley, G., Redfern, J., Hodgetts, D., George, A. D., & Wach, G. D. (2018). The applicability of modern tidal analogues to pre-vegetation paralic depositional models. Sedimentology, 65(6), 2171-2201.

Brink, R., Mehrtens, C., & Maguire, H. (2019). Sedimentology and petrography of a Lower Cambrian transgressive sequence: Altona formation (Potsdam Group) in Northeastern New York. Bulletin of Geosciences, 94(3)

Brivio, L., Ghinassi, M., D'Alpaos, A., Finotello, A., Fontana, A., Roner, M., & Howes, N. (2016). Aggradation and lateral migration shaping geometry of a tidal point bar: An example from salt marshes of the northern venice lagoon (italy). Sedimentary Geology, 343, 141-155.

Buatois, L. A., & Mángano, M. G. (2003). Sedimentary facies, depositional evolution of the upper Cambrian-Lower Ordovician Santa Rosita formation in Northwest Argentina. Journal of South American Earth Sciences, 16(5), 343-363.

Buatois, L. A., & Mángano, M. G. (2002). Trace fossils from carboniferous floodplain deposits in western Argentina: Implications for ichnofacies models of continental environments. Palaeogeography, Palaeoclimatology, Palaeoecology, 183(1-2), 71-86.

Burns, C. E., Mountney, N. P., Hodgson, D. M., & Colombera, L. (2017). Anatomy and dimensions of fluvial crevasse-splay deposits: Examples from the Cretaceous Castlegate Sandstone and Neslen Formation, Utah, USA. Sedimentary Geology, 351, 21-35.

Burns, C. E., Mountney, N. P., Hodgson, D. M., & Colombera, L. (2019). Stratigraphic architecture and hierarchy of fluvial overbank splay deposits. Journal of the Geological Society, 176(4), 629-649.

Calder, J. H. (1994). The impact of climate change, tectonism and hydrology on the formation of Carboniferous tropical intermontane mires: the Springhill coalfield, Cumberland Basin, Nova Scotia. Palaeogeography, Palaeoclimatology, Palaeoecology, 106(1-4), 323-351.

Calder, J. H. (1998). The carboniferous evolution of Nova Scotia. Geological Society, London, Special Publications, 143(1), 261-302.

Cheeseman, J. M. (2015). The evolution of halophytes, glycophytes and crops, and its implications for food security under saline conditions. New Phytologist, 206(2), 557-570.

Clark, J. S. (1988). Particle motion and the theory of charcoal analysis: Source area, transport, deposition, and sampling. Quaternary Research, 30(1), 67-80.

Cleal, C. J., & Thomas, B. A. (2005). Palaeozoic tropical rainforests and their effect on global climates: is the past the key to the present?. Geobiology, 3(1), 13-31.

Cohen, K. M., Finney, S. C., Gibbard, P. L., & Fan, J. (2013). The ICS international chronostratigraphic chart. Episodes, 36(3), 199-204.

Cotter, E. (1977). The evolution of fluvial style, with special reference to the central Appalachian Paleozoic.

Cotter, E., & Graham, J. R. (1991). Coastal plain sedimentation in the late Devonian of southern Ireland; hummocky cross-stratification in fluvial deposits?. Sedimentary Geology, 72(3-4), 201-224.

Crowley, T. J., & Baum, S. K. (1991). Estimating Carboniferous sea-level fluctuations from Gondwanan ice extent. Geology, 19(10), 975-977.

D'Alpaos, A., Ghinassi, M., Finotello, A., Brivio, L., Bellucci, L. G., & Marani, M. (2017). Tidal meander migration and dynamics: A case study from the Venice lagoon. Marine and Petroleum Geology, 87, 80-90.

Dalrymple, R. W., Zaitlin, B. A., & Boyd, R. (1992). Estuarine facies models; conceptual basis and stratigraphic implications. Journal of Sedimentary Research, 62(6), 1130-1146.

Davies, N. S., & Gibling, M. R. (2010a). Cambrian to Devonian evolution of alluvial systems: The sedimentological impact of the earliest land plants. Earth-Science Reviews, 98(3-4), 171-200.

Davies, N. S., & Gibling, M. R. (2010b). Paleozoic vegetation and the Siluro-Devonian rise of fluvial lateral accretion sets. Geology, 38(1), 51-54.

Davies, N. S., Gibling, M. R., & Rygel, M. C. (2011). Alluvial facies evolution during the Palaeozoic greening of the continents: Case studies, conceptual models and modern analogues. Sedimentology, 58(1), 220-258.

Davies, N. S., & Shillito, A. P. (2018). Incomplete but intricately detailed: The inevitable preservation of true substrates in a time-deficient stratigraphic record. Geology, 46(8), 679-682.

Davies, N. S., Shillito, A. P., & McMahon, W. J. (2019). Where does the time go? Assessing the chronostratigraphic fidelity of sedimentary geological outcrops in the Pliocene–Pleistocene Red Crag Formation, Eastern England. Journal of the Geological Society, 176(6), 1154-1168.

Davies, N. S., Shillito, A. P., Slater, B. J., Liu, A. G., & McMahon, W. J. (2020). Evolutionary synchrony of Earth's biosphere and sedimentary-stratigraphic record. Earth-Science Reviews, 102979.

Davies, S. J., & Gibling, M. R. (2003). Architecture of coastal and alluvial deposits in an extensional basin: The Carboniferous Joggins Formation of Eastern Canada. Sedimentology, 50(3), 415-439.

Decombeix, A. L., Meyer-Berthaud, B., & Galtier, J. (2011). Transitional changes in arborescent lignophytes at the Devonian–Carboniferous boundary. Journal of the Geological Society, 168(2), 547-557.

Diessel, C. F. (2010). The stratigraphic distribution of inertinite. International Journal of Coal Geology, 81(4), 251-268.

DiMichele, W. A., Pfefferkorn, H. W., & Phillips, T. L. (1996). Persistence of Late Carboniferous tropical vegetation during glacially driven climatic and sea-level fluctuations. Palaeogeography, Palaeoclimatology, Palaeoecology, 125(1-4), 105-128.

DiMichele, W. A., Montañez, I. P., Poulsen, C. J., & Tabor, N. J. (2009). Climate and vegetational regime shifts in the late Paleozoic ice age earth. Geobiology, 7(2), 200-226.

DiMichele, W. A., Cecil, C. B., Montañez, I. P., & Falcon-Lang, H. J. (2010). Cyclic changes in Pennsylvanian paleoclimate and effects on floristic dynamics in tropical Pangaea. International Journal of Coal Geology, 83(2-3), 329-344.

Drever, J. I. (1994). The effect of land plants on weathering rates of silicate minerals. Geochimica Et Cosmochimica Acta, 58(10), 2325-2332.

El-ghali, M. A. K. (2005). Depositional environments and sequence stratigraphy of paralic glacial, paraglacial and postglacial Upper Ordovician siliciclastic deposits in the Murzuq basin, SW Libya. Sedimentary Geology, 177(3-4), 145-173.

Eriksson, K. A., & Simpson, E. L. (1998). Controls on spatial and temporal distribution of Precambrian eolianites. Sedimentary Geology, 120(1-4), 275-294.

Evans, J. E., Maurer, J. T., & Holm-Denoma, C. S. (2019). Recognition and significance of Upper Devonian fluvial, estuarine, and mixed siliciclastic-carbonate nearshore marine facies in the San Juan Mountains (Southwestern Colorado, USA): Multiple incised valleys backfilled by lowstand and transgressive systems tracts. Geosphere, 15(5), 1479-1507.

Falcon-Lang, H. (1998). The impact of wildfire on an early Carboniferous coastal environment, North Mayo, Ireland. Palaeogeography, Palaeoclimatology, Palaeoecology, 139(3-4), 121-138.

Falcon-Lang, H. J. (2000). Fire ecology of the Carboniferous tropical zone. Palaeogeography, Palaeoclimatology, Palaeoecology, 164(1-4), 339-355.

Falcon-Lang, H. J. (2003). Response of Late Carboniferous tropical vegetation to transgressive-regressive rhythms at Joggins, Nova Scotia. Journal of the Geological Society, 160(4), 643-648.

Falcon-Lang, H. J., & Bashforth, A. R. (2005). Morphology, anatomy, and upland ecology of large cordaitalean trees from the Middle Pennsylvanian of Newfoundland. Review of Palaeobotany and Palynology, 135(3-4), 223-243.

Fielding, C. R. (2006). Upper flow regime sheets, lenses and scour fills: Extending the range of architectural elements for fluvial sediment bodies. Sedimentary Geology, 190(1-4), 227-240.

Fielding, C. R., Allen, J. P., Alexander, J., & Gibling, M. R. (2009). Facies model for fluvial systems in the seasonal tropics and subtropics. Geology, 37(7), 623-626.

Fielding, C. R., Frank, T. D., Birgenheier, L. P., Rygel, M. C., Jones, A. T., & Roberts, J. (2008). Stratigraphic imprint of the late Palaeozoic ice age in Eastern Australia: A record of alternating glacial and nonglacial climate regime. Journal of the Geological Society, 165(1), 129-140.

Fischer, W. W. (2018). Early plants and the rise of mud. Science, 359(6379), 994-995.

Flowers, T. J., & Colmer, T. D. (2015). Plant salt tolerance: Adaptations in halophytes. Annals of Botany, 115(3), 327-331.

Foster, G. L., & Rohling, E. J. (2013). Relationship between sea level and climate forcing by CO2 on geological timescales. Proceedings of the National Academy of Sciences, 110(4), 1209-1214.

Fraser, A. J., & Gawthorpe, R. L. (1990). Tectono-stratigraphic development and hydrocarbon habitat of the Carboniferous in Northern England. Geological Society, London, Special Publications, 55(1), 49-86.

Fraser, A. J., & Gawthorpe, R. L. (2003). An atlas of Carboniferous basin evolution in Northern England Geological Society.

Gawthorpe, R. L., Gutteridge, P., Leeder, M. R., & Arthurton, R. S. (1989). Late Devonian and Dinantian basin evolution in Northern England and North Wales. The Role of Tectonics in Devonian and Carboniferous Sedimentation in the British Isles, 6, 1-23.

Gensel, P. G., Kotyk, M. E., & Basinger, J. F. (2001). Morphology of Above-and below-ground structures in Early Devonian (Pragian–Emsian) plants. Plants Invade the Land: Evolutionary and Environmental Perspectives, , 83.

Gibling, M. R. (2006). Width and thickness of fluvial channel bodies and valley fills in the geological record: A literature compilation and classification. Journal of Sedimentary Research, 76(5), 731-770.

Gibling, M. R., Bashforth, A. R., Falcon-Lang, H. J., Allen, J. P., & Fielding, C. R. (2010). Log jams and flood sediment buildup caused channel abandonment and avulsion in the Pennsylvanian of Atlantic Canada. Journal of Sedimentary Research, 80(3), 268-287.

Gibling, M. R., & Davies, N. S. (2012). Palaeozoic landscapes shaped by plant evolution. Nature Geoscience, 5(2), 99-105.

Glasspool, I. J., Edwards, D., & Axe, L. (2004). Charcoal in the Silurian as evidence for the earliest wildfire. Geology, 32(5), 381-383.

Graham, J. (2010). The Carboniferous geology of north mayo. Irish Journal of Earth Sciences, 25-45.

Graham, J. R. (1996). Dinantian river systems and coastal zone sedimentation in Northwest Ireland. Geological Society, London, Special Publications, 107(1), 183-206.

Greb, S. F., Storrs, G. W., Garcia, W. J., & Eble, C. F. (2016). Late Mississippian vertebrate palaeoecology and taphonomy, Buffalo W allow Formation, western Kentucky, USA. Lethaia, 49(2), 199-218.

Gurnell, A. (2014). Plants as river system engineers. Earth Surface Processes and Landforms, 39(1), 4-25.

Hack, J. T. (1975). Dynamic equilibrium and landscape evolution. Theories of Landform Development, 1, 87-102.

Heckel, P. H. (2008). Pennsylvanian cyclothems in Midcontinent North America as far-field effects of waxing and waning of Gondwana ice sheets. Resolving the Late Paleozoic Ice Age in Time and Space; Fielding, CR, Frank, TD, Isbell, JL, Eds, 275-290.

Hillier, R. D., Edwards, D., & Morrissey, L. B. (2008). Sedimentological evidence for rooting structures in the Early Devonian Anglo-Welsh basin (UK), with speculation on their producers. Palaeogeography, Palaeoclimatology, Palaeoecology, 270(3-4), 366-380.

Hoffmann, T., Erkens, G., Gerlach, R., Klostermann, J., & Lang, A. (2009). Trends and controls of Holocene floodplain sedimentation in the rhine catchment. Catena, 77(2), 96-106.

Holbrook, J., & Miall, A. D. (2020). Time in the rock: a field guide to interpreting past events and processes from a fragmentary siliciclastic archive. Earth-Science Reviews, 103121.

Ilgen, A. G., Heath, J. E., Akkutlu, I. Y., Bryndzia, L. T., Cole, D. R., Kharaka, Y. K., ... & Suarez-Rivera, R. (2017). Shales at all scales: Exploring coupled processes in mudrocks. Earth-Science Reviews, 166, 132-152.

Istanbulluoglu, E., & Bras, R. L. (2005). Vegetation-modulated landscape evolution: Effects of vegetation on landscape processes, drainage density, and topography. Journal of Geophysical Research: Earth Surface, 110(F2)

Jackson, R. G. (1976). Depositional model of point bars in the lower Wabash River. Journal of Sedimentary Research, 46(3), 579-594.

Johnson, B. D. (1984). The great fire of Borneo: Report of a visit to Kalimantan-Timur a year later, May 1984 World Wildlife Fund-UK.

Johnson, S. M., & Dashtgard, S. E. (2014). Inclined heterolithic stratification in a mixed tidal–fluvial channel: Differentiating tidal versus fluvial controls on sedimentation. Sedimentary Geology, 301, 41-53.

Johnston, J. D., Coller, D., Millar, G., & Critchley, M. F. (1996). Basement structural controls on carboniferous-hosted base metal mineral deposits in Ireland. Geological Society, London, Special Publications, 107(1), 1-21.

Kakeh, N., Coco, G., & Marani, M. (2016). On the morphodynamic stability of intertidal environments and the role of vegetation. Advances in Water Resources, 93, 303-314.

Kennedy, K. L., Gibling, M. R., Eble, C. F., Gastaldo, R. A., Gensel, P. G., Werner-Zwanziger, U., & Wilson, R. A. (2013). Lower Devonian coaly shales of Northern New Brunswick, Canada: Plant accumulations in the early stages of terrestrial colonization. Journal of Sedimentary Research, 83(12), 1202-1215.

Kennedy, M., Droser, M., Mayer, L. M., Pevear, D., & Mrofka, D. (2006). Late Precambrian oxygenation; inception of the clay mineral factory. Science, 311(5766), 1446-1449.

Ketzer, J. M., Morad, S., Evans, R., & Al-Aasm, I. S. (2002). Distribution of diagenetic alterations in fluvial, deltaic, and shallow marine sandstones within a sequence stratigraphic framework: Evidence from the Mullaghmore formation (Carboniferous), NW Ireland. Journal of Sedimentary Research, 72(6), 760-774.

Kim, Y., Lee, C., & Lee, E. Y. (2018). Numerical analysis of sedimentary compaction: Implications for porosity and layer thickness variation. J. Geo. Soc. Korea, 54(6), 631-640.

Kleinhans, M. G., Buskes, C. J., & de Regt, H. W. (2005). Terra incognita: Explanation and reduction in earth science. International Studies in the Philosophy of Science, 19(3), 289-317.

Kleinhans, M. G., de Vries, B., Braat, L., & van Oorschot, M. (2018). Living landscapes: Muddy and vegetated floodplain effects on fluvial pattern in an incised river. Earth Surface Processes and Landforms, 43(14), 2948-2963.

Knighton, D. (2014). Fluvial forms and processes: a new perspective. Routledge.

Lambeck, K., Rouby, H., Purcell, A., Sun, Y., & Sambridge, M. (2014). Sea level and global ice volumes from the Last Glacial Maximum to the Holocene. Proceedings of the National Academy of Sciences, 111(43), 15296-15303.

Lazarus, E. D., & Constantine, J. A. (2013). Generic theory for channel sinuosity. Proceedings of the National Academy of Sciences, 110(21), 8447-8452.

Li, G., Li, P., Liu, Y., Qiao, L., Ma, Y., Xu, J., & Yang, Z. (2014). Sedimentary system response to the global sea level change in the east china seas since the last glacial maximum. Earth-Science Reviews, 139, 390-405.

Lokhorst, I. R., Braat, L., Leuven, J. R., Baar, A. W., Van Oorschot, M., Selaković, S., & Kleinhans, M. G. (2018). Morphological effects of vegetation on the tidal-fluvial transition in Holocene estuaries. Earth Surface Dynamics, 6(4), 883-901.

Long, D. (2011). Architecture and depositional style of fluvial systems before land plants: A comparison of Precambrian, Early Paleozoic and modern river deposits. From River to Rock Record: The Preservation of Fluvial Sediments and their Subsequent Interpretation, 97, 37-61.

Love, S. E., & Williams, B. P. (2000). Sedimentology, cyclicity and floodplain architecture in the lower old red sandstone of SW wales. Geological Society, London, Special Publications, 180(1), 371-388.

Martinius, A. W., & Van den Berg, J H. (2011). Atlas of sedimentary structures in estuarine and tidally-influenced river deposits of the Rhine-Meuse-Scheldt system EAGE Houten.

Maynard, J. R., & Leeder, M. R. (1992). On the periodicity and magnitude of Late Carboniferous glacio-eustatie sea-level changes. Journal of the Geological Society, 149(3), 303-311.

McMahon, W. (2018). Pre-vegetation alluvium: Geological evidence for river behaviour in the absence of land plants. PhD Thesis,

McMahon, W. J., & Davies, N. S. (2018a). Evolution of alluvial mudrock forced by early land plants. Science, 359(6379), 1022-1024.

McMahon, W. J., & Davies, N. S. (2018b). The shortage of geological evidence for pre-vegetation meandering rivers. Fluvial Meanders and their Sedimentary Products in the Rock Record, 119-148.

Miall, A. (2014). The emptiness of the stratigraphic record: a preliminary evaluation of missing time in the Mesaverde Group, Book Cliffs, Utah, USA. Journal of Sedimentary Research, 84(6), 457-469.

Miall, A. D. (2015). Updating uniformitarianism: stratigraphy as just a set of 'frozen accidents'. Geological Society, London, Special Publications, 404(1), 11-36.

Mikulaš, R., Mešķis, S., Ivanov, A., Lukševičs, E., Zupiņš, I., & Stinkūlis, Ģ. (2013). A rich ichnofossil assemblage from the Frasnian (Upper Devonian) deposits at Andoma Hill, Onega Lake, Russia. Bulletin of Geosciences, 88(2).

Mills, S. M. (1989). The greater Yellowstone postfire assessment, Greater Yellowstone Coordinating Committee.

Mjøs, R., & Prestholm, E. (1993). The geometry and organization of fluviodeltaic channel sandstones in the Jurassic Saltwick Formation, Yorkshire, England. Sedimentology, 40(5), 919-935.

Myrow, P. M., Lamb, M. P., & Ewing, R. C. (2018). Rapid sea level rise in the aftermath of a Neoproterozoic snowball earth. Science, 360(6389), 649-651.

Nelsen, M. P., DiMichele, W. A., Peters, S. E., & Boyce, C. K. (2016). Delayed fungal evolution did not cause the Paleozoic peak in coal production. Proceedings of the National Academy of Sciences, 113(9), 2442-2447.

Nichols, G., & Jones, T. (1992). Fusain in Carboniferous shallow marine sediments, Donegal, Ireland: The sedimentological effects of wildfire. Sedimentology, 39(3), 487-502.

Okolo, S. A. (1983). Fluvial distributary channels in the fletcher bank grit (Namurian R2b), at Ramsbottom, Lancashire, England. Modern and ancient fluvial systems (pp. 421-433) International Association of Sedimentologists Special Publication 6.

Olivo, M. S., RombolA, C., Loinaze, V. S. P., & Kietzmann, D. A. (2019). Integrated sedimentological and palynological analysis from early cretaceous estuarine deposits in the southern-central Neuquén Basin, Argentina. Journal of South American Earth Sciences, 92, 246-264.

Paola, C., Ganti, V., Mohrig, D., Runkel, A. C., & Straub, K. M. (2018). Time not our time: Physical controls on the preservation and measurement of geologic time. Annual Review of Earth and Planetary Sciences, 46, 409-438.

Patriat, M., Ellouz, N., Dey, Z., Gaulier, J., & Kilani, H. B. (2003). The Hammamet, Gabes And Chotts Basins (Tunisia): A review of the subsidence history. Sedimentary Geology, 156(1-4), 241-262.

Pfefferkorn, H. W., Alleman, V., & Iannuzzi, R. (2014). A greenhouse interval between icehouse times: Climate change, long-distance plant dispersal, and plate motion in the Mississippian (Late Visean–Earliest Serpukhovian) of Gondwana. Gondwana Research, 25(4), 1338-1347.

Plink-Björklund, P. (2005). Stacked fluvial and tide-dominated estuarine deposits in high-frequency (fourth-order) sequences of the Eocene central basin, Spitsbergen. Sedimentology, 52(2), 391-428.

Pollen-Bankhead, N., & Simon, A. (2009). Enhanced application of root-reinforcement algorithms for bank-stability modeling. Earth Surface Processes and Landforms, 34(4), 471-480.

Polo, C. A., Melvin, J., Hooker, N. P., Rees, A. J., Gingras, M. K., & Pemberton, S. G. (2018). The ichnological and sedimentological signature of a late Paleozoic, postglacial marginal-marine and shallow-marine, tidally influenced setting: The Wudayhi Member of the Nuayyim Formation (Unayzah Group) in the subsurface of central and eastern Saudi Arabia. Journal of Sedimentary Research, 88(9), 991-1025.

Raymond, A., & Phillips, T. L. (1983). Evidence for an Upper Carboniferous mangrove community. Biology and ecology of mangroves (pp. 19-30) Springer.

Renwick, W. H. (1992). Equilibrium, disequilibrium, and nonequilibrium landforms in the landscape. Geomorphology, 5(3-5), 265-276.

Revil, A., Grauls, D., & Brévart, O. (2002). Mechanical compaction of sand/clay mixtures. Journal of Geophysical Research: Solid Earth, 107(B11), ECV 11-15.

Rygel, M. C., Fielding, C. R., Frank, T. D., & Birgenheier, L. P. (2008). The magnitude of Late Paleozoic glacioeustatic fluctuations: a synthesis. Journal of Sedimentary Research, 78(8), 500-511.

Sánchez, T. M., & Benedetto, J. L. (2007). The earliest known estuarine bivalve assemblage, Lower Ordovician of northwestern Argentina. Geobios, 40(4), 523-533.

Savage, J. E., Bradshaw, M. A., & Bassett, K. N. (2013). Marginal marine depositional setting and correlation of the Devonian Sperm Bluff Formation (Taylor Group), Southern Victoria Land, antarctica. Antarctic Science, 25(6), 767-790.

Schmedemann, N., Schafmeister, M., & HOFFMANN, G. (2008). Numeric de-compaction of Holocene sediments. Polish Geological Institute Special Papers, 23, 87-94.

Schutter, S. R., & Heckel, P. H. (1985). Missourian (early Late Pennsylvanian) climate in Midcontinent North America. International Journal of Coal Geology, 5(1-2), 111-140.

Scott, A. C., & Glasspool, I. J. (2006). The diversification of Paleozoic fire systems and fluctuations in atmospheric oxygen concentration. Proceedings of the National Academy of Sciences, 103(29), 10861-10865.

Sevastopulo, G. D. (1981). Lower carboniferous. A Geology of Ireland, 147-171.

Sevastopulo, G. D., & Wyse Jackson, P. N. (2009). Carboniferous: Mississippian (Tournaisian and Viséan). The Geology of Ireland.Dunedin Academic Press, Edinburgh, 215, 269.

Singh, B. P., & Andotra, D. S. (2000). Barrier-lagoon and tidal cycles in Palaeocene to middle Eocene Subathu Formation, NW Himalaya, India. Tertiary Research, 20(1/4), 65-78.

Sisulak, C. F., & Dashtgard, S. E. (2012). Seasonal controls on the development and character of inclined heterolithic stratification in a tide-influenced, fluvially dominated channel: Fraser river, Canada. Journal of Sedimentary Research, 82(4), 244-257.

Skolnick, H. (1958). Observations on fusain. AAPG Bulletin, 42(9), 2223-2236.

Smith, D. G. (1976). Effect of vegetation on lateral migration of anastomosed channels of a glacier meltwater river. Geological Society of America Bulletin, 87(6), 857-860.

Smith, D. G., Hubbard, S. M., Leckie, D. A., & Fustic, M. (2009). Counter point bar deposits: Lithofacies and reservoir significance in the meandering modern peace river and ancient McMurray formation, Alberta, Canada. Sedimentology, 56(6), 1655-1669.

Sønderholm, M., & Tirsgaard, H. (1998). Proterozoic fluvial styles: Response to changes in accommodation space (Rivieradal sandstones, eastern North Greenland). Sedimentary Geology, 120(1-4), 257-274.

Stanley, S. M. (2005). Earth system history Macmillan.

Stouthamer, E. (2001). Sedimentary products of avulsions in the Holocene Rhine–Meuse Delta, the Netherlands. Sedimentary Geology, 145(1-2), 73-92.

Surdam, R. C., Dunn, T. L., MacGowan, D. B., & Heasler, H. P. (1989). Conceptual models for the prediction of porosity evolution with an example from the Frontier Sandstone, Bighorn Basin, Wyoming.

Tabor, N. J., & Poulsen, C. J. (2008). Palaeoclimate across the Late Pennsylvanian–Early Permian tropical palaeolatitudes: a review of climate indicators, their distribution, and relation to palaeophysiographic climate factors. Palaeogeography, Palaeoclimatology, Palaeoecology, 268(3-4), 293-310.

Thomas, R. G., Smith, D. G., Wood, J. M., Visser, J., Calverley-Range, E. A., & Koster, E. H. (1987). Inclined heterolithic stratification—terminology, description, interpretation and significance. Sedimentary Geology, 53(1-2), 123-179.

Thornes, J. B. (2009). Catchment and channel hydrology. Geomorphology of desert environments (pp. 303-332) Springer.

Tipper, J. C. (2015). The importance of doing nothing: Stasis in sedimentation systems and its stratigraphic effects. Geological Society, London, Special Publications, 404(1), 105-122.

Torsvik, T. H., & Cocks, L. R. M. (2004). Earth geography from 400 to 250 Ma: a palaeomagnetic, faunal and facies review. Journal of the Geological Society, 161(4), 555-572.

van Asselen, S., Stouthamer, E., & Van Asch, T. W. (2009). Effects of peat compaction on delta evolution: a review on processes, responses, measuring and modeling. Earth-Science Reviews, 92(1-2), 35-51.

van de Lageweg, Wietse I, Braat, L., Parsons, D. R., & Kleinhans, M. G. (2018). Controls on mud distribution and architecture along the fluvial-to-marine transition. Geology, 46(11), 971-974.

van Dijk, W. M., van de Lageweg, Wietse I, & Kleinhans, M. G. (2013). Formation of a cohesive floodplain in a dynamic experimental meandering river. Earth Surface Processes and Landforms, 38(13), 1550-1565.

van Kessel, T., Vanlede, J., & de Kok, J. (2011). Development of a mud transport model for the Scheldt estuary. Continental Shelf Research, 31(10), S165-S181.

van Wijk, J., Koning, D., Axen, G., Coblentz, D., Gragg, E., & Sion, B. (2018). Tectonic subsidence, geoid analysis, and the Miocene-Pliocene unconformity in the Rio Grande rift, southwestern United States: Implications for mantle upwelling as a driving force for rift opening. Geosphere, 14(2), 684-709.

Varela, A. N., Richiano, S., Paz, D. M., Tettamanti, C., & Poiré, D. G. (2019). Sedimentology and stratigraphy of the Puesto El Moro Formation, Patagonia, Argentina: Implications for Upper Cretaceous paleogeographic reconstruction and compartmentalization of the Austral-Magallanes basin. Journal of South American Earth Sciences, 92, 466-480.

Vennin, E., Kolodka, C., Asghari, A., Thomazo, C., Buoncristiani, J., Goodarzi, H., & Desaubliaux, G. (2015). Discussion on palaeozoic discontinuities in the Kuh-E Surmeh area (Zagros, Iran). Marine and Petroleum Geology, 66, 1073-1092.

Walling, D. E., & He, Q. (1998). The spatial variability of overbank sedimentation on river floodplains. Geomorphology, 24(2-3), 209-223.

Woodroffe, C. D. (2002). Coasts: Form, process and evolution Cambridge University Press.

Worthington, R. P., & Walsh, J. J. (2011). Structure of Lower Carboniferous basins of NW Ireland, and its implications for structural inheritance and Cenozoic faulting. Journal of Structural Geology, 33(8), 1285-1299.

Wright, V. P. (1990). Equatorial aridity and climatic oscillations during the early Carboniferous, Southern Britain. Journal of the Geological Society, 147(2), 359-363.

Yokoyama, Y., Lambeck, K., De Deckker, P., Johnston, P., & Fifield, L. K. (2000). Timing of the Last Glacial Maximum from observed sea-level minima. Nature, 406(6797), 713-716.

Zhang, J., & Zhang, Z. (2008). Sedimentary facies of the Silurian tide-dominated paleo-estuary of the Tazhong area in the Tarim Basin. Petroleum Science, 5(2), 95-104.

Zhang, L., Buatois, L. A., Mángano, M. G., Qi, Y., Zhang, X., Sun, S., & Tai, C. (2017). Early Triassic estuarine depauperate Cruziana ichnofacies from the Sichuan area of South China and its implications for the biotic recovery in brackish-water settings after the End-Permian mass extinction. Palaeogeography, Palaeoclimatology, Palaeoecology, 485, 351-360.

Appendix A: Nature and rate of allogenic forcing

The Carboniferous case study represents a drowning estuary valley, displaying an overall fluvial to marine transition (Figure 2), likely in response to relative sea level rise. The mechanism forcing this sea level rise is not well-constrained for the stratigraphic interval of the studied succession. Relative sea level rise induced by tectonic subsidence and eustatic sea level rise in response to the melt-off of terrestrial ice sheets are both feasible mechanisms. In this appendix, the most likely mechanism is deduced through a novel approach based on the relation between the time recorded in individual beds and outcrops and the time span the succession could represent.

11.1. Outline

The sedimentary record is 'more gap than record'. In successions representing 10^3 to 10^6 years, individual beds and outcrops only record a fraction of that time span in the order of 10^{-4} – 10% (Paola et al., 2018, Miall, 2014, Miall 2015, Hollbrook and Miall, 2020). Sedimentary non-deposition or stasis appears to be the norm (Tipper, 2015; Davies and Shillito, 2018) and pack away most of the time span in a sedimentary succession.

Knowing only a small bit of time is recorded in individual outcrops, one may estimate the time span of a given sedimentary succession by summing and extrapolating the 'aggradation time' of individual outcrops that the sedimentary succession comprises. Through similar means, one may gauge whether a proposed time span for a given succession is realistic or not.

This appendix discusses which of three proposed scenarios and their associated time spans are realistic given the cumulative 'aggradation time' in the studied succession. The scenarios considered are relative sea level rise through: (1) tectonic subsidence, spanning several million years; (2) 'slow' climatically-induced eustatic sea level rise, spanning several tens of thousands of years; and (3), 'rapid' climatically-induced eustatic sea level rise, spanning several thousands of years.

11.2. Method

The sedimentary succession is approached from hierarchically different stratigraphic scales and corresponding timescales (Figure 20) in order to estimate the time span the succession may represent under the three proposed scenarios and to estimate the cumulative 'aggradation time' recorded in the outcrops of the succession.

The highest order is that of the stratigraphic succession, comprising a series of outcrops. A stratigraphic succession records sedimentary processes within a 'geological' timescale, *e.g.* the drowning of a valley over the course of millennia to millions of years.

At the middle order are outcrops and their stratigraphic context, recording sedimentary processes within a 'physical geography' timescale, *e.g.* laterally migrating fluvial channels over the course of several decades, or encroaching marine influence in conduits over the course of centuries to millennia.

The lowest order in the hierarchy in the succession is that of individual outcrops and its beds and bedforms. These record dynamic sedimentary processes within a 'human' timescale, *e.g.* a dune migration several metres over the course of hours to days, or floodplain accumulation lasting a few decades (Miall, 2015; Davies et al., 2020).

The challenges outlined above are tackled by going down the 'sedimentary hierarchy'. Uncertainties arising at one scale are fenced off at a hierarchically lower scale:

1. the forcing mechanism on a geological timescale driving the fluvial to marine transition is tackled by estimating the time it takes to deposit the thickness of the succession, yielding the 'succession time'. With tectonic subsidence and climatically-

induced sea level rise as main candidates, how long does it take for each mechanisms to deposit the succession?

2. by employing typical sedimentation rates for the facies and their outcrops, the time it has taken to deposit these packages is estimated. The yielded 'aggradation time' of the packages in the entire succession is compared to the time encompassed in the entire succession as determined in (1), resulting in an estimate of the fraction of 'succession time' recorded in the outcrops. Knowing the sedimentary record is more 'gap than record', which of the scenarios outlined in (1) is realistic? Under the realistic scenario(s), was the sedimentary system in a state of flux or one of equilibrium?
3. looking at the level of individual outcrops and beds, do erosional or aggradational features dominate, or is a more steady-state prevalent?

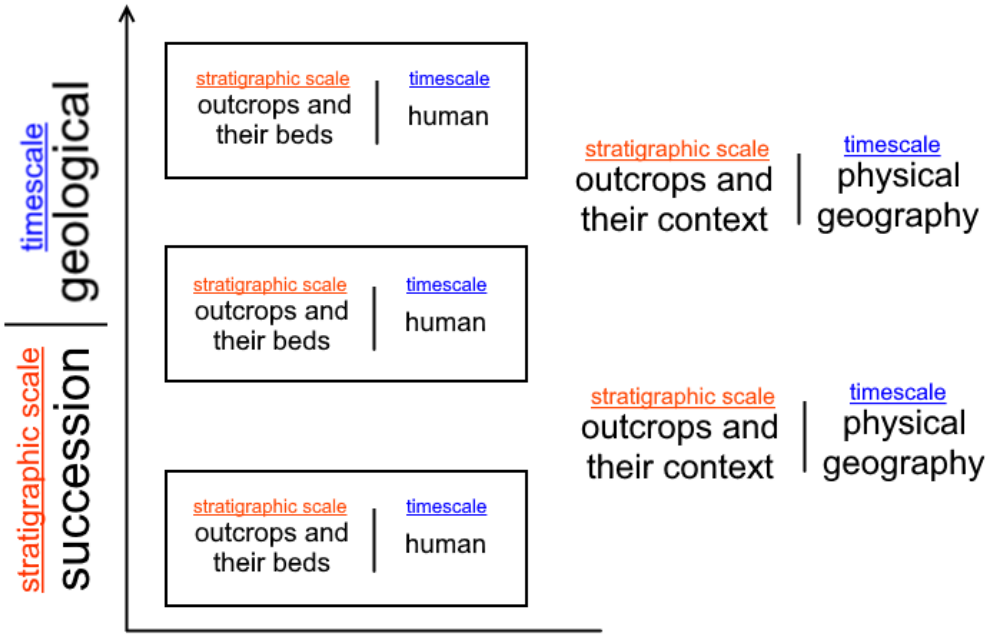

Figure 20: *Graphic overview of the stratigraphic scales and their corresponding timescales, and how these relate to one another.*

11.3. Highest order: succession stratigraphic scale | geological timescale

At the hierarchically highest order of the sedimentary succession the forcing mechanism pushing the relative sea level rise is explored. There are two candidates: relative sea level rise by tectonic subsidence, or climatically-induced eustatic sea level rise by ice cap melting. It is assumed sediment supply during this relative sea level rise was sufficient.

To estimate the amount of time it would have taken these mechanisms to transition the palaeolandscape from a full fluvial environment to a near-shore estuarine environment, the thickness of the studied succession is considered. Alluvial fan conglomerates of facies AC-1 are not taken into account as their base is not constrained well. To deposit the volume of sediments of the studied succession, it is assumed an equal volume of accommodation space needed to be created by the mechanisms under consideration. However, the 80 metres of studied stratigraphy (sans alluvial fan conglomerates) as exposed today at Shawly Point underwent differential compaction by burial after deposition, reducing sediment porosity and thus the thickness of the strata. That means the thickness of the strata as observed in outcrop do not represent the 'depositional volume' of the strata. Therefore, the strata need to be 'decompacted' first.

11.3.1. Compaction

The degree of compaction of a sedimentary package depends on the maximum burial depth it underwent (Kim et al., 2018). The burial history of the studied succession is not known and detailed research is outside the scope of this study, but a range of burial scenarios and the resulting strata compaction are explored.

Additionally, differential compaction of different lithologies result in varying degrees of compaction between packages of the succession. Muds lose the majority of their porosity in the first 30 metres of burial, the rate of compaction waning with deeper depths (Athy, 1930; Aqrawi, 1995). Conversely, sands retain their porosity under shallow burial and only start compacting markedly when buried deeper than *ca.* 50 metres (Kim et al., 2018). This differential compaction between muds and sands would mean that under a shallow burial scenario, the succession as exposed would be volumetrically 'biased' towards sandstones.

Furthermore, sediments were compacted while the succession was building. This 'syn-depositional' compaction reduces strata thickness and creates accommodation space for subsequent deposits, limiting the need for an allogenic forcing to create accommodation space. That means the volume of the succession would not require an equal volume of (allogenically forced) accommodation space. This syn-depositional compaction is not considered in the reconstructed thickness. Mitigating this complication would call for computer modelling, which is beyond the scope of this study. The succession is treated as if its sediments did not compact until the entire succession was deposits, after which it was buried and compacted instantaneously.

11.3.2. Burial scenarios

To estimate the degree of compaction, three burial scenarios and their resultant compaction are explored: 10 metres, 100 metres, 1 kilometre. An upper limit value for the maximum burial depth is *ca.* 3-5 km, as strata in the succession did not undergo metamorphism or (extensive) diagenetic alterations (*e.g.* mineral alteration, cementation) (Surdam et al., 1989).

The strata of the succession are grouped by realm (fluvially-dominated, mixed-energy, marine-dominated) and by lithology (sandstones and mudstone, silts and shales). Note that the conglomerates at the base of the succession are not taken into account. Rates of compaction for these lithologies at various burial depths are taken from literature (Table 2).

The three burial scenarios – 10 metres, 100 metres, 1 km – yield a decompacted thickness of 97.6 metres, 105.3 metres and 178.6 metres, respectively (Figure 21, Table 6). Thickness reduction half (1 km burial) is not likely as the geometry of the sedimentary structures observed in outcrop and the geometry of architectural elements (*e.g.* the cosets of IHS-A in Figure 7A) are close to those found in modern, active environments. The scenario for 1 km is therefore rejected, leaving a range of *ca.* 10 to 100 metres for the maximum burial depth the studied succession experienced. That translates to a decompacted thickness of *ca.* 98 to 105 metres, a compaction of 17 to 23%, accounted for mostly by compaction of muds.

With two burial scenarios and their resultant decompacted succession thickness established, the time encompassed in them can be explored based on the two forcing mechanisms discussed previously.

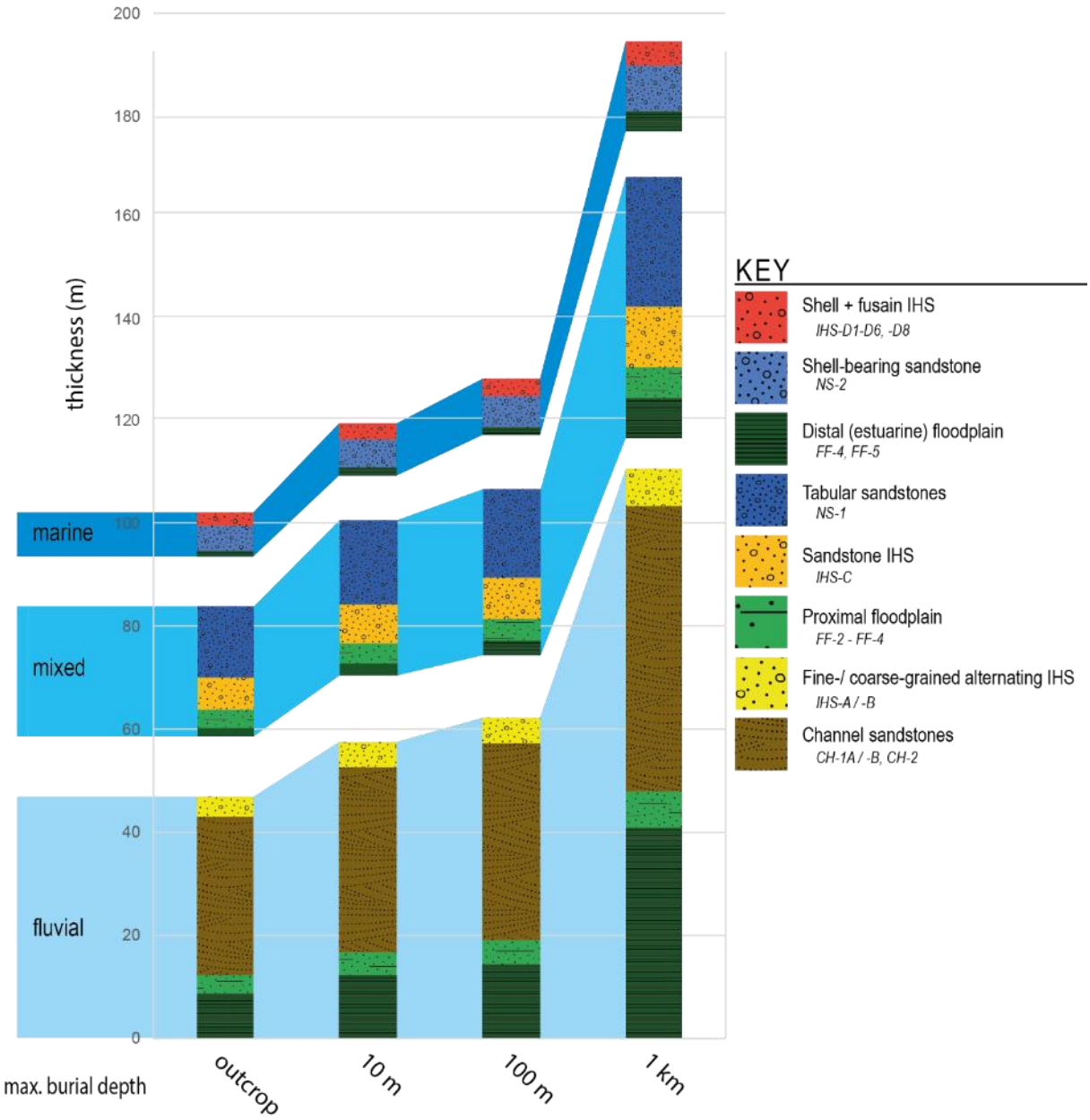

Figure 21: *graphic representation of the outcrop thickness and decompacted thickness of grouped strata under three burial scenarios.*

Table 6*: rates of compaction and resultant strata thickness for three burial scenarios (10m, 100m, 1km), grouped by environmental realm and lithology. Note that the conglomerates at the base of the succession are not taken into account.*

				Max. thickness reduction in scenario			(Decompacted) thickness			
realm	facies	interpretation	lithology	10 m	100 m	1 km	outcrop	10 m	100 m	1 km
fluvial dominated	FF-2, FF-3, FF-4	floodplain (distal)	mudstone and shales	30%	40%	79%	8.6 m	12.3 m	14.3 m	40.9 m
	FF-1, F-5	floodplain (prox.)	sandstone (intercal. with silts)	15%	20%	45%	3.8 m	4.5 m	4.8 m	6.9 m
	CH-1A/B, CH-2	channel and bars	sandstone	15%	20%	45%	30.6 m	36.0 m	38.3 m	55.6 m
	IHS-A, IHS-B	channel point bar	sandstone (primarily)	15%	20%	45%	4 m	4.7 m	5.0 m	7.2 m
mixed energy	FF-2, FF-3, FF-4	estuarine 'floodplain' (distal)	mudstone and shales	30%	40%	79%	1.6 m	2.3 m	2.7 m	7.6 m
	FF-1, F-5	estuarine 'floodplain' (prox.)	sandstone (intercal. with silts)	15%	20%	45%	3.4 m	4.0 m	4.3 m	6.1 m
	IHS-C	estuarine point bar	sandstone (primarily)	15%	20%	45%	6.4 m	7.5 m	8.0 m	11.6 m
	NS-1/NS-2	estuarine sand flat	sandstone	15%	20%	45%	13.8 m	16.2 m	17.3 m	25.0 m

tidal dominated	FF-4, IHS-D7	(estuarine) floodplain, fines	shelly siltstones and mudstone	25%	35%	74%	1 m	1.3 m	1.5 m	3.8 m
	NS-2	nearshore sand flat	shelly sandstone	15%	20%	45%	4.8 m	5.6 m	6.0 m	8.7 m
	IHS-D1-D6, D8	fusain-rich point bar	shelly and fusain-rich sandstone	15%	20%	45%	2.6 m	3.1 m	3.3 m	4.7 m
			Entire succession	17%	23%	55%	80.6 m	97.6 m	105.3 m	178.6 m

Thickness reduction percentages are estimated from values in literature on Holocene deposits for shallow burial depths (10-100m), Aqrawi (1995) and from seismics and modelling studies for deep burial depths (1 km), Kim et al. (2018), Revil et al. (2002), Schmedemann et al. (2008).

11.3.3. Time span the succession represents

Few age constraints are known for the formation in the studied section. The onset of sedimentation, marked by the *Roulough Conglomerate Formation*, is thought to be of Viséan age (*ca.* 350 Ma) (Graham, 1996), but no upper limit is known. The present author aims to gauge the time span the succession encompasses by estimating how long it would take to deposit the *ca.* 100 metre succession representing this fluvial to marine transition, assuming ample sediment availability.

A base level rise creating sufficient accommodation space for the succession to be deposited could be forced by (a combination of) two main mechanisms: climatic eustatic sea level rise and/or tectonic subsidence. As is elaborated on below, both mechanisms are feasible considering the climatic and geological context of the studied succession. Recent analogues for climatically-forced sea level change are used. Tectonic subsidence rates are derived from literature on basins in a similar (extensional) tectonic regime. Two climatically-forced scenarios are discussed first, followed by scenarios with tectonic subsidence as the forcing mechanism.

Climatic eustatic sea level rise

The Viséan age of the studied succession places the sediments in a wider context of the Late Palaeozoic Ice Age (Ketzer et al., 2002; Fielding et al., 2008) with climate oscillating between glacial and non-glacial conditions (Ketzer et al., 2002; Pfefferkorn et al., 2014).

Past sea level rise during deglaciation provides an order of magnitude for the rate of sea level rise. Mean sea level rise during deglaciation trends to *ca.* 5 mm/yr when multiple deglaciation periods stretching from the Eocene to the Quaternary are considered (Foster and Rohling, 2013). Mean sea level rise after the Last Glacial Maximum (~35 ka) was more rapid and approximated 15 mm/yr (Lambeck et al., 2014).

At the 'slow' rate of sea level rise of 5 mm/yr and assuming a decompacted thickness of the studied succession of 97 to 105 metres, the fluvial to marine transition would span *ca.* 19.5 to 21 ky. Assuming a 'rapid' sea level rise of 15 mm/yr, the succession would span 6.5 to 7 ky (Table 7).

A base level rise of *ca.* 100 metres is near the upper end of reported Carboniferous sea level fluctuations - 42 m (Maynard and Leeder, 1992), 60 m (Crowley and Baum, 1991), 100 m (Alekseev et al., 1996), but within the 130 metres reported for the deglaciation following the Last Glacial Maximum (*ca.* 21 Ka) (Yokoyama et al., 2000). Sea level rise superimposed on tectonic subsidence would bridge the 'base level gap'. A scenario with tectonic subsidence in conjunction with climate-forced eustatic sea level rise is beyond the scope of this study and not explored. Tectonic subsidence as the sole mechanism is explored below.

Tectonic subsidence

The studied succession is deposited in the Donegal Basin, one of several extensional basins formed in the Lower Carboniferous (Worthington and Walsh, 2011). Tectonic subsidence could therefore be a realistic mechanism for relative base level rise.

Studies on other extensional basins under tectonic subsidence report typical subsidence rates in the order of 35 m/Myr, or 0.035 mm/yr (Patriat et al., 2003; van Wijk et al., 2018). Relative base level rise forced solely by tectonic subsidence yields a time span recorded in the succession of 2 - 4.2 My (Table 7).

A tectonically-forced rate of base level rise is three orders of magnitude (10^3) lower than climatically-forced base level change. For a scenario in which tectonic subsidence act in conjunction with climate-forced eustatic sea level rise, the latter rate would have to be much slower for tectonic subsidence to have a marked contribution to overall base level rise. Such a scenario is not considered in this study, however.

Table 7: *Time span reflected in the studied succession of two burial scenarios with a maximum burial depth of 10 m or 100 m, under base level rise forced by tectonic subsidence, 'slow' climatically-forced eustatic sea level rise, and 'rapid' climatically-forced eustatic sea level rise.*

	burial scenario	10 m	100 m
	decompacted thickness	98 m	105 m
forcing scenario	rate of relative sea level rise		
slow climatic	*5mm/yr*	19.5×10^3 yr	21×10^3 yr
rapid climatic	*15mm/yr*	6.5×10^3 yr	7×10^3 yr
tectonic subsidence	*0.035mm/yr*	$2\times10^6 – 3.9\times10^6$ yr	2.1×10^6 yr

11.4. Middle order: outcrop context scale | 'physical geography' timescale

11.4.1. Time span recorded in the outcrops

At the hierarchically middle order, the amount of time stored in individual facies and outcrops are explored. Individual outcrops record sedimentary processes on the 'human' timescale, *e.g.* a dune migrating several metres in hours to days, or floodplain muds accumulating over the span of decades. Each sedimentary process has a characteristic aggradation rate and different facies are dominated by differing sedimentary processes (Table 8). Aggradation rates are derived from literature on Holocene analogues. However, human interference on late Holocene systems significantly affected sediment supply and aggradation rates since Iron age times (*ca.* 1000 B.C.) (Hoffmann et al., 2009). Hence, pre-Iron aggradation rates are used for floodplain aggradation rates. Four groups of facies are identified, each with a unique characteristic aggradation rate:

1. Proximal floodplain facies are dominated by the aggradation of sheet-like layers of fine-grained sands and silts, at a characteristic aggradation rate of cm's/yr (Walling and He, 1998; Hoffmann et al., 2009). Comprises facies FF-1, FF-2 and FF-5.
2. Distal floodplain facies are dominated by the aggradation of sheet-like layers of silts and muds, at a characteristic aggradation rate of mm's/yr (Walling and He, 1998; Hoffmann et al., 2009). Comprises facies FF-3 and FF-4.
3. Channel facies are dominated by bedload deposition of (coarse-grained) sands and (point) bar migration, at a characteristic aggradation rate of cm's/h (Allen, 2008).

Comprises facies CH-1A, CH-1B, CH-2, CH-3, IHS-A, IHS-B, IHS-C, IHS-D and NS-2.

4. Sandflats in the succession are dominated by parallel lamination deposited under upper flow regime conditions, at a characteristic aggradation rate of mm's/min (Paola et al., 1989; Fielding, 2006). Comprises facies NS-1.

Employing again the decompacted succession, the thickness of all the strata of each group are summed and multiplied with their characteristic aggradation rate, yielding the total 'aggradation time' for each group. The sum of the aggradation times of each group yields the total amount of time recorded in the succession (Table 9). The total time recorded in the succession ranges from 2.6 - 8.85 ky.

Table 8: *Facies groups, constituent facies, order of magnitude of their aggradation rate and the values used in calculations on each group's total aggradation time.*

Facies group	Facies	aggradation magnitude	range of values used in calculations	
1 proximal floodplain	FF-1, FF-2, FF-5	cm's per year	2-6 cm/yr	$2\text{-}6\times10^{-2}$ m/yr
2 distal floodplain	FF-3, FF-4	mm's per year	2-6 mm/yr	$2\text{-}6\times10^{-3}$ m/yr
3 channel facies	CH-1A/-B – CH-3, IHS-A – IHS-D, NS-2	cm's per hour	2-6 cm/h	$1.75\text{-}5.25\times10^{2}$ m/yr
4 UFR sandflat	NS-1	mm's per minute	2-6 mm/min	$1.1\text{-}3.3\times10^{3}$ m/yr

Table 9: *Time recorded in each facies group and total time recorded in the succession under the two burial scenarios (10 m and 100 m) explored.*

	decompacted thickness		amount of time recorded	
Facies group	scenario 10 m	scenario 100 m	scenario 10 m	scenario 100 m
1 proximal floodplain	8.5 m	9.1 m	$1 - 4\times10^{2}$ yr	$1.5 - 4.5\times10^{2}$ yr
2 distal floodplain	15 m	17 m	$2.5 - 7.5\times10^{3}$ yr	$2.8 - 8.5\times10^{3}$ yr
3 channel facies	51.3 m	54.6 m	$9\times10^{-5} - 2.8\times10^{-4}$ yr	$1.0\times10^{-4} - 3.1\times10^{-4}$ yr
4 UFR sandflats	21.8 m	23.3 m	$6.8\times10^{-6} - 2.1\times10^{-5}$ yr	$7.4\times10^{-6} - 2.2\times10^{-5}$ yr
		Total time recorded	$2.6 - 7.8\times10^{3}$ yr	$2.95\text{-}8.85\times10^{3}$ yr

11.4.2. Rejecting 'rapid climate sea level rise' scenario

The time recorded in the deposits of the succession lies in the range of $2.95\text{-}8.85\times10^{3}$ yr. If the rapid climatic scenario as outlined in (1) is true, the succession would reflect $6.5\text{-}7.0\times10^{3}$ yr. That would mean 40-100% of that time would be recorded in the deposits.

If the slow climatic scenario as outlined in (1) is true, the succession would reflect $19.5\text{-}21\times10^{3}$ yr. That would mean 10-40% of that time would be recorded in the deposits.

If the tectonic subsidence scenario is true, the succession would reflect 2.1-4.2×10^6 yr. That would mean *ca.* 0.1% of that time would be recorded in the deposits.

A near complete and continuous stratigraphic record in dynamic environments like fluvial and estuarine ones is very unlikely (van de Lageweg et al., 2018), leading to the rejection of the rapid climatic scenario. In the near-shore environment of the succession, one would expect transgressive erosional surfaces when sea level rise was as rapid as deglaciation after the Last Glacial Maximum (*ca.* 21 ka) (Li et al., 2014). The absence of these corroborates rejection of the rapid climatic scenario, leaving the slow climatic and tectonic subsidence scenarios as viable options.

11.4.3. Sedimentary system (dis)equilibrium

The landscapes of sedimentary systems and the landforms they comprise – *e.g.* a fluvial landscape comprising channels, erosional hillslopes and oxbow lakes – have an equilibrium state which some landform processes tend towards over longer timescales (Renwick, 1992). An equilibrium is not static but sees landforms emerging, altering and disappearing. For example, fluvial channel meander length can remain stable under dynamic equilibrium conditions, but individual channels still erode, aggrade and migrate.

When external forcing perturbates these processes, a new equilibrium state may be attained after a certain 'response time', usually in the order of 10^4 years or more (Renwick, 1992). For example, meander lengths change during this 'response time', trending to their new equilibrium state. If an external forcing acts over a period longer than the landscape's response time ('slow external forcing'), short-term equilibrium may be maintained in the landscape while shifting gradually to a new equilibrium state over the course of its response time. This gradual shift is usually termed 'dynamic equilibrium' (Hack, 1975). External forcing acting more over a period shorter than the landscape's response time ('rapid external forcing') render the landscape to be in a state of geomorphic disequilibrium, trending to the new equilibrium state in a non-stable manner (Allen, 2008).

The time span encompassed in the climatic scenario is shorter than the typical landscape response time. That would render the system state of the studied succession in a state of disequilibrium as it adjusts and trends to a new equilibrium state under rapid external forcing. Conversely, the system would shift gradually in dynamic equilibrium if it was forced by tectonic subsidence, as the time span encompassed in the tectonic scenario is longer than the landscape response time. In what state was the sedimentary system?

11.5. Lowest order: outcrop beds scale | 'human' timescale

A system in disequilibrium under a sea level rise quicker than the response time of the system would be one of aggradation, assuming ample sediment supply. Deposition must keep up with the accommodation space being created at a rate of 5 mm/yr, similar to Eocene-Quaternary deglaciation events relative sea level rise rates. Quick-paced aggradation would manifest as climbing ripples at the scale of outcrops and individual beds (Myrow et al., 2018). Erosional features, such as erosive top bed boundaries and truncated cross-beds, would be limited. Up to 40% of the 'aggradation time' would have to be preserved and stored in stratigraphy, further limiting the potential for erosional features to develop.

However, ample evidence for the removal of aggradation time by erosion is observed in the studied succession, despite the overall gradual nature of it. Wide exposures of laterally migrating channels (facies CH-1A, Fig. 5A) suggest extensive autogenic reworking and little

vertical movement, suggesting a limited rate of base level rise. The erosional top of floodplain beds (Fig. 11A) records removal of, perhaps copious amounts of, aggradation time. At the level of individual beds, truncated cross-beds (Fig. 7A) record the removal of ripples. The line of evidence seems to point to a landscape in a state of dynamic equilibrium, with external forcing acting over timescales longer than the geomorphic response time.

11.6. Summary

The scenario of base level rise forced by tectonic subsidence fits this the best. The 'slow' climatic scenario is rejected. However, this conclusion relies on a framework of assumptions with broad implications: (1) sediment supply must have been ample to keep up with any hypothesized rate of base level rise so to exclude erosion by sediment starved streams. In a scenario with rapid relative sea level rise, sediment starvation and therefore erosion is not unlikely; (2) syn-depositional' compaction while the succession was building limits the amount of base level rise needed to deposit the entire thickness of the studied succession. That shortens the time span hypothesized in the three forcing scenarios, but is not considered; and, (3) the rate of base level rise at which (near-)completely preserved, climbing ripples are formed is unclear. The assumption that these should be observed under the 'slow' climatic scenario could consequently be invalid.

Appendix B: Raw data tables for mudrock abundance and IHS presence

#	Reported age	Mudrock %	Architecture	Comments	Main references
1	Early to Medial Cambrian	17%	-	sub-equatorial arid climate	Brink et al. (2019)
2	Late Cambrian to Early Ordovician	15%	IHS	-	Buatois et al. (2003)
3	Early Ordovician	30%	-	-	Sánchez et al. (2007)
4	Late Ordovician	8%		polar climate	El-Ghali et al. (2005)
5	Ordovician to Early Silurian	0%	-	-	Bradley et al. (2018)
6	Silurian	12%	-	-	Zhang et al. (2008)
7	Late Silurian	35%	IHS	-	Hiller et al. (2004)
8	Devonian	6%	-	-	Savage et al. (2013)
9	Medial to Upper Devonian	19%	-	-	Mikulaš et al. (2013)
10	Upper Devonian	18%	IHS	semi-arid climate; formation age debated	Evans et al. (2019)
11	Medial Mississippian (Carboniferous)	16%	IHS	alternating humid and arid climate	this study
12	Late Mississippian	35%	IHS	alternating humid and arid climate	Greb et al. (2016)
13	Late Carboniferous to Medial Permian	12%	IHS	post-glacial ameliorating climate	Polo et al. (2018)
14	Late Permian	43%	-	-	Vennin et al. (2015)
15	Early Triassic	25%	-	-	Zhang et al. (2017)
16	Early Jurassic	45%	-	high latitude climate	Oluassen et al. (2018)
17	Medial Jurassic	21%	IHS	equatorial humid climate	Al-Hussaini et al. (2019)
18	Early to Medial Jurassic	53%	IHS	age debated	O'Conner et al. (2018)
19	Early Cretaceous	24%	IHS	temperate humid climate	Olivo et al. (2019)
20	Late Cretaceous	50%	IHS	-	Varela et al. (2019)

#	Palaeo-environment	sub-environment	mudstone %	siltstone %	shale %
1	estuary to shoreface	estuary	17		
2	estuary	estuary	0	15	0
3	estuary	estuary	0	30	0
4	estuary	estuary	0	8	0
5	estuary	macrotidal estuary	0	0	0
6	estuary	fluvial head of tide-dominated estuary		12	
7	estuary	estuary	35	0	0
8	wave-dominated delta	estuary	6	0	0
9	estuary	brackish environment	10	9	0
10	estuary	estuary	0	0	18
11	estuary	estuary	0	0	0
12	estuary	fluvial-dominated channel		0	35
13	marginal-marine	estuary		12	0
14	estuary	wave-dominated estuary	43	0	0
15	estuary	estuary	25	0	0
16	estuary	tide-dominated estuary	45	0	0
17	estuary	estuary	21	0	0
18	estuary	estuary	53	0	0
19	estuary	wave-dominated estuary	24	0	0
20	estuary	estuary	50	0	0

#	Reported age		Mudrock %	Architecture	Comments	Main references
1	Early to Medial Cambrian	Early-Med Cm.	17%	-	sub-equatorial arid climate	Brink et al. (2019)
2	Late Cambrian to Early Ordovician	Late Cm.-Early O.	15%	IHS	-	Buatois et al. (2003)
3	Early Ordovician	Early O.	30%	-	-	Sánchez et al. (2007)
4	Late Ordovician	Late O.	8%		polar climate	El-Ghali et al. (2005)
5	Ordovician to Early Silurian	O.-Early S.	0%	-	-	Bradley et al. (2018)
6	Silurian	Sil.	12%	-	-	Zhang et al. (2008)
7	Late Silurian	Late S.	35%	IHS	-	Hiller et al. (2004)
8	Devonian	Dev.	6%	-	-	Savage et al. (2013)
9	Medial to Upper Devonian	Med-Late D.	19%	-	-	Mikulaš et al. (2013)
10	Upper Devonian	Late D.	18%	IHS	semi-arid climate; formation age debated	Evans et al. (2019)
11	Medial Mississippian (Carboniferous)	Med M.	16%	IHS	alternating humid and arid climate	this study
12	Late Mississippian	Late M.	35%	IHS	alternating humid and arid climate	Greb et al. (2016)
13	Late Carboniferous to Medial Permian	Late C.-Med P.	12%	IHS	post-glacial ameliorating climate	Polo et al. (2018)
14	Late Permian	Late P.	43%	-	-	Vennin et al. (2015)
15	Early Triassic	Early T.	25%	-	-	Zhang et al. (2017)
16	Early Jurassic	Early J.	45%	-	high latitude climate	Oluassen et al. (2018)
17	Medial Jurassic	Med J.	21%	IHS	equatorial humid climate	Al-Hussaini et al. (2019)
18	Early to Medial Jurassic	Early-Med J.	53%	IHS	age debated	O'Conner et al. (2018)
19	Early Cretaceous	Early K.	24%	IHS	temperate humid climate	Olivo et al. (2019)
20	Late Cretaceous	Late K.	50%	IHS	-	Varela et al. (2019)